

### **Preamble**

This work is unique: it revives the traditions of honest science of the 18th and 19th centuries. Prominent representatives of this science include, for example, Pierre-Simon Laplace and Simon Newcomb.

The results of this paper refute the speculations of modern mainstream science about dark matter, dark energy, black holes, big bangs, gravitational waves, etc. That's why establishment journals don't publish this work.

At the end of the paper is attached a Discussion in which my answers and explanations are given to the reviewers' comments. This Discussion reveals the details and subtleties of the problem of contemporary science, which go far beyond the scope of the paper.

# Development of Multilayer Models of Globular Star Clusters and Study of Their Evolution

Joseph J. Smulsky

Institute of Earth's Cryosphere, Tyum. SC of SB RAS, Federal Research Center, Tyumen, Russia

Email: [jmulsky@mail.ru](mailto:jmulsky@mail.ru)

**How to cite this paper:** Smulsky, J.J. (2024) Development of Multilayer Models of Globular Star Clusters and Study of Their Evolution. *Journal of Modern Physics*, 15, 1246-1300.

<https://doi.org/10.4236/jmp.2024.158051>

**Received:** May 6, 2024

**Accepted:** July 26, 2024

**Published:** July 29, 2024

Copyright © 2024 by author(s) and Scientific Research Publishing Inc. This work is licensed under the Creative Commons Attribution International License (CC BY 4.0).

<http://creativecommons.org/licenses/by/4.0/>



Open Access

## Abstract

Usually, models of globular star clusters are created by analyzing their luminosity and other observation parameters. The goal of this work is to create stable models of globular clusters based on the laws of mechanics. It is necessary to set the coordinates, velocities and masses of the stars so that as a result of their gravitational interaction the globular cluster is not destroyed. This is not an easy task, and it has been solved in this paper. Using an exact solution of the axisymmetric gravitational interaction of  $N$ -bodies, single-layer spherical structures were created. They are combined into multilayer models of globular clusters. An algorithm and a program for their creation is described. As a result of solving the problem of gravitational interaction of  $N$  bodies, evolution of 5-, 10-, and 15-layer structures was studied. During the inter-body interaction, there proceeds a transition from the initial specially organized structure to a structure with bodies, uniformly distributed in space. The number of inter-body collisions decreases, and the globular cluster model passes into the stable form of its existence. The collisions of bodies and the acquisition of rotational motion and thermal energy by them are considered. As a result of the passage to scaled dimensions, the results were recalculated to the conditions of globular star clusters. The periods of rotation and the temperatures of merged stars are calculated. Attention is paid to a decreased central-body mass in the analyzed models of globular star clusters.

## Keywords

$N$ -Body Problem, Solution, Globular Star Clusters, Properties

## 1. Introduction

Globular star clusters are spherical or somewhat flattened formations that contain from tens of thousands to a million stars [1]-[6]. The average density of

substance in globular clusters is 0.4 stars per cubic parsec (pc) [7]. In the center, the density increases up to 100 - 1000 stars/pc<sup>3</sup>. The diameter of clusters can reach tens of parsecs [5]. Globular star clusters are common objects in the Universe: there are about 150 of them in our Galaxy alone [2]. They are old formations. The age of many of them exceeds 10 billion years (Gyr) [2] [5] and even exceeds 13.8 Gyr [7], *i.e.*, the age of the Universe assumed in the “Big Bang” theory. Therefore, in recent decades, astronomers have reduced the age of globular clusters. However, after the James Webb Space Telescope discovered distant galaxies with an age exceeding 13.8 Gyr, the age of very old globular clusters is now raised to 26.7 Gyr [8]. It should be noted that relatively young globular clusters are observed in the Magellanic clouds, satellites of our Galaxy, and in other galaxies [5] [9]-[11].

There also exist dwarf spheroidal galaxies. Such galaxies are predominantly satellites of other galaxies, but they also occur as isolated objects [12]. The nuclei of galaxies and their surrounding halos also have a spherical shape. Thus, the spherical shape of stellar associations is often found in the Universe. Therefore, researchers believe that uncovering the mechanisms behind the existence of globular clusters will provide insight into processes in denser systems such as galactic nuclei [3].

Various methods are used to model stellar associations such as globular star clusters and galaxies [5] [3] [13]. In some of them, the entire cluster zone is considered as a continuous medium, and in others, as a set of objects with random kinematic characteristics. The latter models are not deterministic. In deterministic models, each body has its own size, mass, coordinates, and velocity. The gravitational interaction of each such body with any other body is investigated. Therefore, the position and velocity of any body are known at any time.

Depending on the method of solving the N-body problem, such models can differ significantly [4] [5]. For example, computer programs implementing such methods generally fall into four groups [6]. The most common programs for solving the N-body problem are the programs NBODY 2 - NBODY 6 [10] [14] developed by S.J. Aarseth [13]. Those programs, such as NBODY 6 [6], use the Hermite method based on the expansion of coordinates and velocity of bodies in Taylor series. This approach uses three derivatives [6]. In the process of solving the N-body problem, bodies can approach each other. At such moments, a step division algorithm is activated, and at small distances between bodies the calculation is terminated. Therefore, various regularization methods are introduced [4] [6] [13]. When two bodies approach together, as a rule, switching to the algorithm for the exact solution of the two-body problem is used. When three bodies approach each other, other algorithms are employed. Such regularization avoids slowing down the calculation process, but simultaneously leads to a loss of overall solution accuracy. That is why an additional effect is introduced, namely the tidal one [6] [13]. This effect is also added to take into account the influence due to objects located outside the globular cluster.

In these problems, one of the main tasks is the assignment of initial conditions, in particular, coordinates and velocities of bodies. For this purpose, many different methods were used [13]. In the most common of them, based on the brightness distribution and the number of stars in a cluster, the initial mass function (IMF) of the cluster [5] [14] or the initial concentration function [15] [16] are calculated. With their help, the velocity of stars at a certain radius from the cluster center can be found. The stars are then made statistically distributed in space. It should be noted that this leads to a violation of the determinism of the problem.

Since the positions and velocities of bodies obtained in this way can lead to the destruction of the globular cluster model, they must be further corrected and adapted [4] to avoid undesirable effects.

In many works on solving the N-body problem it was noted that there is only one exact solution to this problem, that for the two-body problem [4] [13]. An exact solution of the N-body problem is required for testing computer programs for numerical solution [13].

In fact, such solutions do exist. We have obtained some of them [17], for example, one solution for N bodies located axisymmetrically on a plane [18]. We should also mention a second solution, in which there are N2 concentric layers around a central body, each layer containing N3 bodies [19]. In this case, the entire structure rotates around its axis as a whole and the masses of one body in each layer are different.

In the present paper, globular cluster models are created based on the solution of the first problem [20] [21]. The solution to this problem exists for any number N of bodies. In this case, the central body may be absent. It should be noted that this planar axisymmetric N-body problem was also solved for Coulomb interaction [22]. Its solution exists only in the presence of a central particle, *i.e.* positively charged nucleus, and with the number of peripheral particles, *i.e.* electrons,  $N_3 < 473$ .

Thus, by solving the planar axisymmetric N-body problem, the masses of the central and peripheral bodies, and their coordinates and velocities, are determined. As a result of research [20] [21], it was found that with a uniform arrangement of bodies in space, they move along the same orbits as on the plane. It should be noted here that those orbits can be a circle, an ellipse, a parabola, or a hyperbola. In the present work, globular clusters with circular orbits of bodies were treated. In such clusters, all bodies have certain masses, coordinates and velocities, that is, the cluster is strictly deterministic, with its motion being strictly pre-defined in the future.

For solving the N-body problem, we have developed a system called Galactica. This system was used to solve a number of problems in celestial and cosmic dynamics [23] [24]. The guide for working with Galactica is available in [25], the text of the program for gravitational interaction is published in [24], and the entire system is freely available<sup>1</sup>. The Galactica system is a universal program. It

<sup>1</sup><http://wgalactica.ru/smull1/smulski/GalactW/>

can be used for calculating Coulomb interactions in the micro-world [22]. A guide to working with the Galactica system in this case is published in [26].

The Galactica program uses a highly accurate solution method. Like in the NBODY 6 program, the coordinates and velocities of bodies in it are expanded into Taylor series, with derivatives up to the sixth order inclusive taken into account. Due to this, the accuracy in solving Solar-system dynamics problems is several orders of magnitude higher than, for example, the accuracy offered by NASA programs [27] [28].

When solving the problem of evolution of the Solar system, a number of authors have arrived at a conclusion about Solar-system instability, which will manifest itself after 20 million years [29] [30]. Using the Galactica system, the problem of evolution of the Solar system over a period of 100 million years was solved, and it was shown that, on the contrary, the Solar system will remain stable, with no tendency to its changes observed [31] [32]. This is due to the greater accuracy of the Galactica program.

The Galactica program uses no regularization when bodies approach each other. At each step, accuracy is controlled and, if necessary, the step size is changed. When the bodies come in contact, they combine into one body, whose kinematic parameters can be determined as governed by the mechanics laws. Therefore, the resultant bodies have angular momentum, *i.e.* spins, and thermal energies. From these quantities, one can calculate the period of rotation of the body and its temperature. It should be noted here that Galactica has a number of functions that allow one to analyze and study the results obtained when solving the N-body problem.

In this way, the interactions of bodies in a spherical single-layer structure were analyzed [20] [21]. The construction of such a structure was substantiated, its development in the process of inter-body interaction was demonstrated, and evolution was studied. Such a structure presents a model of a globular star cluster with a rarefied core. In the present work, multilayer structures with each layer created according to the single-layer structure construction algorithm have been considered. The algorithm for constructing such structures is substantiated, issues concerning the choice of parameter values for these structures are discussed, and the evolution of several models of multilayer structures is studied. During this work, various phenomena and properties of modeled structures were revealed, with considerable attention having been given to the study of modeled objects. Such phenomena also occur in globular star clusters.

The structure of the paper is as follows. The method for constructing globular clusters is described at the beginning. The evolution of 5, 10, and 15-layer globular cluster models is then considered. Then their general properties are described. These studies were carried out in dimensionless form. Further, the results obtained are presented in dimensional form in the scale of a globular cluster. At the end of the paper, models of the central body are studied, which makes it possible to reduce its mass by tens of times.

## 2. Basic Principles in Constructing Multilayer Structures

A layered structure is created from a number of structures distributed over a sphere [20] [21]. The single-layer structure is based on solving the problem of interaction of  $N_3$  peripheral bodies with a mass  $m_i = m_1$  located axisymmetrically on a plane around a central body of mass  $m_0$  [18] [33] [34]. Such a structure unfolds in space as follows. The second peripheral body  $m_2$  (Figure 1(a)), together with the other bodies  $m_3, m_4, \dots, m_p, \dots, m_{N_3}$ , is rotated in the  $x_1y_1$ -plane through an angle  $\Delta\psi$  counted from the position of the first body. Then, through the  $x_2$ -axis passing through the second body, the entire plane with the bodies  $m_2 - m_{N_3}$  is rotated through an angle  $\Delta\theta$  from the initial plane. The velocity vectors of these bodies are also located in a new plane. Such a process of rotations through the angles  $\Delta\psi$  and  $\Delta\theta$  is performed sequentially for all bodies from  $m_3$  to  $m_{N_3}$ . As a result, a structure distributed in space is formed (Figure 2(a)), in which the coordinates and velocities of bodies during their interaction allow them to move in space with periods almost the same as those on the plane. By changing the increments  $\Delta\psi$  and  $\Delta\theta$ , one can create various spherical structures.

There are also a number of other possibilities that allow one to create various structures using rotations through angles  $\Delta\psi$  and  $\Delta\theta$ . In the works by Smulsky [20] [21], four such possibilities were analyzed. In the fourth case, not the bodies  $m_i$  themselves but the pericenters of their orbits  $P_{c,i}$  are located on the initial circle (Figure 1(b)). The orbit can be an ellipse, a parabola, or a hyperbola. Peripheral bodies have similar orbits with eccentricity  $e$ , each body being located at an angular distance  $\varphi_{0,i}$  from its pericenter  $P_{c,i}$ . In this case, the bodies in the layer will be located in a 3D region remote from the pericenter radius  $R_p$  to the apocenter radius  $R_a$ .

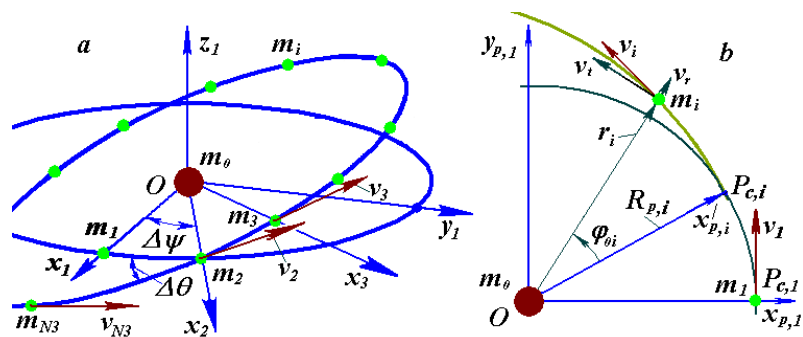


**Figure 1.** Geometric and kinematic characteristics of a single-layer axisymmetric structure comprising  $N_3$  bodies, with a central body of mass  $m_0$  and peripheral bodies of mass  $m_i = m_1$ : (a) rotations of bodies and their velocities through angles  $\Delta\psi$  and  $\Delta\theta$ ; (b) polar coordinates  $r_i$  and  $\varphi_{0,i}$  of the peripheral body  $m_i$  over a trajectory section; the polar angle  $\varphi_{0,i}$  is reckoned from the orbit pericenter  $P_{c,i}$

This option was used for creating multilayer structures. However, in the study reported in this paper there was no need to use elliptical orbits, therefore all treated structures were created with zero eccentricity.

Let there be  $N_2$  layers in a multilayer structure, enumerated with numbers  $j =$

1, 2, ...,  $N_2$ . Consider the coordinates and velocities of a body in layer  $j$  at its initial on-plane position. The bodies on the ring of layer  $j$  are evenly spaced with an interval  $\Delta\varphi_j = 2\pi/N_{3,j}$ . Those bodies move along orbits with an eccentricity  $e$ . They are located at an angular distance from the pericenters of their orbits (**Figure 1(b)**), which are reckoned from the axis  $x_{p,j,i}$

$$\varphi_{0,j,i} = (i_j - 1) \cdot \Delta\varphi_j, \quad i_j = 1, 2, \dots, N_{3,j}. \tag{1}$$

Note that, in contrast to **Figure 1(b)**, in formula (1) and in subsequent formulas, an additional subscript indicating the layer number  $j$  is introduced.

From the trajectory equation of the peripheral body [18] [33], one can determine the distance of bodies  $r_{j,i}$  from the origin  $O$ , their radial velocity  $v_{r,j,i}$  and the transversal velocity  $v_{t,j,i}$ . Then, in the coordinate system  $x_{p,j,i}y_{p,j,i}z_{p,j,i}$  with the  $x_{p,j,i}$ -axes passing through the pericenter  $P_{c,j,i}$  (**Figure 1(b)**), the coordinates and velocities of the peripheral bodies can be written as

$$x_{p,j,i} = r_{j,i} \cdot \cos \varphi_{0,j,i}; \quad y_{p,j,i} = r_{j,i} \cdot \sin \varphi_{0,j,i}; \quad z_{p,j,i} = 0; \tag{2}$$

$$v_{xp,j,i} = v_{r,j,i} \cdot \cos \varphi_{0,j,i} - v_{t,j,i} \cdot \sin \varphi_{0,j,i}; \tag{3}$$

$$v_{yp,j,i} = v_{r,j,i} \cdot \sin \varphi_{0,j,i} + v_{t,j,i} \cdot \cos \varphi_{0,j,i}; \quad v_{zp,j,i} = 0.$$

As a result of solving the problem of gravitational interaction of bodies in an axisymmetric structure [18] [33] [34], the trajectory equation for a peripheral body in the polar coordinate system  $r_{j,i}(\varphi_{0,j,i})$  is obtained in the form

$$r_{j,i} = \frac{R_{p,j}}{(\alpha_{1,j} + 1) \cdot \cos \varphi_{0,j,i} - \alpha_{1,j}}, \tag{4}$$

where  $R_{p,j}$  is the pericenter radius, *i.e.* the radius of the point on the orbit with the smallest distance to the origin  $O$  in **Figure 1(b)**;

$$\alpha_{1,j} = \mu_{1,j} / (R_{p,j} \cdot v_{p,j}^2); \tag{5}$$

$$\mu_{1,j} = -G(m_{j,0} + m_{j,1} \cdot f_{N_{3,j}}); \tag{6}$$

$$f_{N_{3,j}} = 0.25 \sum_{i_j=2}^{N_{3,j}} \frac{1}{\sin[\pi(i_j - 1)/N_{3,j}]}. \tag{7}$$

In formulas (5)-(7), the following designations are used:  $\alpha_{1,j}$  is the trajectory parameter;  $\mu_{1,j}$  is the interaction parameter; and  $f_{N_{3,j}}$  is the contribution due to the action of  $N_{3,j} - 1$  peripheral bodies on one of the bodies.

Depending on the value of trajectory parameter  $\alpha_1$ , the orbits of peripheral bodies can be circles ( $\alpha_1 = -1$ ), ellipses ( $-1 < \alpha_1 < -0.5$ ), parabolas ( $-1 < \alpha_1 < -0.5$ ), or hyperbolas ( $-0.5 < \alpha_1 < 0$ ). The time of motion of a body along the trajectory also depends on  $\alpha_1$  [18] [33] [34].

Below, four other parameters of the orbit of peripheral bodies will be needed [33] [34]: the orbital period

$$P_j = -\frac{2\pi\alpha_{1,j} \cdot R_{p,j}}{v_{p,j}(-2\alpha_{1,j} - 1)^{3/2}}, \tag{8}$$

the velocity at the pericenter

$$v_{p,j} = \sqrt{\mu_{1,j} / (\alpha_{1,j} \cdot R_{p,j})}, \tag{9}$$

the eccentricity of the orbit

$$e_j = -(1 + 1/\alpha_{1,j}), \tag{10}$$

and the semi-major axis of the orbit

$$a_j = R_{p,j} (2\alpha_{1,j} + 1) / \alpha_{1,j}. \tag{11}$$

The radial velocity of a peripheral body is given by [33] [34]

$$v_{r,j,i} = \pm v_{p,j} \sqrt{(\alpha_{1,j} + 1)^2 - (\alpha_{1,j} + R_{p,j} / r_{j,i})^2}. \tag{12}$$

The radial velocity is positive when the body moves from pericenter to apocenter, and negative when returning back. The transversal velocity is written as [33]:

$$v_{t,j,i} = v_{p,j} \cdot R_{p,j} / r_{j,i} \tag{13}$$

Providing that the masses of the bodies  $m_{j0}$  and  $m_{j1}$ , the pericenter radii  $R_{p,j}$  and the trajectory parameters  $\alpha_{1,j}$  or the eccentricities  $e_j$  are given, expressions (1)-(13) determine the coordinates and velocities of peripheral bodies in all  $N_j$  layers of the flat structure.

In order to be able to vary the structures, the coefficient  $k_\varphi$  of the angle between the bodies in the layer and the coefficient  $k_{\varphi v}$  of the angle of rotation of the velocity vector are introduced, with the help of which these angles can be expressed as

$$\Delta\psi = k_\varphi \cdot \Delta\varphi; \quad \Delta\theta = k_{\varphi v} \cdot \Delta\varphi, \tag{14}$$

where  $\Delta\varphi_j = 2\pi / N_{3,j}$ .

This algorithm will be used to create a multilayer structure consisting of  $N_j$  layers. The orbit of the bodies in a layer is given by the eccentricity  $e$  and the major semi-axis  $a$ . Using expression (10), the trajectory parameter  $\alpha_{1,j}$  is determined by the eccentricity  $e$ , and according to formula (11), the pericenter radius  $R_{p,j}$  can be expressed in terms of the semi-axis of the orbit  $a_j$  as follows:

$$R_{p,j} = a_j \cdot \alpha_{1,j} / (2\alpha_{1,j} + 1). \tag{15}$$

It was shown [33] that with a centrally symmetrical arrangement of bodies in space, the force of the outer layer on the mass inside is zero. On the other hand, the force of action of such a structure on a mass located outside is equal to the force of action of a material point located in the center of the structure and having a mass equal to the mass of this structure. Therefore, for each layer, starting from  $j = 2$ , we assume that its center has a central body with mass  $m_{j0}$  equal to the mass of all bodies inside the layer  $j$ , *i.e.*

$$m_{j,0} = m_{j-1,0} + N_{3,j-1} m_{j-1,1}. \tag{16}$$

As already noted, a flat multilayer structure described by expressions (1)-(16) turns into a spatial one following successive rotations through angles  $\Delta\psi$  and  $\Delta\theta$ . These rotations are to be executed for each layer. The algorithm for applying



these rotations was presented in [20] [21] as variant 4. Therefore, we do not reproduce it here.

In addition to this algorithm, three more operations have been added. The first operation is related with the refinement of the distance between the bodies in one layer (Figure 2(a)). The first peripheral body 1 is located on the  $x$ -axis to be followed by bodies 2, 3, 4, and so on, located at almost identical distances from each other. The last body 99 is not at the same distance from the first body. An algorithm for refining the coefficient  $k_\varphi$  in formula (14) was developed. This algorithm allows one to calculate the angle  $\Delta\psi$  between the bodies so that the distance between the first and the last body be the same as between all other bodies. For this purpose, the coordinates of the body with number  $N_{3,j} + 1$  are calculated. If these coordinates coincide with the coordinates of the first body, then the distance between the bodies  $N_{3,j}$  and 1 will be the same as the distance between the other bodies. The calculation is performed by the method of successive approximations until a relative change in the coefficient  $k_\varphi$  of the specified accuracy EPS is reached. As a rule, the coefficient  $k_\varphi$  for six iterations is determined with a relative accuracy  $\text{EPS} = 1 \times 10^{-10}$ .

The second operation is related to the correction of the position of bodies at the points of self-intersection of their initial location line (Figure 2(b)). For this purpose, the number  $N_3$  of bodies in the layer is calculated so that the body on the line crossing the gap between two bodies is approximately at the same distance from them. We denote the average distance between bodies as  $d_m$ , and the minimum distance between the bodies  $i_1$  and  $i_2$  as  $d_{mn}$ , where the bodies  $i_1$  and  $i_2$  are located on different parts of the initial location line. Then, the length of this line is

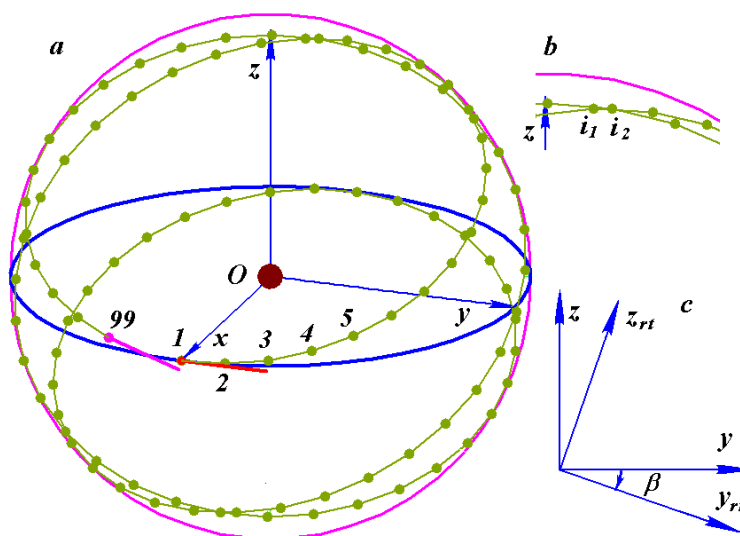


**Figure 2.** Arrangement of 99 bodies in one layer at  $k_\varphi = 1.7$  and  $k_{\varphi v} = 1$  in the  $xyz$  coordinate system: (a) in the uncorrected layer, the distance between the 99<sup>th</sup> body and body 1 differs from the distances between other bodies; the segments show the velocity vectors of the 1<sup>st</sup> and 99<sup>th</sup> body; (b) correction of distances in the regions of self-intersection of the layer; (c) rotation of the layer through an angle  $\beta$ .

$$l_0 = N_3 d_m, \tag{17}$$

and the distance from the  $x$ -axis, on which the body with number  $i = 1$  is located, to the body with number  $i_1$  is

$$l_1 = (i_1 - 1) d_m. \tag{18}$$

The distance to the body with number  $i_2$  will be greater by  $d_{mn}$ :

$$l_2 = (i_1 - 1) d_m + d_{mn}. \tag{19}$$

Suppose that, with a new number of bodies  $N'_3$ , the body  $i_2$  is located in the middle between the bodies  $i_1$  and  $i_1 + 1$ , so that the distance to this body is

$$l'_2 = (i_1 - 1) d'_m + 0.5 d'_m = d'_m (i_1 - 0.5). \tag{20}$$

Since the length of the initial location line  $l_0$  remains unchanged, then  $l'_2$  equals  $l_2$ ; from here, taking into account formula (17) for  $d'_m$ , we obtain a new number of bodies in the layer:

$$N'_3 = \frac{N_3 (i_1 - 0.5)}{i_1 - 1 + d_{mn}/d_m}. \tag{21}$$

The new amount of bodies  $N'_3$  calculated by formula (21) must be rounded up to the nearest integer number. As a rule, the new number of bodies thus obtained makes it possible to increase the minimum distance  $d_{mn}$  between the bodies  $i_1$  and  $i_2$  (**Figure 2(b)**) to acceptable values.

The third operation consists in the uniform rotation of the layers, starting from the second layer, in clockwise direction around the  $x$ -axis through an angle  $\beta_j$  (**Figure 2(c)**). The coordinate axes of the rotated layer are denoted as  $y_r z_{rt}$ . The projections onto the axes of the  $yz$  coordinate system are

$$y = y_r \cos \beta + z_r \sin \beta; \quad z = -y_r \sin \beta + z_r \cos \beta. \tag{22}$$

The angle of rotation of the  $j$ -th layer is given by the expression

$$\beta_j = (j - 1) \cdot \Delta\beta, \tag{23}$$

where  $\Delta\beta = 2\pi/N_2$ .

### 3. Software for Creating Multilayer Structures

For performing multiple calculations when creating a multilayer spherical structure, an MLSpStr2.for program has been developed. This program consists of three parts implementing the following operations: 1) reading the initial parameters; 2) construction of the multilayer structure; 3) creating a file with initial conditions for the Galactica system.

In the present paper, a dimensional/non-dimensional method of treating data is used. When setting values of structural parameters, the Solar system is used as an analogue providing parameter ratios. After the structure is created, its dynamics and evolution are analyzed in dimensionless form. The results are discussed in dimensional form with parameter values inherent to globular star clusters.

The main initial parameters are read from the data file MLSpStr2.dat. In this file, the following structural parameters are specified:  $N_2$  is the number of layers;  $N_{30}$  is the initial number of peripheral bodies in the first layer;  $mi$  is the initial mass of the central body and all first-layer bodies;  $p_{m0}$  is the fraction of the mass  $mi$  due to the central body;  $A_{sm}$  is the semi-axis of the orbits of first-layer peripheral bodies in astronomical units (AU);  $e$  is the eccentricity of the orbits of peripheral bodies;  $k_a$  is the coefficient of the semi-axes of the layers, starting from the second layer;  $k_{N3}$  is the coefficient of the number of bodies on these layers;  $k_{\varphi 0}$  and  $k_{\varphi v}$  are the coefficients of the initial angles of bodies and their velocities when constructing the structure; EPS is the allowed error in calculating  $k_{\varphi}$  for the body's angle;  $I_{nx}$  is the key for initiating the uniform rotation of layers around the  $x$ -axis;  $I_{cm}$  is the key for issuing the coordinates and velocities of peripheral bodies in the information file MLSpStr2Err; and  $\rho_b$  is the absolute density of bodies. Note that the density of bodies  $\rho_b$  expressed in  $\text{kg}/\text{m}^3$  is necessary for calculating their radii. The radii of bodies are used in the Galactica program when calculating the inter-body collisions. The MLSpStr2.dat file also specifies a number of other parameters required for Galactica.

The above-listed data completely determine the parameters of the central body and first-layer bodies. The semi-axis of the orbits of the rest layers is calculated as

$$a_j = A_{sm} \cdot AU \cdot (1 + k_a (j-1)), \quad (24)$$

where AU is the astronomical unit, and the number of bodies in a layer is determined in proportion to the semi-axis of the orbit:

$$N_{3,j} = N_{3,1} \cdot k_{N3} \cdot (a_j / a_1). \quad (25)$$

The masses of peripheral bodies are identical in each layer. This mass is calculated from the difference between the mass  $m_j$  and the central-body mass, and from the number of bodies  $N_{3,1}$ .

After reading the initial parameters of the structure, the algorithm presented above calculates the coordinates and velocities of all bodies involved. Calculation results are issued in the form of three output files: fN3fvout.dat, MLSpStr2Err and, for example, MS15c49b.dat. The file fN3fvout.dat contains the layer numbers  $j$ , the number  $N_{3,j}$  of bodies, the coefficients  $k_{\varphi j}$  and  $k_{\varphi v j}$ , the semi-axes  $a_j$  expressed in meters, and the mass  $m_j$  of one peripheral body in kg.

In the MLSpStr2Err file, for each layer, the period  $P_j$  in sidereal years, the number of bodies  $N_{3,p}$ , the average distance between bodies  $d_m$  in meters, the minimum distance  $d_{mn}$  between the bodies  $i_1$  and  $i_2$  at the point of intersection of their location line with indication of their numbers  $i_1$  and  $i_2$  are output. The distance between bodies 2 and 3 is output as  $d_m$ . In addition, the number of iterations in the calculation of coefficient  $k_{\varphi j}$  and the two last values of this coefficient are indicated.

Then, the summary information for all layers is given, including the minimum distance between the bodies in the entire structure with indication of the

layer and body numbers; the dimensionless coordinates and velocities of the center of mass of the entire system, and the first body in the first layer. For the center of mass, these values should be zero, and their non-zero values indicate the level of error in creating the system. For example, for a fifteen-layer structure MS15c49b.dat with the number of bodies  $N = 5866$ , the values of interest are at the level of  $2 \times 10^{-17}$  when the program is compiled with double precision, *i.e.* when the number length is 16 significant digits. This level of error indicates that the error is in fact extremely low.

At the end of this file, the initial data specified in the MLSpStr2.dat file are output. Thus, the MLSpStr2Err file is a kind of a passport of the created structure: it contains all necessary information about it.

Additionally, in the MLSpStr2Err file the coordinates and velocities of all bodies in the layers in dimensional form are output when the key Icm in the initial data file MLSpStr2.dat is set to 1. The MLSpStr2Err file is also intended for issuing error messages when the MLSpStr2.for program is running. When an error occurs, its decryption is written to this file.

Based on the initial data specified in the MLSpStr2.dat file, a structure is created, with the desired dimensions of layers and the number of bodies in them, according to the algorithm (24)-(25). In creating structures with a different algorithm, an additional source data file fN3fvinp.dat is used. The latter file specifies the layer numbers  $j$ , the number of bodies  $N_{3,j}$ , the coefficients  $k_{\varphi,j}$  and  $k_{\varphi v,j}$ , the semi-axes  $a_j$  in meters, and the mass of one peripheral body  $m_j$  in kg. Based on these data, a multilayer structure is created. In this case, the mass of the central body is calculated based on the initial data file MLSpStr2.dat. Providing that a source data file fN3fvinp.dat is available, the MLSpStr2 program creates a structure from the data contained in this file; otherwise, algorithm (24)-(25) is used for this purpose.

The file of initial conditions for the Galactica program, for example, MS15c49b.dat, contains the masses, the coordinates, the velocities, and the radii of bodies, as well as a number of other parameters necessary for calculating the system dynamics and evolution. The Galactica system [23] [25] makes it possible to calculate the dynamics of a multilayer structure and study its evolution in time. In addition, Galactica is used to accomplish the creation of the structure. According to the algorithm presented above, a structure is created in which bodies in the layers are organized in a certain order. After their interaction for some time, the bodies will become evenly distributed over space. For implementing this distribution, the Galactica system is used.

A file of initial conditions such as MS15c49b.dat uses dimensionless values [25]. All body masses in it are related to the total mass of the system  $m_s$ . Time  $T$  is expressed in hundreds of periods of revolution  $P_1$  of first-layer bodies, where the periods  $P_1$  are determined from the initial data according to formula (8). For this, the time factor

$$k_t = 1/(100 \cdot P_1) \quad (26)$$

is introduced. The geometric dimensions in the Galactica program are related to the quantity

$$A_m = \left( G \cdot m_{ss} / k_t^2 \right)^{1/3}, \quad (27)$$

where  $G$  is the gravitational constant.

The program Galactica integrates the differential equations for bodies that interact according to the Newton law of gravitation. For example, in dimensionless form these equations as projected onto the  $x$ -axis look as follows:

$$\frac{d^2 x_j}{dT^2} = - \sum_{k \neq j}^N \frac{m_{o,k} (x_j - x_k)}{r_{jk}^3}, \quad j = k = 1, 2, \dots, N, \quad (28)$$

where  $x_j = x_{C,j} / A_m$  is the dimensionless coordinate of the  $j$ -th body;  $x_{C,j}$  is the dimensional coordinate of the  $j$ -th body relative to the center of mass of the entire structure, and  $m_{o,k} = m_k / m_{ss}$  is the dimensionless mass of the  $k$ -th body.

As already noted, the Galactica system, with a set of necessary tools for solving problems, is available in free access. Its description is presented in the GalDiscrp.pdf file in Russian, and in the GalDiscrpE.pdf file in English. The MLSpStr2 program, the data file MLSpStr2.dat, and the structure files mentioned here are available<sup>2</sup>.

#### 4. First Five-Layer Structures

When creating a structure, one must decide on the choice of parameters specified in the MLSpStr2.dat file. Some of these parameters were identified during the creation and study of single-layer spherical structures [20] [21]. The structures considered below have the following dimensional parameters: the initial mass of the central body and first-layer bodies is equal to the Solar-system mass  $m_i = 1.99179 \times 10^{30}$  kg, with the mass fraction due to the central body being  $p_{m0} = 0.99$ ; the semi-axis length of first-layer bodies is equal to one astronomical unit, *i.e.*  $a_1 = 149.595$  million km. In this case, the period of revolution of first-layer bodies is  $P_1 = 1$  sidereal year. The rest parameters are as follows:  $A_{sm} = 1$ ;  $e = 0$ ;  $k_a = 1$ ;  $k_{N3} = 1$ ;  $k\varphi = 2.83$ ;  $k_{qv} = 1$ ;  $EPS = 1 \times 10^{-10}$ ; and  $\rho_b = 5 \cdot 10^3$  kg/m<sup>3</sup>. Note that the body masses are in the following correspondence to the masses of Solar-system bodies:  $m_0 = 0.991m_s$  and  $m_1 = 0.354m_{sa}$ , where  $m_s$  is the mass of the Sun, and  $m_{sa}$  is the mass of Saturn. The five-layer structures with these parameters, shown in **Figure 3**, are created with a uniform rotation of the layers around the  $x$ -axis, that is, with the key  $I_{nx} = 1$ .

According to formula (24), the sizes  $a_j$  of the layers in the five-layer structure MS05c99d.dat increase with each layer by the semi-axis of the orbit of first-layer bodies, and, according to formula (8), their periods  $P_j$  are equal to 2.80; 5.07; 7.66; and 10.46 periods of first-layer bodies. According to formula (25), the numbers of bodies in the layers, 99, 198, 297, 396, and 495, also increase by the number of bodies in the first layer. The total number of bodies is  $N = 1486$ . In **Figure 3(a)**, the segments show the velocity vectors of the 2<sup>nd</sup> and 1486<sup>th</sup> body.

<sup>2</sup><http://wgalactica.ru/smul1/smulski/Data/MLSpStr/>

Unlike in **Figure 1** and **Figure 2**, here the enumeration of bodies begins from the central body ( $m_1$ ), with the first body in the first layer designated as  $m_2$ . At the point of self-intersection of the line of formation of layers 2 and 4, the distance between bodies was respectively 66 and 14 times shorter than the average distance between bodies. Therefore, when calculating the motion of bodies in the structure using the Galactica system, intense collisions of bodies and their merging began at these places. **Figure 3(b)** shows the configuration of the structure at time  $T = 1.01$ , *i.e.*, after 101 revolutions of first-layer bodies. There happened 91 collisions in this structure, while 88 bodies have acquired double masses, one a triple mass, and one body experienced a collision with the central body.

**Figure 3(c)** shows the distribution of relative body distances  $r_{r1}$  from the center of mass depending on the body numbers  $k = 1, 2, \dots, N$  at time  $T = 1.01$ . The lines show the distances  $r_{r1}$  at  $T = 0$ . These distances are normalized by the semi-axis of the orbits of first-layer bodies  $a_1$ , *i.e.*  $r_{r1} = r/a_1$ . As it is seen, the greatest distance of one of the bodies reaches  $20a_1$ . The points on the horizontal axis indicate the numbers of bodies that have merged with other bodies. It is seen that there are empty regions, or voids, in the 2<sup>nd</sup> and 4<sup>th</sup> layers, *i.e.*  $r_{r1} = 0$ . In these places, there were small distances between bodies at the intersections of their location line. Therefore, at these places intense collisions of bodies occurred during their interaction.

In order to exclude such collisions, an MS05c99c.dat structure was created, in which the numbers of bodies  $N_{3,2}$  and  $N_{3,4}$  in layers 2 and 4 were corrected according to formula (21); as a result, the layers have become incorporating one additional body. Therefore, the total number of bodies in this structure (**Figure 3(d)**) has become  $N = 1488$ . In general appearance, this structure differs little from the previous one (see **Figure 3(a)**).

It should be noted that algorithm (21) for correcting the number of bodies  $N_{3,j}$  in a layer is not included in the MLSpStr2.for program. Therefore, new numbers of bodies in layers must be entered using an additional file fn3fvinp.dat.

When calculating the motion of bodies in this structure for time  $T = 1.05$ , *i.e.*, for almost the same period as in the case of the previous structure, the number of collisions was found to equal 38. Thus, the elimination of the minimum distances in the second and fourth layers has led to a reduction in collisions by 2.4 times. During the time  $T = 1.95$  (**Figure 3(e)**), there were 44 collisions in total. In this case, 40 double-mass bodies were formed, and one body had acquired a quadruple mass. In addition, there was one collision with the central body. Thus, during the second time interval  $\Delta T = 0.9$ , there occurred a total of six collisions. In the latter structure (**Figure 3(e)**), the bodies are more uniformly distributed over space than in the previous structure shown in **Figure 3(b)**.

**Figure 3(f)** shows the distribution of relative body distances for the second structure. The spread of distances in this structure is much smaller than in the previous one (**Figure 3(c)**). The greatest distance of one of the bodies is  $13a_1$ . There are also no voids in the region of the 2<sup>nd</sup> and 4<sup>th</sup> layers.

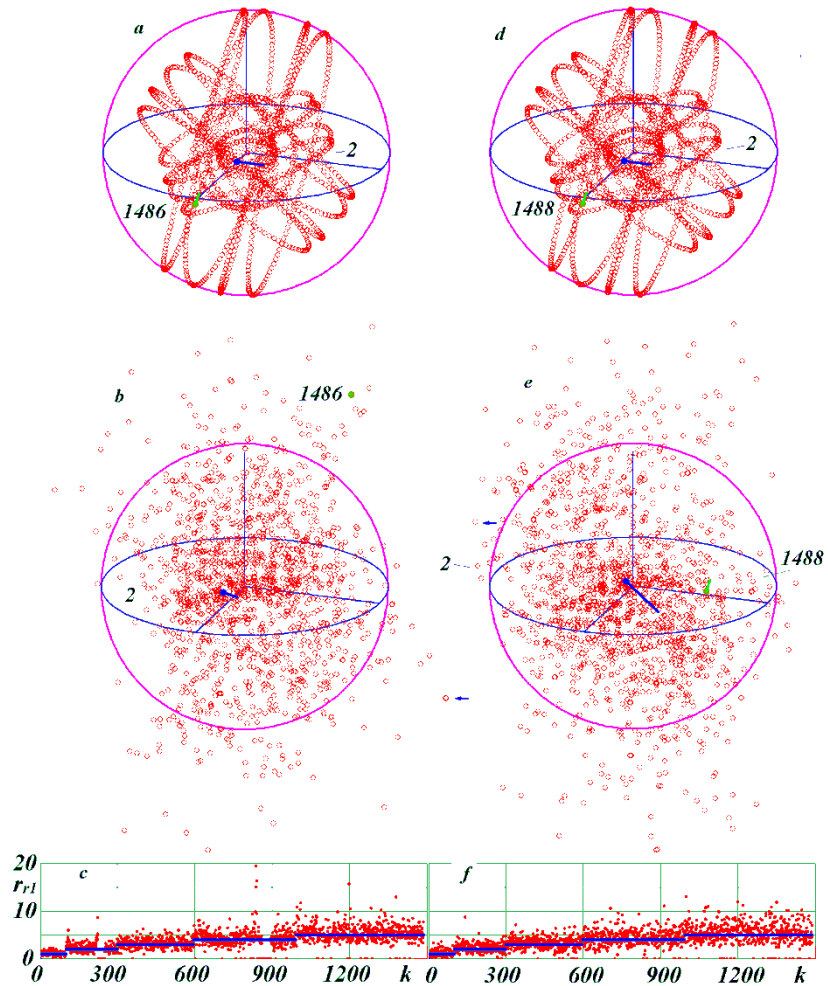


**Figure 3.** Two five-layer structures at the beginning ((a), (d)) and by the end of the interaction ((b), (e)) of their constituent bodies: (a)-(c) MS05c99d.dat; (d)-(f) MS05c99c.dat; the first body of the first layer  $m_2$  is on the  $x$ -axis; the velocity vectors of bodies  $m_2$  and  $m_N$  are shown as segments; the lines in the graphs (c) and (f) show the body distances  $r_{i1}$  from the center of mass at time  $T=0$ .

For the two structures considered above, the problems of interaction of bodies were calculated in the Galactica system with a step  $dT = 1 \times 10^{-7}$ . Files with kinematic parameters of the structures were issued after  $K13 = 1 \times 10^5$  steps. This number of steps corresponded to the time interval  $\Delta T = 0.01$ , which was equal to the period of revolution of first-layer bodies. For the structure MS05c99d.dat, 101 files were issued, and for the structure MS05c99c.dat, 195 files.

## 5. Evolution of the Five-Layer Structure

### 5.1. General Changes

In the structures shown in **Figure 3**, the layers were successively rotated about the  $x$ -axis; as a result, these structures became asymmetric. In this connection, the MS05c99e.dat structure was created with the same parameters as the MS05c99c.dat structure, but without the rotation of layers, that is, with the pa-

parameter  $I_{nx} = 0$ . As evident from **Figure 4(a)**, the former structure is more symmetrical. It has  $N = 1488$  bodies, and the layer parameters in it are the same as in the MS05c99c.dat structure. After 196 revolutions of first-layer bodies, that is, at  $T = 1.96$ , the structure under consideration (see **Figure 4(b)**) also proved to be more symmetrical than the previous configuration (**Figure 3(e)**). However, the spread of body distances  $r_{r1}$  in it (**Figure 4(c)**) is somewhat greater than in the previous structure (**Figure 3(f)**). The greatest distance of a body from the center of mass is  $r_{r1max} = 15.7$  in comparison with  $r_{r1max} = 13.1$  in the previous structure. It also exhibits slightly more collisions, namely, 46, compared with the previous structure with 44 collisions. Note that body 1434 exhibits the greatest distance from the center of mass  $r_{r1max} = 15.7$ .

The dynamics of inter-body collisions in the structure under consideration is shown in **Figure 4(d)**. By the time  $T = 1.96$ , 40 bodies with a double mass and 3 bodies with a triple mass have formed in this structure. As it is seen from **Figure 4(d)**, collisions occur more frequently during the initial time interval of  $T < 0.5$ , and less frequently during the interval  $T > 0.7$ . Initially, the rate of collisions is equal to  $v_{imp} = 64$  collisions per 100 revolutions of first-layer bodies and, then,  $v_{imp} = 8$ . That is, the rate of collisions has decreased by eight times. If we relate the rate of collisions to the number of bodies, then in the last section it will be  $v_{imp1} = v_{imp}/N = 5.4 \times 10^{-3}$ .

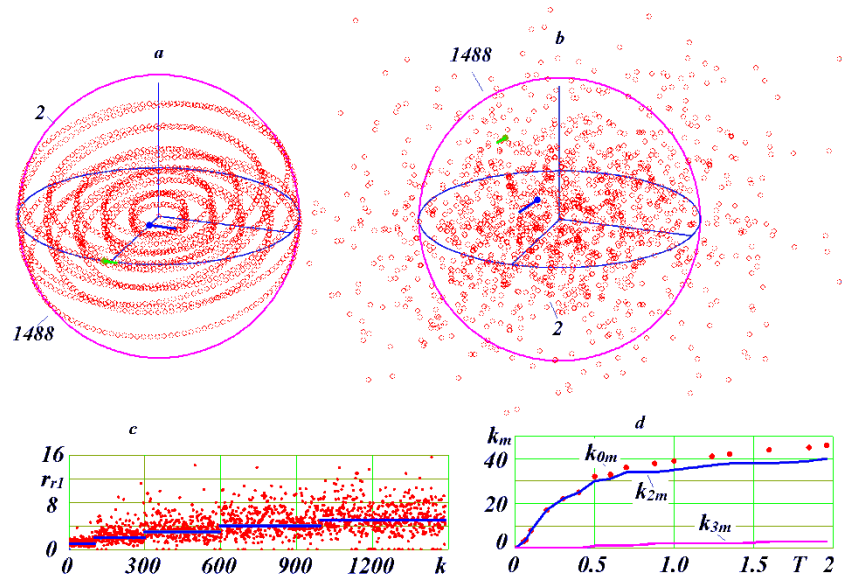


**Figure 4.** Layer structure MS05c99e.dat without layer rotations. (b) at time  $T = 1.96$ . Part (d) of the figure shows the dynamics of collisions:  $k_{0m}$  is the number of collisions;  $k_{2m}$  is the number of formed bodies with a mass of  $2m_1$ ;  $k_{3m}$  is the number of formed bodies with a mass of  $3m_1$ . For the rest designations see **Figure 3**.

From the visual analysis of the structures, it follows that the remains of their initial organization shown in **Figure 4(a)** still persist by the time  $T = 0.1$ , whereas by the time  $T = 0.2$  they are no longer observed. That is why we can assume



that, from the latter moment, a structure with a disordered arrangement of bodies has been created, with its appearance changing little in the future. When the rate  $v_{imp}$  reaches the second stage of its change, we can assume that the dynamics of the structure has passed into the stable phase of its existence.

### 5.2. Trajectories of Individual Bodies

The trajectories of bodies in different layers were studied: that of first-layer body 2, that of third-layer body 401, and those of bodies 1434 and 1488 in the last layer. The study was carried out for two time intervals, initial  $T = 0 - 0.15$  (Figure 5(a), Figure 5(b)) and final  $T = 1.81 - 2.11$  (Figures 5(c)-(e)).

Over the initial time interval, body 2 first moves in a circle (see Figure 5(a)) with a period  $P_1 = 0.01$ . Its orbit lies in the  $xy$ -plane. Over time, the orbit becomes elliptical, and the period of revolution increases slightly. Over a finite time interval (Figure 3(c)), the orbital eccentricity of body 2 increases to  $e = 0.385$ , but the dimensions of the orbit show a decrease, and the period also decreases and becomes shorter than 0.01. In the 3D graph of Figure 5(e), it is seen that the orbit of body 2 rotates in space, and with each revolution of this body

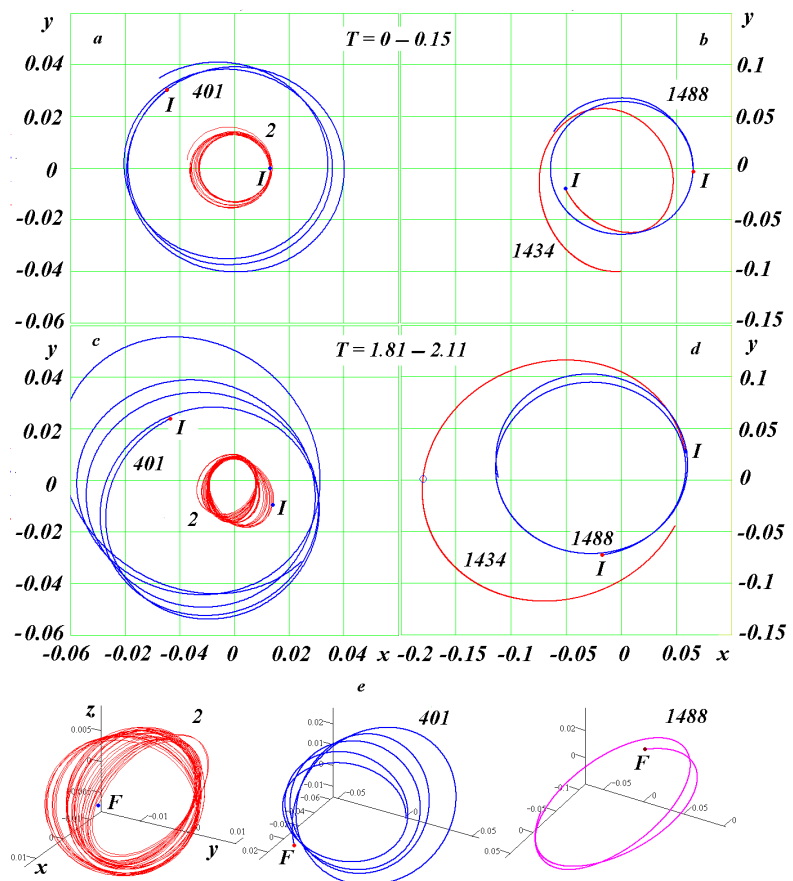


**Figure 5.** Trajectories of bodies 2, 401, 1434, and 1488 over the initial ((a), (b)) and final (c)-(e) periods of evolution of the MS05c99e.dat structure: *I* and *F* are the initial and final points of the trajectories; (e) three-dimensional images of the trajectories; the circle in image (d) shows the position of body 1434 at time  $T = 1.96$ .

around the center of mass, this body departs farther and farther from the  $xy$ -plane.

The orbit of body 401 over the initial time interval (**Figure 5(a)**) during the first revolution of the body is approximately a circle with a period of  $P_2 = 0.028$ . Then, the trajectory becomes elliptical, and the period of revolution increases slightly. Over a finite time interval (**Figure 5(c)**), the eccentricity reaches a value  $e = 0.373$ , the orbit size increases, and the period reaches  $1.25P_2$ . As it is seen from **Figure 5(e)**, here the orbit rotates in space with each body revolution.

The orbit of body 1488, the last body in the fifth layer, over the initial time interval (**Figure 5(b)**) is a circle with a period of revolution  $P_5 = 0.1046$ . Over the final time interval (**Figure 5(d)**), the orbit is already elliptical with an eccentricity  $e = 0.349$ , and the period has increased by a factor of 1.6. From **Figure 5(e)**, it is evident that the orbit of body 1488 changes in space little during this time.

**Figure 5(b)** shows that during the first revolution the orbit of the most distant body 1434 exhibits notable changes. Over the final time interval (**Figure 5(d)**), the orbit is already an ellipse with an eccentricity  $e = 0.491$  and a period of 0.30, while the initial period of revolution of five-layer bodies is 0.1046. That is, here the period has increased three-fold.

It should be noted that the orbits are exactly ellipses, parabolas and hyperbolas only in the two cases: 1) the interaction involves two bodies, and 2) the interaction involves  $N$  bodies located axisymmetrically on one plane [18]. That is why under an elliptic trajectory we mean a trajectory bounded in space, while under hyperbolic and parabolic trajectories we understand infinite trajectories. In the latter case, the velocity of a body on a parabolic trajectory tends to zero at infinity.

### 5.3. Dynamics of Encounters of an Individual Body with Other Bodies

Changes in the orbit of body 1434 occur when this body approaches other bodies. The approaches of body 1434 over the initial time interval are shown in **Figure 6**. Plotted on the vertical axis are the numbers of bodies  $k$  to which the body  $i = 1434$  comes in proximity. Such bodies are marked with points or with

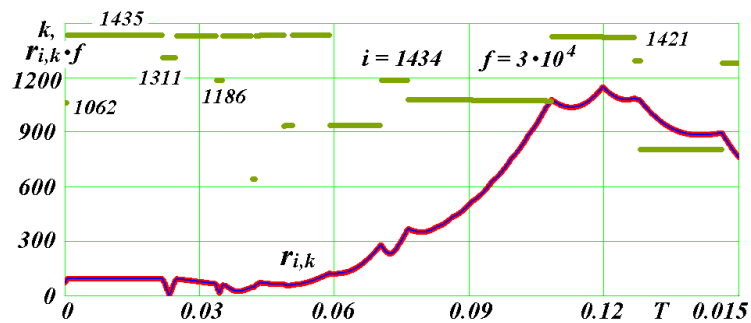


**Figure 6.** Approach of body  $i = 1434$  by bodies  $k$  to a distance  $r_{i,k}$  for the number of integration steps  $KI3 = 3000$  made with a time step of  $dT = 1 \times 10^{-7}$  over the initial time interval  $T = 0 - 0.15$ . The dimensionless distance  $r_{i,k}$  in the graph is increased by  $f = 3 \times 10^4$  times.

horizontal segments if the points overlap. Also indicated on the vertical axis is the distance  $R_{ik}$  at the moment of approach of body 1434 to body  $k$ . The distance  $R_{ik}$  is increased by the factor  $f$ . The distance  $R_{ik}$  is defined as the minimum distance of a body  $i$  from other bodies over the number of integration steps KL3, where KL3 is a parameter of the Galactica system. In the case under consideration, the integration was performed with a step  $dT = 1 \times 10^{-7}$ .

As it follows from **Figure 6**, at the initial time  $T = 0$  body 1434 passes at a distance of  $2.40 \times 10^{-3}$  from body 1062, which is at the intersection of the initial location line. In this case, the distance between the bodies on this line is  $3.17 \times 10^{-3}$ , that is, of the same order.

Then, body 1434 moves with an almost constant distance to the neighboring body 1435 until the time  $T = 2.16 \times 10^{-2}$ ; and then at time  $T = 2.32 \times 10^{-2}$  it approaches body 1311 to a distance  $R_{ik} = 1.66 \times 10^{-4}$ . The latter distance corresponds to 90 radii of the body. Then, at time  $T = 3.44 \times 10^{-2}$  the body approaches body 1186 to a distance of  $R_{ik} = 5.84 \times 10^{-4}$ . These two approaches lead to a significant change in the trajectory of the body of interest, with its orbit becoming elliptical. The body moves away from all bodies to a distance  $R_{ik} = 3.83 \times 10^{-2}$  from the nearest body 1421 at time  $T = 0.12$ . This is the most distant point of its orbit, after which body 1434 starts approaching the center of the structure again. At this point, the distance of body 1434 from the center is  $r = 0.109$ .

As a result of subsequent interactions, the orbital eccentricity increases in magnitude, and at the apocenter by the time  $T = 1.96$  (**Figure 5(d)**) the body moves away from the center to a distance  $r = 0.205$ , which value is 3.14 times greater than the initial size of the structure.

#### 5.4. Determining the Trajectory Parameters of a Distant Body

When considering the results of calculations for the motion of bodies in the structures shown in **Figure 3(b)**, **Figure 3(d)**, and **Figure 4(b)**, it becomes necessary to determine the type of motion of remote bodies. This allows one to determine whether such a body is a body of this structure or it is a body ejected out of it. For solving this problem, it is necessary to perform a special study of the trajectory of such body. Consider a method based on the results of the two-body problem, which will give an answer to the question of interest without performing special studies.

For a body remote from the structure, we can assume that it is affected by the entire structure with mass  $m_{ss}$  located in its center of mass. Then, similarly to (5), the parameter of the body trajectory will be

$$\alpha_1 = \mu_1 / (R_p \cdot v_p) \quad (29)$$

where  $R_p$  and  $v_p$  are the pericenter radius of the body and its velocity in pericenter, and the interaction parameter is  $\mu_1 = -Gm_{ss}$ . As a result of calculations made using the Galactica program, we obtain the coordinates  $x, y, z$  and the velocities  $v_x, v_y, v_z$  of the body in the center-of-mass system. From the definition of the scalar product of the radius vector  $\mathbf{r}$  of the body and its velocity vector  $\mathbf{v}$ , we

can write

$$xv_x + yv_y + zv_z = r \cdot v \cdot \cos \beta_1, \tag{30}$$

where  $\beta_1$  is the angle between the vectors  $\mathbf{r}$  and  $\mathbf{v}$

$$r = \sqrt{x^2 + y^2 + z^2}; \quad v = \sqrt{v_x^2 + v_y^2 + v_z^2}.$$

Then, from formula (30) we obtain the following expression for the angle  $\beta_1$ :

$$\cos \beta_1 = \frac{xv_x + yv_y + zv_z}{r \cdot v} \tag{31}$$

The radial velocity  $v_r$  is directed along the radius vector  $\mathbf{r}$ , and the transversal velocity  $v_p$  in the direction perpendicular to the latter velocity, so that

$$v_r = v \cdot \cos \beta_1; \quad v_t = v \cdot \sin \beta_1. \tag{32}$$

On the other hand, according to the two-body problem [33] [34], the radial and transversal velocities, similarly to (12) and (13), can be written as follows:

$$v_r = \pm v_p \sqrt{(\alpha_1 + 1)^2 - (\alpha_1 + R_p/r)^2}; \quad v_t = v_p \cdot R_p/r. \tag{33}$$

Equating the right-hand sides in the velocity  $v_t$  from formulas (32) and (33), we obtain the pericentric velocity

$$v_p = \frac{v \cdot r \cdot \sin \beta_1}{R_p}, \tag{34}$$

and excluding the velocity  $v_r$  from formulas (32) and (33) with taking into account formula (34), we obtain the expression

$$R_p \cos \beta_1 = r \sin \beta_1 \sqrt{(\alpha_1 + 1)^2 - (\alpha_1 + R_p/r)^2}. \tag{35}$$

Three Equations (29), (34) and (35) include three parameters  $\alpha_1$ ,  $R_p$ , and  $v_p$ . As a result of successive substitutions and solutions of quadratic equations, the pericenter radius is obtained in the following form:

$$R_p = \frac{\mu_v \pm \sqrt{\mu_v^2 + r^2 \sin^2 \beta_1 (1 + 2\mu_v/r)}}{1 + 2\mu_v/r} \tag{36}$$

where the designation  $\mu_v = \mu_1/v^2$  is introduced. The quantity  $\mu_v$ , which is measured in meters, is negative,  $\mu_v < 0$ . Expression (36) gives two values of  $R_p$ : with the “-” sign in the case of an elliptical orbit we obtain the apocenter radius  $R_a$ , and in the case of “+”, the pericenter radius  $R_p$ .

Given the pericenter radius  $R_p$ , the pericenter velocity  $v_p$  can be found using expression (34). In the case of  $v_p > 0$ , the orbit is passed counterclockwise. Then, formula (29) can be used to calculate the trajectory parameter  $\alpha_1$ , and formula (10) yields the orbital eccentricity  $e$ . In accordance with formula (4), these parameters make it possible to determine the trajectory of the body, as well as the time of motion along it [33] [34].

In the case of a parabolic or hyperbolic orbit, the velocity at infinity can be calculated as follows:

$$v_{\infty} = v_p \sqrt{2\alpha_1 + 1} \quad (37)$$

For a hyperbolic orbit, the apocenter radius  $R_a$  calculated using expression (36) with the “-” sign turns out to be negative.

For body 1434, the parameters calculated by this algorithm for time  $T = 1.96$  have the following values:  $R_p = 0.0694$ ,  $v_p = 4.638$ ,  $\alpha_1 = -0.669$ ,  $e = 0.494$ ,  $R_a = 0.2049$ , and  $v_a = 1.572$ . Since for an elliptical orbit we have:  $-0.5 > \alpha_1 > -1$ , the trajectory of body 1434 is an ellipse. At time  $T = 1.96$ , the body is at a distance  $r = 0.2049$  and has a velocity  $v = 1.572$ . These parameters coincide with the parameters of the apocenter. As it is seen from **Figure 5(d)**, body 1434 shown with a circle is indeed located at the most distant point of the trajectory from the center, that is, at its apocenter. Therefore, algorithm (29)-(37) presented above can be used to estimate the trajectory of a remote body from its coordinates and velocity at some point in time.

## 6. Evolution of the Ten-Layer Structure

### 6.1. General Changes

Due to the fact that in the structure with layers rotated around the  $x$ -axis (**Figure 3(d)**) there were slightly fewer collisions than in the structure without rotations (**Figure 4(a)**), we have decided to create 10- and 15-layer structures with rotated layers. Such a ten-layer structure is shown in **Figure 7(a)**. The initial parameters of this structure in the MLSpStr2.dat file are the same as those of the structure in **Figure 3(d)**, except for the number of layers, which is set to  $N_2 = 10$ . All close encounters at the self-crossings of the formation line are eliminated. The number of bodies in the layers varies from 99 in the 1st layer to 991 in the 10<sup>th</sup> layer, the semi-axis varies from  $a_1 = 0.0118$  to  $a_{10} = 0.1179$ , and the period, from  $P_1 = 0.0100$  to  $P_{10} = 0.2536$ . The total number of bodies is  $N = 5451$ .

In the previous cases, the calculation of bodies' motion implemented with the help of the Galactica program was carried out with a time step  $dT = 1 \times 10^{-7}$ . At this step, the calculation time for the interval  $\Delta T = 0.01$ , which is equivalent to one revolution of first-layer bodies lasted for 7 hours. For a ten-layer structure with  $N = 5451$ , the calculation time of this interval took 97 hours. For solving the problem over the required time interval, the duration of calculation will exceed one year. Therefore, the solution of problems with such a number of bodies was performed with a step of  $dT = 10^{-6}$  in automatic step selection mode, which can be launched in the Galactica system using the key  $K14 = 3$ . Since the results of calculation are issued following a certain number of integration steps, in the latter case the time interval between these results may be different.

It should be noted that the Galactica system also automatically modifies the step when the bodies approach each other up to a distance of the order of their diameters. These circumstances must be taken into account when analyzing points on the graphs of parameter variation over time.

After 81.5 revolutions of first-layer bodies, *i.e.* at  $T = 0.815$ , the structure is shown in **Figure 7(b)**. By the time  $T = 0.1$ , elements of the initial organization of

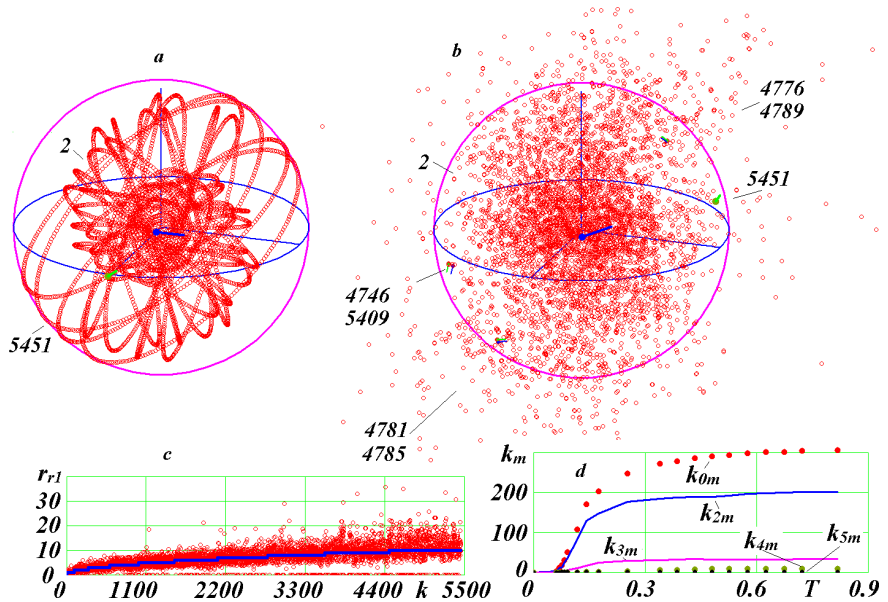


**Figure 7.** The ten-layer structure MS10c99b.dat and its evolution. (b) data at  $T = 0.815$ . Part (d) of the figure shows the dynamics of collisions:  $k_{0m}$  is the number of collisions;  $k_{4m}$  is the number of formed bodies with a mass equal to  $4m_1$ ;  $k_{5m}$  is the number of formed bodies with a mass equal to  $5m_1$ . For other designations, see **Figure 3** and **Figure 4**.

the structure are still preserved, and by the time  $T = 0.2$  they completely disappear. By the time  $T = 0.4$ , the structure acquires a form later showing almost no changes. The scatter of body distances in **Figure 7(c)** is limited to  $40a_1$ . About 30 bodies were ejected over a large distance, the largest of which is  $r_{r1} = 600$  for body 1575.

By the time  $T = 0.815$ , there were 306 collisions, one of which was with the central body. During this period, 202 double-mass bodies, 34 triple-mass bodies, 9 quadruple-mass bodies, and 2 bodies with mass  $5m_1$  were formed. The dynamics of collisions is shown in **Figure 7(d)**. Before the time  $T = 0.061$ , there were no collisions. Then frequent collisions began, with the rate which we will also consider in two regions. On the first interval  $\Delta T = 0.0688 - 0.142$  the rate of collisions is  $v_{imp} = 2158$  collisions per 100 revolutions of first-layer bodies, and on the second interval  $\Delta T = 0.339 - 0.815$  the average rate of collisions is  $v_{imp} = 69.3$ . At the same time, over this time interval there is a tendency towards a further decrease of velocity, possibly to zero at infinity. In this structure, the rate of collisions in the second trajectory section compared with the first section has decreased by 31 times. In this case, the rate of collisions per one body is  $v_{imp1} = 1.27 \times 10^{-2}$ , which value is 2.4 times higher than that in the five-layer structure.

## 6.2. Trajectories of Individual Bodies

**Figure 8** shows the trajectories of the central body 1, first-layer body 57, second-layer body 170, sixth-layer body 1563, and tenth-layer body 5301. These calculations were performed over the interval  $T = 0.663 - 1.021$  with a step  $dT = 1 \times 10^{-7}$ . The trajectory of the central body 1 around the center of mass is irregular

(Figure 8(a)). The three-dimensional appearance of the trajectory is shown in Figure 8(d). Body 1 does not move away from the center of mass to a distance greater than 0.003, which value is 0.23 of the radius of the inner layer.

The orbit of body 57 (Figure 8(b)) continuously rotates in space (Figure 8(e)). The period of revolution of body 57 fluctuates within small limits relative to the period  $1.34 P_1$ , where  $P_1$  is the initial period. The semi-axis of the orbit also oscillates around a value of 0.015. The orbital eccentricity reaches 0.7.

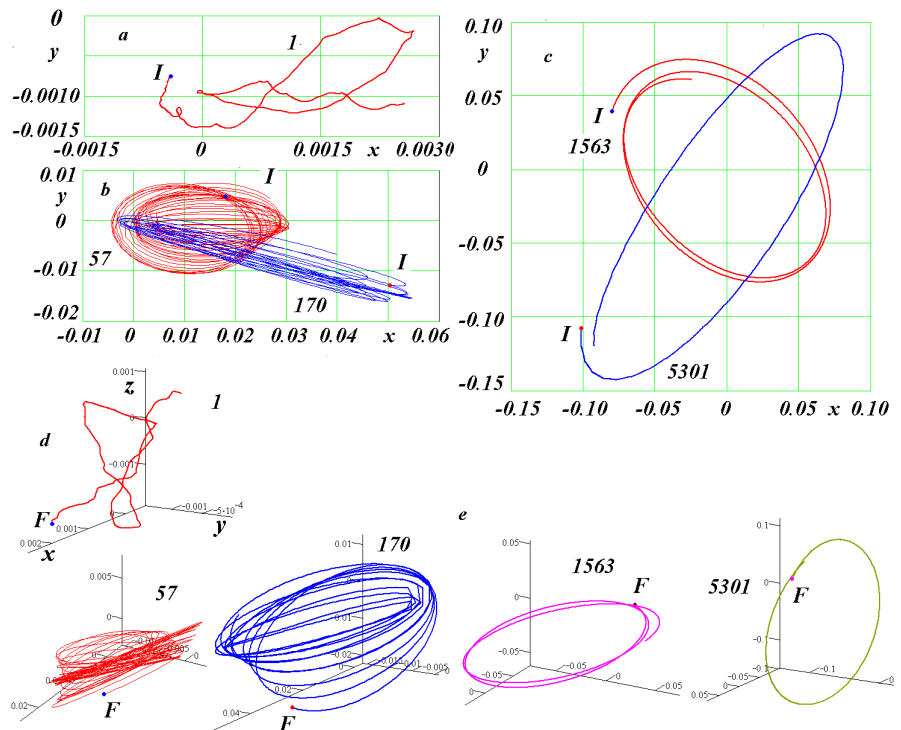


**Figure 8.** Trajectories of the central body 1 and peripheral bodies 57, 170, 1563, and 5301 during the final period ( $T = 0.663 - 1.021$ ) of the evolution of the MS10c99b.dat structure (a)-(c); parts (d) and (e) of the figure show 3D images of the trajectories; and  $I$  and  $F$  are the initial and final points of the trajectories.

The orbit of body 170 is an ellipse with a large eccentricity reaching 0.9 (Figure 8(b)). This orbit also varies in space (Figure 8(e)). The orbital period fluctuates around  $1.16 P_2$ , where  $P_2 = 0.028$  is the initial period.

It should be noted that at the pericenters of the orbits in Figure 8(b) and Figure 8(d) there are trajectory sections with straight segments. This is due to the fact that during the intervals of outputting the trajectory coordinates (with the Galactica system parameter  $K_{li} = 2000$ ), the orbits change more substantially than in other regions.

The trajectory of body 1563 is almost a circle, its eccentricity being  $e = 0.01$  (Figure 8(c)). The orbit slightly changes in space (Figure 8(e)). The orbital period is  $1.2 P_6$ , where  $P_6 = 0.134$ . The semi-axis of the orbit has also changed little compared to the initial one and is equal to  $1.06 a_6$ .

The trajectory of body 5301 is an ellipse with eccentricity  $e = 0.23$  (Figure

**8(c)**). Its plane is almost perpendicular to the  $xy$ -plane (**Figure 8(e)**). That is why on the  $xy$ -plane this trajectory is depicted as a flattened ellipse (**Figure 8(c)**).

As already noted, the distances  $r_{r1}$  of about 30 bodies were outside the graph in **Figure 7(c)**. For some of these bodies, according to algorithm (29)-(36), the types of trajectories and their parameters were determined. At time  $T = 0.815$ , the most remote body 1575 had a distance  $r = 7.076$  and a velocity  $v = 9.735$ . Calculations by algorithm (29)-(36) gave the following results:  $R_p = 0.0560$ ,  $v_p = 11.41$ ;  $\alpha_1 = -0.1371$ ;  $e = 6.293$ ; and  $v_\infty = 9.720$ . With this value of  $\alpha_1$ , the trajectory is a hyperbola. Thus, the body was ejected from the structure along a hyperbolic orbit. At this time, its velocity already approached the velocity at infinity.

For body 1575, the calculations were repeated for the time  $T = 0.385$ , when the distance and velocity were  $r = 2.883$  and  $v = 9.766$ . The parameters of the hyperbolic trajectory were confirmed up to seven digits. These calculations were also performed for the time  $T = 0.1035$ , when the parameters of the body were  $r = 0.1907$  and  $v = 10.450$ . The parameters of the hyperbolic orbit were confirmed to within 4 digits. At this time, the distance  $r$  is close to the radius of the outer layer. It follows from here that algorithm (29)-(36) can be used for determining the trajectories of all bodies outside their main cluster.

These studies were carried out for all remote bodies. It was found that 14 bodies with mass  $m_1$  and 3 bodies with mass  $2m_1$  were ejected from the structure. Two bodies have strongly elongated elliptical orbits, whose apocenter radii  $R_a$  are equal to 0.5646 for body 4601 and 3.024 for body 3032.

### 6.3. Approaches, Collisions, and Merging of Bodies

As already noted, in this structure there are two bodies with a mass of  $5m_1$ . **Figure 9** shows the encounters of one of these bodies, namely body 1951, with other bodies over the interval  $0.069 < T < 0.075$ . The calculations were performed in step correction mode with key Kl4 = 3 and key Kl3 = 300 steps for outputting results. From the time  $T = 0.069$ , body 1951 approaches body 1952, and at time  $T = 7.153 \times 10^{-2}$  the bodies merge together. Then, the approach to body 1950 begins and at time  $T = 7.153 \times 10^{-2}$  the two bodies merge together.

Then, body 1951 approaches body 1953 and at time  $T = 7.172 \times 10^{-2}$  to merge with it. Then, the approach to body 1954 begins, and at time  $T = 7.321 \times 10^{-2}$  there occurs merging with this body. As a result of these four events, the mass of 1951 became equal to  $5m_1$ . Further, at time  $T = 7.321 \times 10^{-2}$  the body 1951 approaches body 1949 to a distance of 14 peripheral-body radii  $R_1 = 1.676 \times 10^{-6}$ , and the bodies diverge. Then, at time  $T = 7.456 \times 10^{-2}$  there occurs an encounter with body 1955 to a distance of  $48R_1$ .

**Figure 10(a)** shows the trajectories of all bodies approaching and colliding with body 1951. These calculations were performed in mode Kl4 = 3 with an initial step  $dT = 0.5 \times 10^{-6}$  (**Figure 10(b)**) over the interval of output steps  $Kli =$



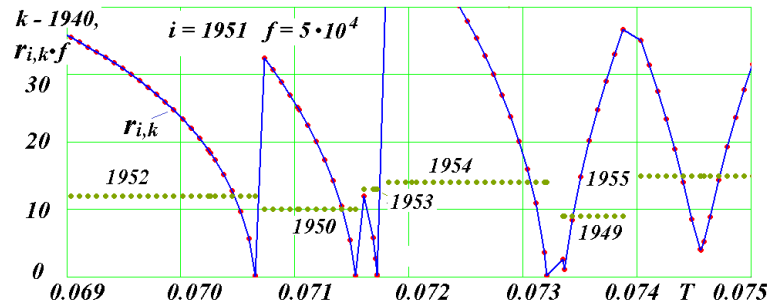


**Figure 9.** Approach of body  $i = 1951$  by bodies  $k$  to a distance  $r_{i,k}$  for the number of integration steps  $KI3 = 300$  made with a step  $dT = 0.5 \times 10^{-6}$  over the initial interval  $T = 0.0690 - 0.0750$ . The dimensionless distance  $r_{i,k}$  in the graph is increased by a factor of  $f = 5 \times 10^4$ , and the number of bodies  $k$  is reduced by 1940.

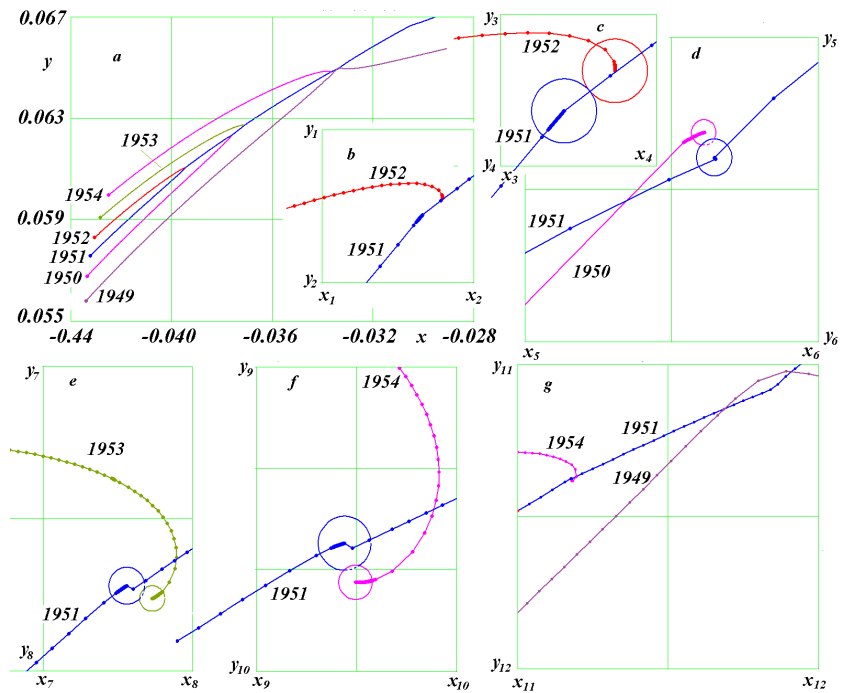


**Figure 10.** The trajectories during the approach and collision of body 1951 with bodies 1949, 1950, 1952, 1953, and 1954. **Table 1** shows the values of  $y_1 - y_{12}$ ,  $x_1 - x_{12}$ .

**Table 1.** The values of the bounds in the graphs  $b, c, d, e, f,$  and  $g$  of **Figure 10**.

	$b$	$c$	$d$	$e$	$f$	$g$
$y_1$	0.06106	$y_3$ 0.061054	$y_5$ 0.06236	$y_7$ 0.06274	$y_9$ 0.06483	$y_{11}$ 0.0650
$y_2$	0.06104	$y_4$ 0.061046	$y_6$ 0.06232	$y_8$ 0.06270	$y_{10}$ 0.066480	$y_{12}$ 0.0645
$x_1$	-0.03948	$x_3$ -0.039470	$x_5$ -0.03762	$x_7$ -0.03715	$x_9$ -0.03372	$x_{11}$ -0.0338
$x_2$	-0.03946	$x_4$ -0.039462	$x_6$ -0.03758	$x_8$ -0.03713	$x_{10}$ -0.03370	$x_{12}$ -0.0333

300. The first approach of body 1951 occurs with body 1952. On the section of approach (**Figure 10(b)**), the calculations were carried out with the interval of output steps  $Kli = 3$ . Body 1952 moves ahead of body 1951 and, as the latter

body approaches the former, it begins to go around it. On a larger scale (**Figure 10(c)**), the diameters of the bodies are marked with circles. The bodies are almost at the same distance from the  $xy$ -plane. The merging of the two bodies occurs when their surfaces come in contact. The condensation of points on the trajectory indicates the inclusion of step correction mode before the collision. The length of the condensation section is proportional to the body velocity. It is seen that the velocity of body 1951 is greater than the velocity of body 1952. This difference may be due to the interaction between these bodies. In this case, the body 1951 is accelerating, and the body 1952, decelerating.

It should be noted that all images in the graphs are drawn to scale, and the values of the limits  $y_1, y_2, x_1, x_2$ , etc. are presented in **Table 1**.

The second approach of body 1951 occurs with body 1950 (**Figure 10(a)**). **Figure 10(d)** shows that the body 1950 catches up with the body 1951, crosses its trajectory, and due to the attraction of this body, the trajectory of body 1950 bends. The merging of the two bodies occurs at the moment of contact. In this case, the  $z$ -coordinate of body 1951 is greater, so the contact occurs below the visible contour of body 1951. As a result of the merging with body 1952, the radius of body 1951 increases to  $1.26R_1$ . Before the collision, the body 1950 was slowing down as a result of the interaction with body 1951, while the body 1951 experienced acceleration.

The third approach of body 1951 occurs with body 1953 (**Figure 10(a)**). It is seen from **Figure 10(e)** that body 1953 moves ahead of body 1951. That is why body 1953 goes around body 1951 and collides with it on the side opposite to the side of approach. In this case, the radius of body 1951 was already  $1.44R_1$ .

As it is evident from **Figure 10(f)**, the fourth approach to body 1954 occurs similarly, yet with the enveloping motion of body 1954 being more pronounced than that of body 1953. This is due to the greater mass of body 1951. This mass is  $4m_1$ , and the radius of 1951 is  $1.59R_1$ . After the merging of body 1951 with body 1954, its mass became  $5m_1$ , and its radius,  $1.71R_1$ . In these two cases (see **Figure 10(e)**, and **Figure 10(f)**), body 1951 more closely approaches the  $xy$ -plane than body 1954; therefore, this plane is partially shaded by this body.

In the four collisions considered above, three bodies approached the target body from the left side and collided with it on the right side (**Figure 10(c)**, **Figure 10(e)**, **Figure 10(f)**). On the other hand, the body approaching the target body from the right side collided with it on the left side (**Figure 10(d)**). At the same time, the greater the mass of body 1951, the greater is the angle through which the approaching body envelopes body 1951.

The approach of body 1949 to body 1951 is shown in **Figure 10(g)**. These calculations were performed with the output interval  $Kli = 30$ . As noted above, in this case the body 1949 approached body 1951 to a distance of  $14R_1$ . At the moment of approach, the velocity of body 1949 was almost three times greater than the velocity of body 1951. That is why the body 1949 overtook body 1951 with a further increase in velocity and went around it by almost  $90^\circ$ . After ap-

proach, the velocity of body 1949 began to decrease.

Despite the above collisions, body 1951 kept moving within the structure. By the end of the studied time interval  $T = 0.815$ , the distance of body 1951 from the center of mass was  $r_{r1} = 7.17$ . Body 1949 was also inside the structure with a distance of  $r_{r1} = 4.28$ .

### 6.4. Spin of the Body and Its Thermal Energy after Collision

When bodies collide, the body formed from them acquires its own angular momentum, which we call spin  $S_p$ , and thermal energy  $E_t$ . The algorithm for calculating these quantities was reported in [33] [34], and its software implementation was described in [24]. **Figure 11(a)** shows the variation of spin projections  $S_{px}$ ,  $S_{py}$ ,  $S_{pz}$  and thermal energy  $E_t$  of body 1951 during its collision with four bodies. As a result of each collision, these quantities changed. The circles in the graphs mark the moments  $T$  of issuing output files by the Galactica program; those files were used to determine the values of interest.

The smallest change in spins occurs during the first collision (point  $2m_1$ ) with body 1952 (**Figure 10(c)**). This collision is close to a frontal impact. As is seen from **Figure 11(a)**, the thermal energy  $E_t$  changes significantly in this case. During the second collision (point  $3m_1$ ) with body 1950, the spin projection  $S_p$  has increased more significantly, and the thermal energy  $E_t$  changed three times less than it did so during the first collision. As it is seen from **Figure 10(d)**, this collision occurred along a tangent line. Other collisions with bodies 1953 and 1954 also occurred in nearly tangential directions. But body 1951 became more

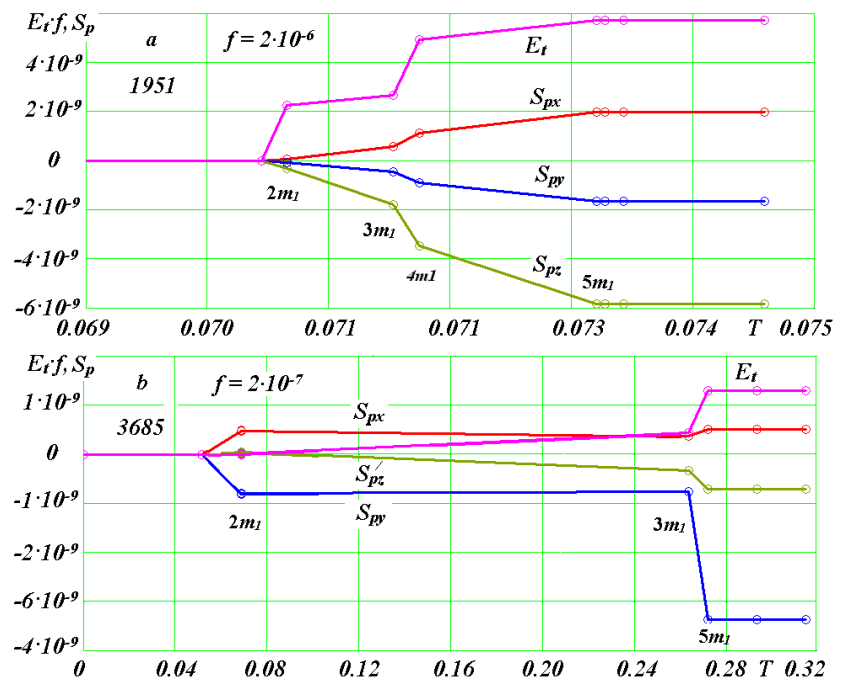


**Figure 11.** Variation of thermal energy  $E_t$  and spin projections  $S_{px}$ ,  $S_{py}$ ,  $S_{pz}$  formed during the merging of bodies 1951 (a) and 3685 (b). The value of  $E_t$  is multiplied by the coefficients  $f = 2 \times 10^{-6}$  (a) and  $f = 2 \times 10^{-7}$  (b).

massive, and the velocity of the approaching bodies increased. Therefore, the increment of spins and thermal energy were significant. As a result, body 1951 acquired thermal energy  $E_t = 2.87 \times 10^{-3}$  and spin modulus  $S_p = 6.385 \times 10^{-9}$ . The spin vector makes an angle  $\beta_2 = -23.8^\circ$  with the  $z$ -axis. Since the angle is negative, body 1951 rotates clockwise.

For comparison, **Figure 11(b)** shows the rotational and thermal characteristics of body 3685, which also has a mass of  $5m_1$ . During the first collision at point  $2m_1$ , the body has acquired a small thermal energy  $E_t$ . During the second collision ( $3m_1$ ), the spin projections  $S_{px}$  and  $S_{py}$  have slightly decreased, while the thermal energy  $E_t$  increased significantly. The third collision at point  $5m_1$  occurred with a body of double mass. In this case, the spin projection  $S_{py}$  dominates. The spin value is  $S_p = 3.48 \times 10^{-9}$ , and its vector makes an angle  $\beta_2 = -78.1^\circ$  with the  $z$ -axis, *i.e.* the axis of rotation of body 3685 is close to the  $xy$ -plane. Its thermal energy is  $E_t = 6.45 \times 10^{-3}$ . Thus, with the same masses of these bodies, body 1951 has a 1.8 times greater spin and 2.2 times lower thermal energy.

## 7. Evolution of the 15-Layer Structure

### 7.1. General Changes

Due to the fact that with an increase in the number of bodies, the time required for calculating the evolution of a structure of interest becomes excessively large, a 15-layer structure was created with a smaller initial number of bodies in the first layer, namely  $N_{3,1} = 49$ . In this case, the absolute peripheral-body mass was 2.02 times greater than that in the previous structures. This structure, contained in the MS15c49b.dat file, is shown in **Figure 12(a)**. All close encounters at self-crossings of the formation line were eliminated by changing the number of bodies in accord with (21). The number of bodies in the layers varies from 47 in the first layer to 733 in the 15<sup>th</sup> layer; the semi-axes, from  $a_1 = 0.0118 - 0.0105$  to  $a_{15} = 0.1573$ ; and the periods, from  $P_1 = 0.0100$  to  $P_{10} = 0.3916$ . The total number of bodies was  $N = 5866$ .

After 77.9 revolutions of first-layer bodies, *i.e.* at  $T = 0.779$ , the structure is shown in **Figure 12(b)**. By the time  $T = 0.2$ , elements of the initial organization of the structure are still preserved, whereas by the time  $T = 0.3$  they completely disappear. By the time  $T = 0.4$ , the structure acquires a form that shows almost no subsequent changes. The scatter of body distances in **Figure 12(c)** is limited to 50 radii of first-layer bodies. About 20 bodies were ejected over a greater distance, the largest of which is  $r_{r1} = 168$  for body 5336.

By the time  $T = 0.779$ , there occurred 164 collisions. In this case, 120 bodies of double mass, 17 bodies of triple mass and 2 bodies of quadruple mass were formed. In addition, there occurred four collisions with the central body.

The dynamics of collisions is illustrated in **Figure 12(d)**. For the interval  $T = 0.085 - 0.286$ , the rate of collisions was  $v_{imp} = 547$  collisions per 100 revolutions of first-layer bodies, and during the second interval  $T = 0.378 - 0.779$ , the aver-

age rate of collisions was  $v_{imp} = 85$ . Thus, over the second time interval the collision rate has decreased by 6.4 times.

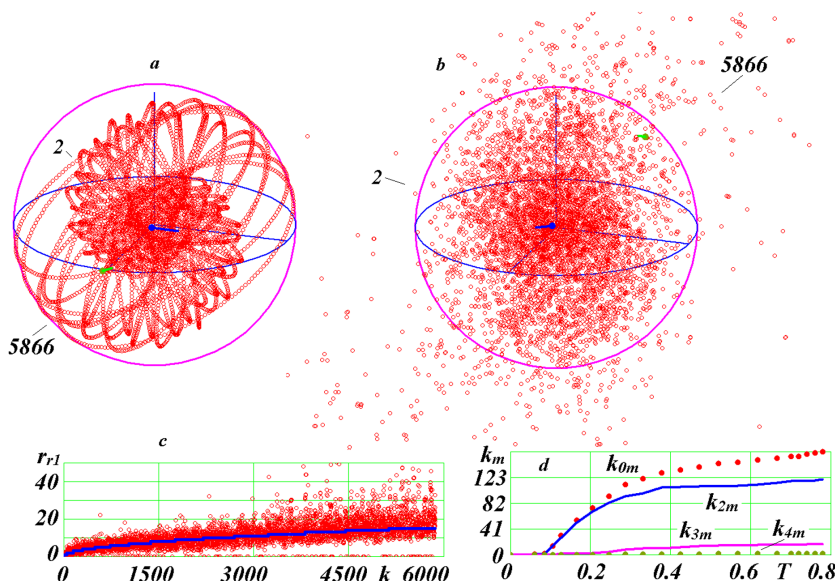


**Figure 12.** The fifteen-layer structure MS15c49b.dat and its evolution. Image *b* shows the structure at time  $T = 0.779$ . For the rest designations, see **Figure 7**.

When compared with the 10-layer structure, the velocity over the second time interval of the 15-layer structure was 1.23 times higher. The velocity per one body,  $v_{impl} = 1.45 \times 10^{-2}$ , is also 1.14 times higher.

### 7.2. Trajectories of Individual Bodies

**Figure 13** shows the trajectories of the central body 1, first-layer body 25, seventh-layer body 1325, and 15<sup>th</sup>-layer body 5660. These calculations were carried out over the interval  $T = 0.597 - 0.853$  with a step  $dT = 1 \times 10^{-7}$ . The trajectory of the central body 1 (**Figure 13(a)**) is irregular and lies in the range of distances  $r < 0.003$  from the center of mass.

The orbit of body 25 is continuously changing in space. Its eccentricity also changes: it decreases up to the time  $T = 0.77$  and then increases. The average value of the eccentricity is  $e = 0.69$ . The period undergoes similar changes, and on average it equals  $0.83P_1$ , where  $P_1 = 0.01$  is the initial period. After  $T = 0.77$ , a significant change in the plane of the orbit occurs (**Figure 13(c)**), both its eccentricity and period increase, and its change in space also becomes more pronounced.

The orbit of body 1325 (**Figure 13(b)**) is an ellipse with eccentricity  $e = 0.408$ . The semi-axis of the orbit is 1.1 times greater than  $a_7 = 0.073$ , where  $a_7$  is the semi-axis of the initial orbit, and the period is 0.95 times less than  $P_7 = 0.1645$ . As it follows from **Figure 13(b)** and **Figure 13(d)**, the orbit changes significantly during one revolution.

The orbit of body 5600 in **Figure 13(b)** and **Figure 13(e)** is represented by its

part smaller than half the body's range of revolution about the center of mass. The distance of the body from the center is  $r = 0.238$  and practically does not change. The slight ellipticity in **Figure 13(b)** is due to the inclination of the orbit to the  $xy$ -plane (see **Figure 13(d)**). The distance  $r$  is  $1.5 a_{15}$ , and the period of revolution of body 5600 is therefore longer than the initial period  $P_{15} = 0.3916$ .

As already noted, the distances  $r_{r1}$  of approximately 20 bodies were beyond the bounds of **Figure 12(c)**. For most of these bodies, algorithm (29)-(36) was used to determine their trajectory types. For bodies 5336, 543, 264, and 5146, remote to distances  $r_{r1} = 168, 125, 115,$  and  $107,$  respectively, the trajectories were hyperbolas, *i.e.* the bodies were ejected out of the structure. In total, six bodies were ejected. In this case, for two bodies, 5146 and 264, the eccentricities were 1.045 and 1.0098, respectively, *i.e.* they are close to unity, which value characterizes a parabolic orbit. For body 5594, remote to  $r_{r1} = 94,$  the orbit is an ellipse with eccentricity  $e = 0.894$ . Other distant bodies also have elliptical orbits.

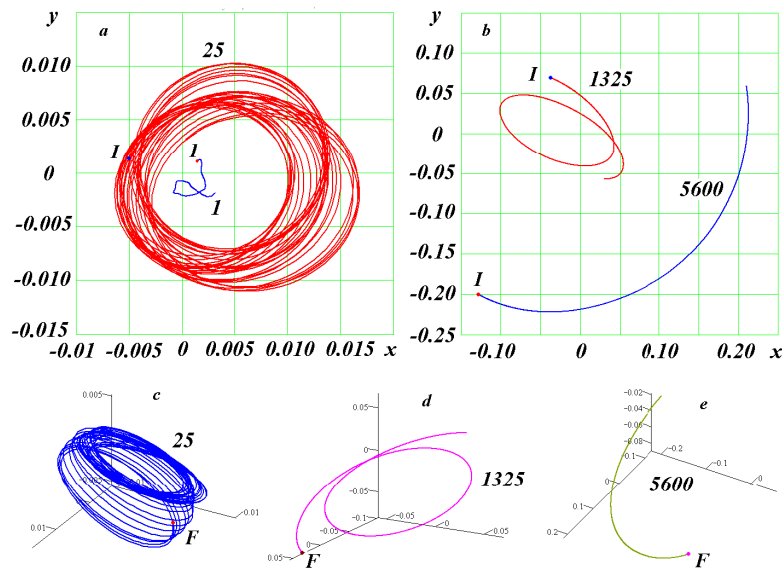


**Figure 13.** Trajectories of the central body 1 and peripheral bodies 25, 1325, and 5600 during the final period ( $T = 0.597 - 0.853$ ) of the evolution of the MS15c99b.dat structure ((a), (b)): shown in parts (c)-(e) of the figure are the three-dimensional images of the trajectories; and  $I$  and  $F$  are the initial and final points of the trajectories.

### 7.3. Approach of a Remote Body

Encounters of the most distant body 5336 with other bodies were studied (**Figure 14**). In the first time interval  $T = 0.184 - 0.193$  (see part *a* of **Figure 14**), this body first passes close to body 5335, and then its approach to body 5333 begins. At time  $T = 0.1854,$  the distance between the bodies  $R_{ik}$  becomes equal to  $4.05 \times 10^{-6},$  this value amounting to 2.15 radii of the body  $R_1,$  *i.e.* the distance between the surfaces of the bodies is  $0.15 \cdot R_1.$  In this case, the velocities of the bodies increase to  $v = 5.53$  for body 5336 and  $v = 5.37$  for body 5333. At the initial time  $T = 0,$  the velocities of both bodies were equal to 2.53. After the approach, the bodies move away from each other and their velocities at the final

time  $T = 0.779$  decrease to  $v = 2.77$  and  $1.87$ , respectively.

In the final time interval  $T = 0.75 - 0.85$ , it is seen that body 5336 is continuously moving away from body 5146, which is also moving away from the structure along a hyperbolic orbit. The distance between the bodies increases almost linearly with an average velocity of  $1.38$ . The bodies move in approximately the same direction: the angle between their velocities is  $8.27^\circ$ .

As for body 5333, after moving away from body 5336, its velocity, as already noted, decreased more significantly, and its motion proceeded along an elliptical orbit with an eccentricity  $e = 0.597$ . At time  $T = 0.779$ , the body is at a distance of  $r_{r1} = 13.87$ . Thus, the ejection of body 5336 has occurred due to its acceleration when approaching body 5333 to a distance  $r = 2.15R_1$ .

In the considered 5, 10, and 15-layer models of globular clusters, the arrangement of the layers relative to each other, the number of bodies in the first layer, and the number of layers changed. All of them are stable and do not destroy. Therefore, with the variations considered, it is possible to create models of globular clusters with any number of layers in them.

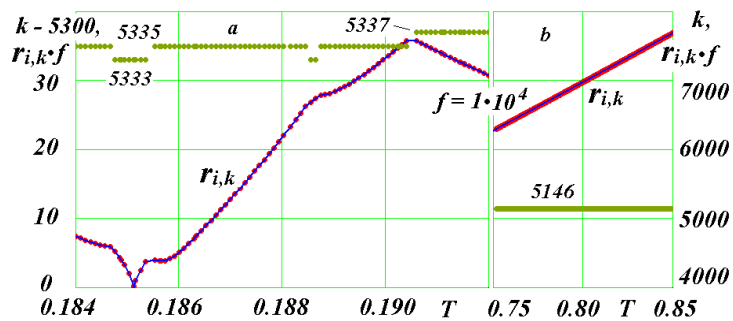


**Figure 14.** Graph of the approaches of body  $i = 5336$  to bodies  $k$  to a distance  $r_{i,k}$  for the number of integration steps  $Kl3 = 400$  with a variable step ( $Kl4 = 3$ ) over the first interval  $T = 0.184 - 0.193$  (a) and over the second interval  $T = 0.75 - 0.85$  (b). The dimensionless distance  $r_{i,k}$  in the graph is increased by a factor of  $f = 1 \cdot 10^4$ , and the number of bodies  $k$  in part a of the figure is reduced by 5300.

## 8. General Characteristics of Structures

### 8.1. Velocity Profiles

In **Figure 15(a)** and **Figure 15(b)**, the points show the velocity profiles of the five-layer MS05c99e.dat structure at the final time  $T = 1.96$ , and the lines show the same profiles at  $T = 0$ . In **Figure 15(a)**, the velocities  $v$  are shown depending on the body numbers  $k$ , and in **Figure 15(b)**, depending on the relative radius  $r_{rN2} = r/r_{N2}$ . At the initial time  $T = 0$ , the line segments mark the velocities of bodies in five layers (**Figure 15(a)**). They decrease stepwise from the first layer to the last fifth layer. After the interaction of bodies proceeding during 196 revolutions of first-layer bodies, the distribution of velocities no longer shows the initial stepping behavior. The velocities were distributed around the initial velocity profile. At the same time, most of the velocities retain the initial trend of decreasing the velocity magnitude with increasing the body number  $k$ .

The zero velocities on the horizontal axis mark the bodies that have merged with other bodies, and their velocities were therefore assigned zero values. Body 76, which is at a distance  $r_{rN2} = 0.082$ , or  $r_{r1} = 0.41$  from the center of mass, has the highest velocity  $v = 14.33$ ; *i.e.* it is located near the central body. All in all, there are eight bodies whose velocities exceed the limit of the graph  $v = 12$ .

The distribution of velocities over body distances  $r_{rN2}$  (**Figure 15(b)**) has a more compact form. In the trajectory section  $r_{rN2} \leq 1$ , the velocities of bodies are distributed uniformly around the initial profile represented by segments. It should be noted that the initial velocity profile is discrete. It is represented by points at which the line breaks.

Consider the reasons for the deviation of velocities from the initial profile. At first the orbits are circles, and then they become ellipses. In the pericenters of the orbits, the bodies have high velocities, and in the apocenters they have lower velocities. In addition, for some bodies the semi-axes of their orbits become smaller, and the velocities become greater. For the other part of the bodies, on the contrary, the semi-axes increase, and the velocities decrease. For these two reasons, there appears a velocity spread relative to the initial profile. Evidently, the action of these two factors is symmetrical with respect to this profile.

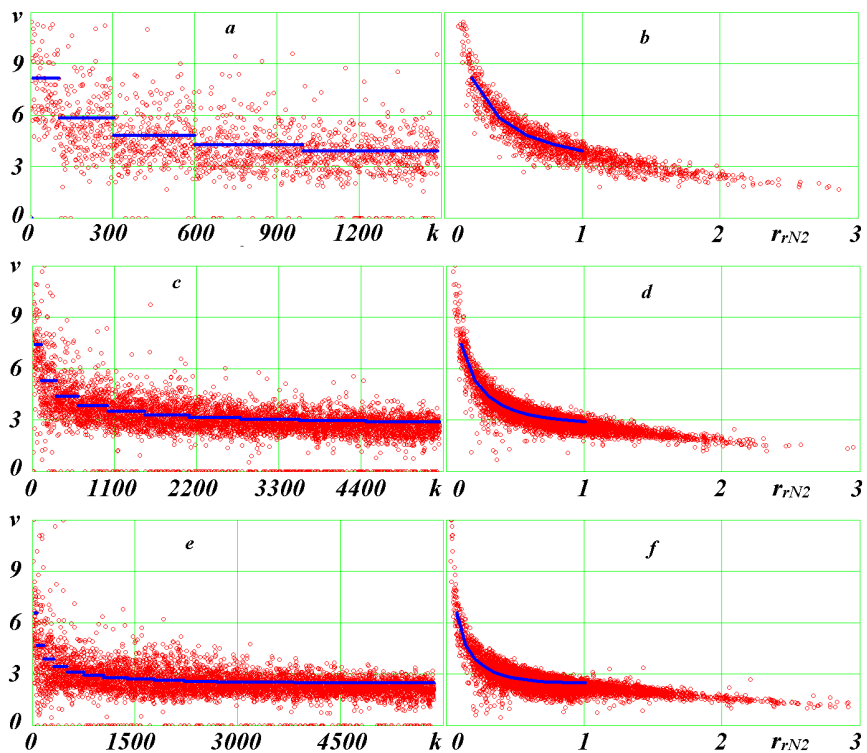


**Figure 15.** Distributions of body velocities  $v$  over their numbers  $k$  and over the relative body distances from the center of mass  $r_{rN2}$  for structures formed by 5 ((a), (b)), 10 ((c), (d)), and 15 ((e), (f)) layers.

According to formulas (12)-(13), the velocity of the bodies at the initial time is equal to



$$v = \sqrt{v_r^2 + v_t^2} = v_p \sqrt{2\alpha_1(1 - R_p/r) + 1}, \quad (38)$$

where the values of  $\alpha_1$ ,  $v_p$ , and  $R_p$  can be calculated using dependencies (4)-(9). For circular orbits with  $r = R_p$ , formula (38) gives the velocities of bodies at the initial time, and for arbitrary distances  $r$  it gives such velocities for all bodies. The above parameters depend on the mass of the bodies within the radius  $r$ , as well as on the number of bodies and their mass at the radius  $r$  (see formulas (6) and (7)). Therefore, expression (38) can be used to estimate the masses of stars in globular clusters from their velocities.

Outside the distances of the graph in **Figure 15(b)**, there is only one body 1434 with  $r_{rN2} = 3.14$ . The velocity of this body,  $v = 1.572$ , falls onto the same dependence  $v(r_{rN2})$  as for other bodies at distances  $r_{rN2}$  close to 3.

The velocity distributions of the ten-layer structure over body numbers (**Figure 15(c)**) are more compact than those for the five-layer structure. The velocities are distributed more uniformly about the initial profile for layers 1 to 8. The distribution of velocities over distances (**Figure 15(d)**) is also more compact compared to the distribution over body numbers. The highest velocity  $v = 17.7$  is exhibited by the body located at a distance of  $r_{rN2} = 0.0227$ , or  $r_{r1} = 0.227$ , so that this body is almost twice as close to the center as in the five-layer structure. A total of four bodies exceed the velocity bounds on the graph. The bounds of the graph over distances are exceeded for 30 bodies, with the largest distance  $r_{rN2} = 60$  belonging to body 1575. The velocity  $v = 9.735$  of this body does not fall on the dependence  $v(r_{rN2})$  for distances close to 3. Starting from  $r_{rN2} = 6$ , the bodies have an ascending velocity profile. This profile can be represented as an average dependence

$$v = -0.526 + 0.171 \cdot r_{rN2} \quad \text{for } r_{rN2} > 6. \quad (39)$$

These bodies leave the structure by moving along hyperbolic orbits.

The 15-layer structure has an even more compact distribution of bodies over their numbers (**Figure 15(e)**). It lasts up to the 14<sup>th</sup> layer. The velocities here are distributed more evenly around the initial velocity profile.

The distribution of velocities over distances is also more compact (**Figure 15(f)**). However, the middle of this distribution noticeably deviates from the initial velocity profile in the region of the last layers. This difference is observed already for the 10-layer structure in **Figure 15(d)**. In the 15-layer structure, the highest velocity  $v = 16.9$  is exhibited by a body located at a distance of  $r_{rN2} = 0.022$ , or  $r_{r1} = 0.33$ . The velocities of only two bodies exceed the velocity bounds in the graph. The bounds of the graph in terms of body distances are exceeded for about 30 bodies with the largest distance  $r_{rN2} = 11.2$  found for body 5336. Its velocity is  $v = 2.763$ . Starting from  $r_{rN2} = 4.4$ , an increasing velocity profile is set:

$$v = -0.964 + 0.333 \cdot r_{rN2} \quad \text{for } r_{rN2} > 4.4 \quad (40)$$

The velocity profiles presented in **Figure 15** for different structures depending on the numbers of bodies and on their distances are similar, but they differ in quantitative characteristics. These quantitative differences are seen from formu-

las (39)-(40) for the ascending sections of velocity profiles. From the analysis of velocity profiles over body numbers at the initial time (**Figure 15(a)**, **Figure 15(c)**, **Figure 15(e)**), it can be inferred that with an increase in the number of layers, the velocity difference between the layers decreases, and the  $v$ -profile asymptotically approaches a horizontal line. Moreover, in the 14<sup>th</sup> layer (**Figure 15(e)**) the velocity becomes minimal,  $v = 2.524$ , and in the 15<sup>th</sup> layer it already increases. This increase in body velocities can also be traced in the velocity profile over distances (**Figure 15(f)**) at  $r_{rN2} \approx 1$  for the final time  $T = 0.779$ .

In order to elucidate the behavior of velocity in structures with a large number of layers, structures MS24c99b.dat with 24 layers (**Figure 16(c)**) and MS34c49b.dat with 34 layers (**Figure 16(d)**) were created. They have approximately the same number of bodies:  $N = 29701$  and  $29156$ , respectively. In the first structure, the number of bodies in the first layer is  $N_{3,1} = 99$ , and in the second,  $N_{3,1} = 49$ . That is why the second structure contains ten extra-layers at an approximately the same number of bodies  $N$ .

The images of the structures, obtained using the Galactica program, are shown in **Figure 16**. They are projections onto the  $xy$ -plane of the structures

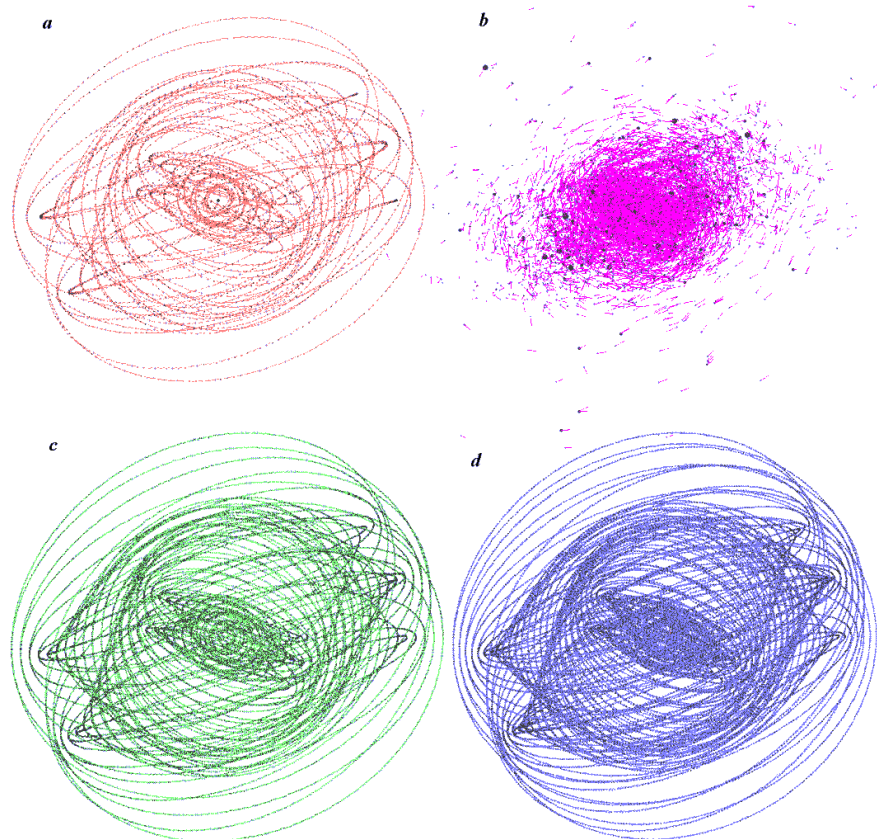


**Figure 16.** Multilayer structures in projections onto the horizontal  $xy$ -plane as represented by the Galactica program: ((a), (b)) MS15c49b; (c) MS24c99b; (d) MS34c49b. Part *b* of the figure shows the 15-layer structure at the time  $T = 0.779$  on the two times reduced scale, the lengths of segments are proportional to body velocities, and the point sizes are proportional to their masses.

pre-rotated around the  $x$ -axis through an angle of  $20^\circ$ . The bodies in the structures are shown as points, and the velocity vectors, as segments. In order not to obscure the images of bodies in the 24-layer and 34-layer structures, the velocity vectors are reduced. Condensation of points in these structures occurs in layers whose mid-planes coincide with the line of sight. In the 15-layer structure at the final time  $T = 0.779$  (**Figure 16(b)**), the enlarged points represent bodies with large masses. Since the graphs show projections of velocities, the small size of segments can be for bodies whose velocity is close to the perpendicular to the  $xy$ -plane. Sets of bodies with velocities directed similarly can be constellations.

All structures in **Figure 16** were obtained with  $\text{Inx} = 1$ , *i.e.* all layers in them were uniformly rotated around the  $x$ -axis. As it is evident from the images of the structures, with an increase in the number of layers their shape approaches the spherical shape: the last structure (**Figure 16(d)**) shows no difference from a sphere.

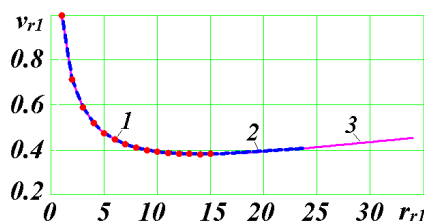


**Figure 17.** Generalized velocity profile at the initial time for multilayer structures: 1—MS15c49b, 2—MS24c99b, and 3—MS34c49b.

When analyzing the velocity profiles of these structures, it turned out that those profiles are similar, and they can be generalized as shown in **Figure 17**. The velocity of bodies  $v_{r1}$  is plotted along the vertical axis. This is the velocity normalized by the maximum velocity, or the body velocity in the first layer  $v_1$ . Plotted along the horizontal axis is the body distance  $r_{r1}$  normalized by the semi-axis  $a_1$  of the first layer. Numbers 1, 2, and 3 mark the velocity profiles of the 15-, 24-, and 36-layer structures. All those profiles form a general dependence. This dependence also determines the velocity profiles of the 5-layer and 10-layer structures. The latter velocity profiles are not shown in **Figure 17**.

The orbits of all bodies in the structures under consideration are circles; that is why their velocities can be calculated using expression (9) with  $r = R_p$  and  $v = v_p$ . From formula (9), it follows that the velocity  $v$  is inversely proportional to  $\sqrt{r}$  and, according to formulas (6) and (16), they vary in proportion to  $\sqrt{m}$ , where  $m$  is the mass of bodies inside the sphere of radius  $r$ . Therefore, with an increase in  $r$ , the velocity decreases unless the mass of the bodies increases so much that its influence becomes predominant.

In the ascending section of the graph in **Figure 17**, the velocity varies non-linearly, and its average change obeys the law

$$v_{r1} = 0.333 + 3.582 \cdot 10^{-3} \cdot r_{r1} \quad \text{for } r_{r1} > 14. \tag{41}$$

For structures 1, 2, and 3 shown in **Figure 17** we have:  $v_1 = 6.590, 5.396,$  and

4.485, respectively. These velocities are given in dimensionless form. They change due to the fact that the dimensional velocities are multiplied by the velocity coefficient  $k_v$ , which, in accordance with formulas (26)-(27), can be determined as follows:

$$k_v = 1/(A_m k_t). \tag{42}$$

The presented values of  $v_1$  vary in proportion to  $k_v$ . It follows from here that the generalized velocity profile in **Figure 17** is also valid in dimensional form.

### 8.2. Angular Momenta

The angular momenta of five structures, from the 5-layer MS05c99b structure to the 34-layer MS34c49b structure, are given in **Table 2** for the initial time  $T = 0$ . This quantity is also called the kinetic momentum. The table shows the projections  $M_x$ ,  $M_y$  and  $M_z$  of the angular momentum onto the coordinate axes  $x$ ,  $y$ ,  $z$ , as well as the absolute value of  $M$ . Based on these projections, the angle  $\beta_3$  between the angular momentum vector  $\mathbf{M}$  and the  $z$ -axis is calculated as follows:

$$\beta_3 = \arctg \frac{\sqrt{M_x^2 + M_y^2}}{M}. \tag{43}$$

In addition, the total orbital momentum of all bodies  $M_{us}$  is given on the condition that the orbits of the bodies lie in the same plane. For circular orbits, the total orbital momentum is defined as follows:

$$M_{us} = \sum_{i=1}^N m_i v_i r_i. \tag{44}$$

The orbital moments of bodies vary from layer to layer. For example, for the

**Table 2.** Orbital ( $M_x, M_y, M_z, M, M_{us}$ ) and rotational ( $S_{sx}, S_{sy}, S_{sz}, S_s$ ) angular momenta in multilayer structures.

Structures	Orbital angular momentum							
	$T$	$M_x$	$M_y$	$M_z$	$M$	$\beta_3$	$M_{us}$	$M/M_{us}$
MS05c99b	0	$8.690 \times 10^{-3}$	$2.295 \times 10^{-4}$	0.02459	0.02608	19.5°	0.02766	0.9428
MS10c99b	0	0.02944	-0.03525	$-3.230 \times 10^{-3}$	0.04603	94.0°	0.09365	0.4915
MS15c49b	0	0.04884	-0.06214	$4.176 \times 10^{-3}$	0.07915	87.0°	0.1554	0.5092
MS24c99b	0	0.07142	-0.09615	0.01974	0.12139	80.6	0.2273	0.5341
MS34c49b	0	0.08392	-0.1167	0.03297	0.14747	77.1	0.2670	0.5523

Structures	Rotational angular momentum (spins)						
	$T$	$S_{sx}$	$S_{sy}$	$S_{sz}$	$S_s$	$\beta_3$	$S_s/M$
MS05c99b	1.96	$3.741 \times 10^{-9}$	$-7.486 \times 10^{-9}$	$8.795 \times 10^{-9}$	$1.214 \times 10^{-8}$	43.6°	$4.655 \times 10^{-7}$
MS10c99b	0.815	$-1.036 \times 10^{-7}$	$-1.587 \times 10^{-7}$	$1.277 \times 10^{-7}$	$2.285 \times 10^{-7}$	56.0°	$4.964 \times 10^{-6}$
MS15c49b	0.779	$5.578 \times 10^{-8}$	$7.778 \times 10^{-7}$	$-4.633 \times 10^{-7}$	$9.070 \times 10^{-7}$	120.7°	$1.146 \times 10^{-5}$

34-layer structure, the angular momentum of the central body is  $2.19 \times 10^{-33}$ , for the first-layer bodies it is  $9.41 \times 10^{-7}$ , and for the 34<sup>th</sup>-layer bodies,  $1.46 \times 10^{-5}$ . It should be noted that the presence of the kinetic moment of the central body is due to its deviation from the center of mass of the structure.

As evident from **Table 2**, the values of kinetic moments  $M$  and  $M_{us}$  increase with the number of layers in the structures. For example, on going from the 5-layer structure to the 34-layer structure the value of  $M_{us}$  increases by almost 10 times. The projections of moments  $M_x$ ,  $M_y$ , and  $M_z$  also vary in a wide range, and they can be either positive or negative. The angular momentum vector  $\mathbf{M}$  is least inclined to the  $z$ -axis for the MS05c99b structure:  $\beta_3 = 19.5^\circ$ . In this structure, there are no rotations of layers about the  $x$ -axis. Therefore, the angular momentum of the structure  $M = 0.02608$  differs little from the orbital momentum of all bodies  $M_{us}$ : their ratio is 0.9428.

In other structures, the layers are uniformly rotated around the  $x$ -axis. This has led to a significant change in the vector  $\mathbf{M}$ . For instance, for the MS10c99b structure we have:  $\beta_3 = 94^\circ$ , *i.e.* the vector  $\mathbf{M}$  lies practically in the  $xy$ -plane. In addition, it is located in the southern hemisphere. Therefore, the total rotation of bodies in the structure proceeds in clockwise direction. In other structures, the total rotation of bodies proceeds counterclockwise.

For the 15-layer structure, we have:  $\beta_3 = 87^\circ$ , *i.e.* the angular momentum vector lies even closer to the  $xy$ -plane, but it is located in the northern hemisphere. Therefore, the total rotation of bodies proceeds counterclockwise. In these two structures, the momentum ratio  $M/M_{us}$  is close to 0.5. In structures with a large number of layers, this ratio slightly increases, and the angle  $\beta_3$  decreases, *i.e.* the vector  $\mathbf{M}$  moves away from the  $xy$ -plane.

In **Table 2**, the values of the kinetic momentum are given for the initial time. The largest relative change in the angular momentum at the final time,  $\delta M_z = 5.8 \times 10^{-5}$ , was found to occur in the MS15c49b structure. This means that the magnitudes of the momentum remain unchanged to four significant digits. This means that the values of the angular momentum given in **Table 2** are also valid for other moments of time.

### 8.3. Rotational Angular Momentum of Bodies and Their Thermal Energies

In **Figure 11**, the change in the spins of a body and its thermal energy was considered when other bodies were successively attached to it. Consider now the spins and thermal energies of all bodies at the final stage of structure formation.

**Figure 18(a)** shows the spin projections  $S_{px}$ ,  $S_{py}$ ,  $S_{pz}$  and thermal energy  $E_t$  for all merged bodies of the 5-layer structure at moment  $T = 1.96$ . The numbers of merged bodies  $i_u$  are plotted along the horizontal axis. The spin projections  $S_{px}$ ,  $S_{py}$ , and  $S_{pz}$  are marked with a cross, a rhombus, and a square, respectively, and the thermal energies are marked with straight segments of a thin line that breaks at body numbers. The break points and the symbols of spin projections falling onto one and the same vertical line with number  $i_u$ , belong to the body  $i_u$ .

All in all, there are  $N_u = 43$  merged bodies. The spin projections (**Figure 18(a)**) vary over wide ranges, and the plots show no dominant direction. The spin modulus  $S_p$  changes from a minimum value of  $2.86 \times 10^{-10}$  to a maximum value of  $2.71 \times 10^{-9}$ , those values differing by one order of magnitude. The average value of spin modulus  $S_{ppm} = 1.21 \times 10^{-9}$  in the graph is shown with a dashed line.

The total value of the angular momentum of the entire 5-layer structure, *i.e.* its spin, is given in **Table 2** as projections  $S_{sx}$ ,  $S_{sy}$ , and  $S_{sz}$ . The total spin modulus is  $S_s = 1.21 \times 10^{-8}$ , *i.e.* it is exactly ten times greater than the average spin of an individual body  $S_{sm}$ . However, there are  $N_u$  bodies in total, and the ratio of the total spin to the sum of the spins of individual bodies is  $S_s/(N_u \cdot S_{ppm}) = 0.23$ . Thus,

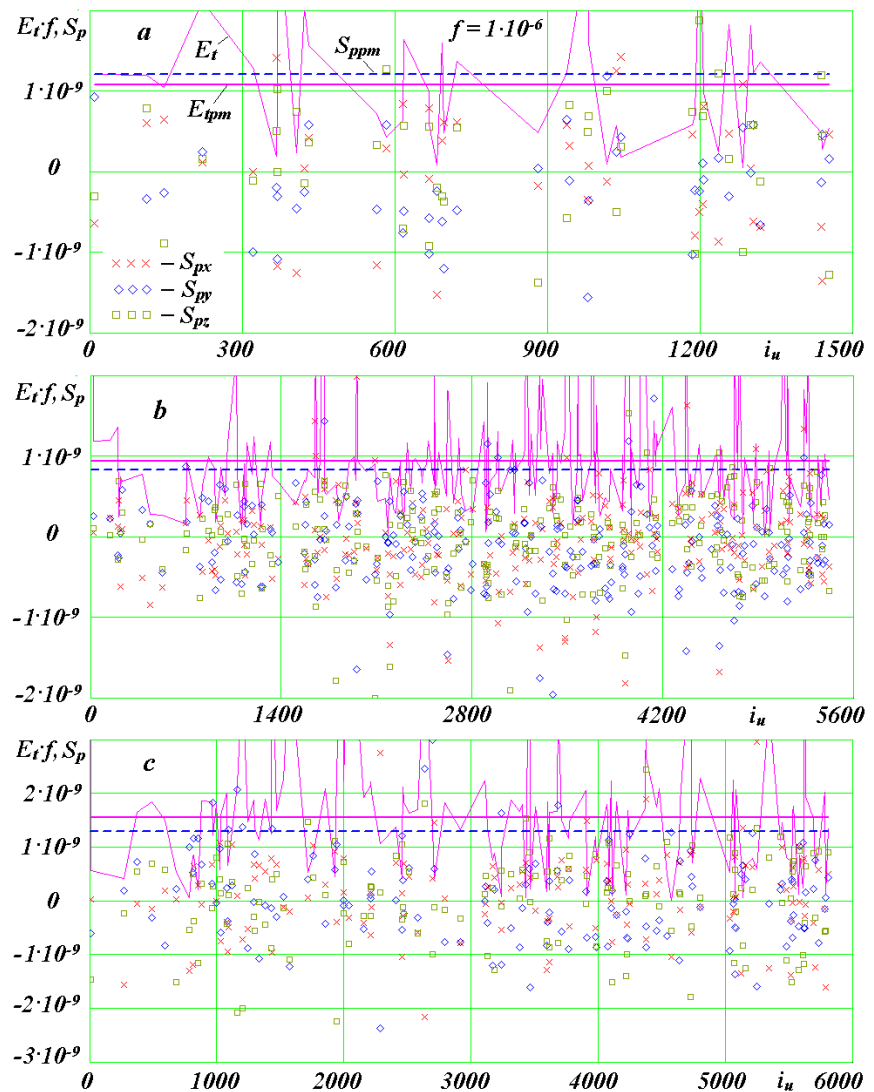


**Figure 18.** Variation of thermal energies  $E_t$  and spins  $S_p$  depending on the numbers of merged bodies in three structures, MS05c99e (a), MS10c99b (b), and MS15c49b (c):  $E_t$  is the thermal energy;  $E_{tpm}$  is the average thermal energy of the peripheral body;  $f = 1 \times 10^{-6}$  is a multiplier;  $S_{px}$ ,  $S_{py}$ ,  $S_{pz}$  are the spin projections; and  $S_{ppm}$  is the mean spin modulus of the peripheral body.

the spins of individual bodies compensate each other to 77%.

As evident from **Table 2**, the total spin of the system is inclined to the  $z$ -axis by an angle  $\beta_3 = 120.7^\circ$ , whereas the kinetic momentum of the system  $\mathbf{M}$  has an inclination angle  $\beta_3 = 19.5^\circ$ . The ratio of these momenta is  $4.66 \times 10^{-7}$ , *i.e.* the rotational momentum is a small fraction of the orbital angular momentum.

The thermal energies  $E_t$  of bodies in **Figure 18** are reduced by a factor  $f = 1 \times 10^{-6}$ . For the 5-layer structure, these energies vary from a minimum value of  $5.85 \times 10^{-5}$  to a maximum value of  $3.24 \times 10^{-3}$ , these values differing by 55 times. The average value of the thermal energy of one body is  $E_{tm} = 1.08 \times 10^{-3}$ , and the thermal energy of all bodies is  $E_{ts} = 0.0466$ .

In the 10-layer structure (**Figure 18(b)**), there are  $N_u = 248$  merged bodies in total. In this system, there was one merging with the central body, so we will consider the parameters of collisions of peripheral bodies without a central body. The spins of these bodies vary from

$2.80 \times 10^{-11}$  to  $6.39 \times 10^{-9}$  at the mean value of  $S_{ppm} = 8.287 \times 10^{-10}$ . In **Figure 18(b)**, the mean value is shown with a dashed line. Here again, the dominating spin direction cannot be identified on the spin projection graphs.

The spin of the central body,  $S_{p1} = 2.13 \times 10^{-7}$ , is 257 times greater than the average spin of the peripheral body. Simultaneously, the total spin of the system (**Table 2**) is  $S_s = 2.29 \times 10^{-7}$ . Therefore, the projection of the spin of the central body determines the direction of the entire spin of the system. The spin makes an angle  $\beta_3 = 56^\circ$  with the  $z$ -axis, while the orbital momentum vector is inclined to this axis by an angle  $\beta_3 = 94^\circ$ . In this case, if one look from the end of the  $z$ -axis onto the  $xy$ -plane, then the total orbital motion will proceed in clockwise direction, and the total rotational motion, counterclockwise.

The thermal energy of peripheral bodies varies from  $5.46 \times 10^{-6}$  to  $6.45 \times 10^{-3}$ , *i.e.* by 1180 times, with the average thermal energy of one body being equal to  $E_{tpm} = 9.44 \times 10^{-4}$ . The thermal energy of the central body is  $E_{ta} = 0.762$ , and that of all bodies,  $E_{ts} = 0.995$ . Thus, the central body makes the main contribution to the thermal energy of the system.

The number of merged bodies in the 15-layer structure is  $N_u = 140$  (**Figure 18(c)**). Here, four bodies have merged with the central body. The spin modules of peripheral bodies vary from  $1.73 \times 10^{-10}$  to  $3.75 \times 10^{-9}$  at an average value of  $S_{ppm} = 1.29 \times 10^{-9}$ . The  $S_{ppm}$ -value is shown in **Figure 18(c)** with a dashed line.

The spin of the central body is  $S_{p1} = 8.99 \times 10^{-7}$ , *i.e.* it exceeds the spin of the peripheral body by 696 times. Simultaneously, the total spin of the system (see **Table 2**) is  $S_s = 9.07 \times 10^{-7}$ , *i.e.* it is almost completely due to the central body. The total spin vector and, consequently, the spin of the central body makes an angle  $\beta_3 = 120.7^\circ$  with the  $z$ -axis. Thus, the total rotational motion with respect to the  $z$ -axis proceeds in clockwise direction, and the total orbital motion with angle  $\beta_3 = 87$  proceeds in an almost vertical plane. The ratio of the total spin to the total angular momentum is  $1.15 \times 10^{-5}$  (see **Table 2**).

The thermal energy of peripheral bodies varies from  $2.25 \times 10^{-5}$  to  $6.46 \times 10^{-3}$

with an average value of  $E_{ipm} = 1.56 \times 10^{-3}$ . The thermal energy of the central body is  $E_{\alpha} = 0.149$ , and that of all bodies is  $E_{is} = 0.366$ . The energy  $E_{\alpha}$  is five times lower than the thermal energy of the central body in the 10-layer structure, despite the fact that there occurred four collisions with the central body. This fact indicates that the collision in the 10-layer structure has occurred at a higher velocity of the peripheral body. In this structure, the spin of the central body is four times less than that in the 15-layer structure. This indicates that the collision in the former structure was more frontal, while the collisions in the latter structure were closer to those occurring along tangential lines.

#### 8.4. Constellations in the Structures

In the images of structures at the final time (**Figure 4**, **Figure 7** and **Figure 12**), we observe close arrangements of bodies to each other involving two, three or more bodies. Some of these arrangements may be due to the coincidence of their visual lines at a sufficiently large distance between the bodies. Another fraction may be due to the short-term convergence of bodies in visual images. However, there may be cases when the bodies form stable associations, that is, constellations. In order to identify constellations in the output files of the Galactica system, a Constns.for program was developed. The output file of Galactica contains the coordinates of bodies at time  $T$ . The output files are generated after a set number of integration steps K13. The Constns.for program determines the number of bodies with numbers  $i$  for which there are bodies with numbers  $k$  located at a distance  $R_{ik} \leq d_{max}$  from body  $i$ . For each body  $i$ , one can find up to six bodies numbered  $k$  with their distances  $R_{ik}$ . The total number of all nearby bodies  $k$  is determined without any restriction, but their numbers and distances  $R_{ik}$  are not memorized.

**Figure 19(a)** shows the results of calculations performed using this program for the ten-layer structure at the final time  $T = 0.815$  for  $d_{max} = 0.003$ . This value of  $d_{max}$  corresponds to the distance between the bodies on the line of their location at time  $T = 0$  (**Figure 7(a)**). For choosing this distance, the distances between closely spaced bodies in **Figure 7(b)** were measured. This distance turned out to be close to 0.003.

Along the horizontal axis, **Figure 19(a)** shows the numbers of bodies  $i$ , and along the vertical line, the numbers of bodies  $k$ . All in all,  $N_{is} = 1032$  bodies  $i$  were found among the total number of bodies in the structure,  $N = 5451$ . If body  $i$  has several close bodies  $k$ , this number of bodies is marked in the graph by the number of points along the vertical line of body  $i$ . The largest number of bodies  $i$  had one close body each, and the smallest, five bodies. There were two such bodies.

It should be noted that the number  $N_{is} = 1032$  includes all bodies that have a close body. Therefore, if each body has one close body, then there will be  $1032/2 = 516$  constellations, and if each body has two close bodies, then there will be  $1032/3 = 344$  constellations, etc.

From **Figure 19(a)**, it is seen that for all bodies, starting from the body  $i = 1000$ , the number of close bodies  $k$  is concentrated on the diagonal line. In



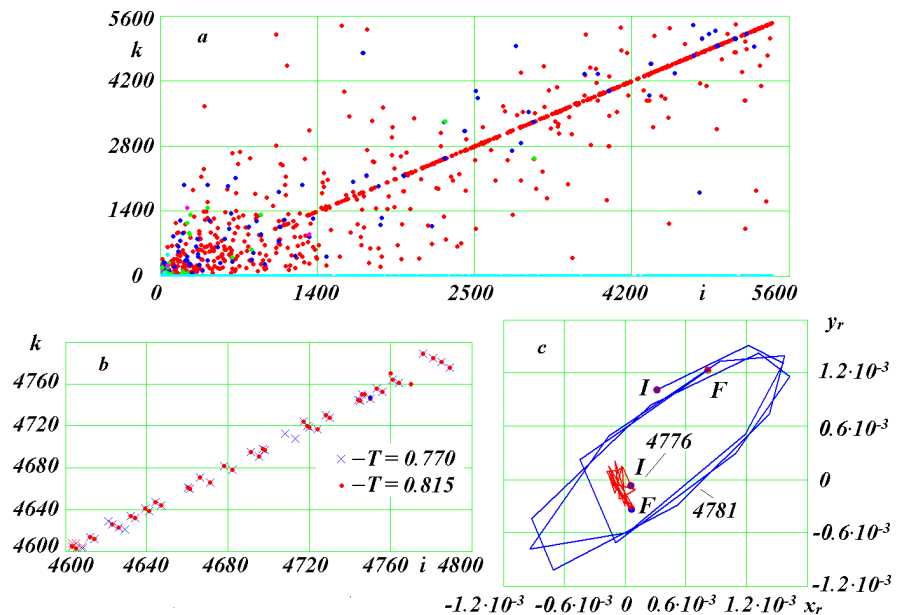


**Figure 19.** Numbers of nearby bodies  $k$  for bodies  $i$  ((a), (b)) and the relative trajectories of bodies in constellations (c) for the ten-layer structure MS10c99b.

**Figure 19(b)**, for bodies  $i = 4600 - 4800$  the graph of nearby bodies is shown on an enlarged scale. The points show the location of bodies at time  $T = 0.815$ . It is seen from the graph that on the diagonal line the bodies  $k$  have numbers close to those of bodies  $i$ . As already noted, the close positions of the bodies determined at the time  $T = 0.815$  may appear occasional. To make sure that these close positions are not occasional, but form constellations, we have to repeat such calculations for another point in time. The results of the calculation for the previous time  $T = 0.770$  are shown with symbols “x”. Most of them coincide with the points for  $T = 0.815$ . Out of 41 cases, there are no matches in only three cases. Therefore, we can assume that in 38 cases of close locations, constellations appear. Of the 38 cases, three are different. Body 4746 has a nearby body 4750; body 4747 has two nearby bodies, 4750 and 5409; and body 4750 also has two nearby bodies, 4746 and 4747. This situation was also confirmed for  $T = 0.770$ . Therefore, the bodies 4746, 4747, 4750 and 5409 form a constellation of four bodies. It follows from here that in the region of bodies  $i = 4600 - 4800$  there are 17 constellations formed by two bodies and one constellation formed by four bodies. In total, out of 200 bodies  $i$  in **Figure 8(b)** there are 18 constellations. Thus, the total number of constellations can be estimated as  $18/200 = 0.09$  of the total number of bodies. Then, there must be  $0.09 \cdot N = 491$  constellations in the ten-layer structure. This estimate is close to the number 516 that was estimated previously from the number of encounters with one body. Therefore, we can assume that up to 9% of all bodies in the structure can form constellations.

The above-mentioned constellation 4746 - 5409 involving four bodies 4746, 4747, 4750 and 5409 is shown in **Figure 20**. Its position at time  $T = 0.770$  is marked with the velocity vectors of bodies 4746 and 5409. The position of this

constellation at the final time  $T = 0.815$  is also shown in **Figure 7(b)**. Evidently, during this time the constellation has moved on the sphere by about  $90^\circ$ .

In this constellation, body 4747 has double mass, and the rest of the bodies have one mass  $m_1$  each. When viewed on a larger scale, body 4747 is in the center, and the rest of the bodies surround it.

Bodies with a mass of  $5m_1$  do not form constellations. Most constellations are created with masses  $m_1$ . In **Figure 19(a)**, there are four cases of bodies  $i$  with mass  $4m_1$ , 13 cases with mass  $3m_1$ , and 76 cases with mass  $2m_1$ . The number of constellations with these bodies will be slightly less, since several bodies with increased masses can enter one constellation.

In the upper right corner of **Figure 19(b)**, four bodies, 4776, 4781, 4785 and 4789, attract attention; one of those bodies, namely, body 4789, has a twice increased mass. It turned out that these bodies form two pairs: 4776 - 4789 and 4781 - 4785. As evident from **Figure 20**, at time  $T = 0.770$  these pairs occupy position in different places of the 10-layer structure. Based on 20 points, starting from the time  $T = 0.7167$ , relative trajectories of the bodies of interest were analyzed: that of body 4776 relative to body 4789 and that of body 4781 relative to body 4785. **Figure 19(c)** shows the relative trajectories of these bodies, *i.e.* 4776 and 4781, as projected onto the  $xy$ -plane. Relative coordinates are denoted as  $x_r$  and  $y_r$ . From the initial point  $I$  to the final point  $F$ , body 4781 makes a little more than three revolutions around body 4789. The average interval between the points is  $\Delta T = 5.195 \times 10^{-3}$ . The orbit of body 4781 is an ellipse with semi-axis  $a = 1.69 \times 10^{-3}$  and eccentricity  $e = 0.255$ . The orbital period is  $P = 0.0325$ .

The orbit of body 4776, from the initial point  $I$  to the final point  $F$ , is represented with intersecting segments, since the period of revolution of this

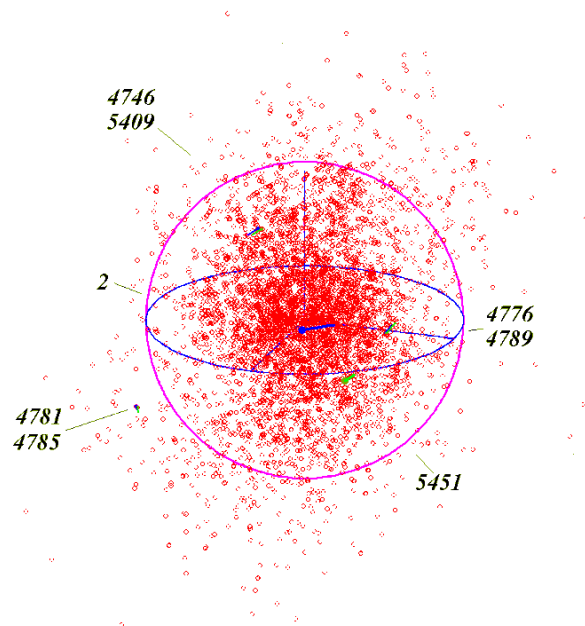


**Figure 20.** Position of three constellations 4746 - 5409, 4776 - 4789, and 4781 - 4785 in the ten-layer structure MS10c99b at time  $T = 0.770$ .

body is comparable with the interval  $\Delta T$  between the points. The orbit of the body is an ellipse with axis  $a = 3.12 \times 10^{-4}$  and eccentricity  $e = 0.513$ . The period of revolution of body 4776 is given by formula (8). It equals  $P = 3.15 \times 10^{-3}$ , a value ten times shorter than the period of revolution of body 4781. During this time interval, body 4776 makes 31 revolutions about body 4789. The position of these two constellations at time  $T = 0.770$  is shown in **Figure 20**, and at the final time  $T = 0.815$ , in **Figure 7(b)**. During this time interval, the motion of these constellations over the sphere has occurred through an angle of not more than  $45^\circ$ .

Calculations were performed using the Constns.for program with a doubled distance  $d_{max} = 6 \times 10^{-3}$ . For time  $T = 0.815$ , 2650 bodies  $i$  that approached other bodies  $k$  to a distance  $d \leq d_{max}$  were identified. In this case, the number of bodies  $k$  reached 19 for body  $i = 93$ . For time  $T = 0.770$ , there were 2715 bodies  $i$  with the largest number of bodies  $k$  equal to 17 for body  $i = 84$ . For this case, the selected first few bodies were not confirmed for the time  $T = 0.815$ . Over the interval of change of bodies  $i = 4600 - 4800$  (**Figure 19(b)**), the cases of discrepancy noted earlier have coincided in this case. Thus, a twofold increase in the distance  $d_{max}$  makes it possible to identify constellations with more distant bodies and with a large number of such bodies.

Similar calculations were also performed for the 5- and 15-layer structures. For the five-layer structure, at the final time  $T = 1.96$ , at  $d_{max} = 3.16 \times 10^{-3}$ , 367 bodies  $i$  approaching other bodies  $k$  to a distance  $R_{ik} \leq d_{max}$  were identified. The number of bodies  $k$  reached 5. The distribution of bodies on a graph similar to that of **Figure 19(a)** was more uniform, and there was no concentration of bodies along the diagonal line.

For the 15-layer structure with  $d_{max} = 5.3 \times 10^{-3}$ , at the final time  $T = 0.780$ , 1843 bodies  $i$  that approached other bodies  $k$  to a distance  $R_{ik} \leq d_{max}$  were identified. The largest number of bodies  $k$  was 7. The distribution of bodies in a graph similar to **Figure 19(a)** was also more uniform, but with lower concentrations of bodies near the diagonal line. The diagonal line could also be traced, but it started from  $i = 2000$ .

## 9. Structure Scaling

### 9.1. Dimensionless Parameters of Structures

As noted above, in the MLSpStr2.for program, files of structures with initial conditions are created in dimensionless form using parameters  $m_{sp}$ ,  $A_m$ , and  $k_i$  [25]. The dimensionless parameters of the structures are indicated in **Table 3**. Here, the number of bodies  $N$  varies from 1488 to 29,701; the mass of the central body  $m_0$ , from 0.8683 to 0.1427; the mass of peripheral bodies  $m_1$ , from  $9.332 \times 10^{-5}$  to  $2.532 \times 10^{-5}$ ; the radius of the central body  $R_{a_0}$ , from  $2.171 \times 10^{-5}$  to  $3.965 \times 10^{-5}$ ; the radii of peripheral bodies  $R_{a_i}$ , from  $1.220 \times 10^{-6}$  to  $1.884 \times 10^{-6}$ ; the semi-axis of the orbit of first-layer bodies  $a_1$ , from 0.0149 to 0.008587; and the semi-axis of the orbit of last-layer bodies  $a_{N_2}$ , from 0.0652 to 0.2427. All struc-

tures have a dimensionless mass  $m_{ss} = 1$  and the same period of revolution of first-layer bodies,  $P_1 = 0.01$ . The period of revolution of last-layer bodies  $P_{N_2}$  varies from 0.1046 to 0.7475.

As already noted, the dimensional semi-axes of these structures are identical, and the dimensional masses of peripheral bodies in the 5-, 10-, and 24-layer structures are also identical. In the 15- and 34-layer structures, the masses are twice as large. Yet, the dimensionless semi-axes and the masses of bodies are different in all structures. The passage to dimensionless quantities is related with the masses of structures, and those masses are different. Thus, the identical dimensional parameters in dimensionless form also become different.

The last column of **Table 3** indicate the relative outer radius  $r_{95rN_2}$  of the structures whose evolution was studied. This radius was determined at the final time as the largest distance from the center of mass of 95% of the bodies, *i.e.* this is the size of the structure with 95% confidence. Evidently, for all structures the value of  $r_{95rN_2}$  is approximately the same, with an average value  $r_{95rN_2,m} = 1.662$ . Only 5% of all bodies are located at a distance from the center larger than  $r_{95rN_2,m}$ .

**Table 3.** Dimensionless parameters of the structures used in modeling spherical star clusters: the dimensionless mass of the structure is  $m_{ss} = 1$ ; the rotation period of first-layer bodies  $P_1 = 0.01$  is the same for all structures.

Structures	$N$	$m_0$	$m_1,$ $\times 10^{-5}$	$Ra_0,$ $\times 10^{-5}$	$Ra_1,$ $\times 10^{-6}$	$a_1,$ $\times 100$	$a_{N_2}$	$P_{N_2}$	$r_{95rN_2}$	$T_{kin}$	$-U$	$R_v$
MS05c99e	1488	0.8683	8.859	3.965	1.853	1.304	0.0652	0.1046	1.753	1.564	3.105	0.161
MS10c99b	5451	0.6426	6.557	3.586	1.676	1.179	0.1179	0.2535	1.522	2.169	4.260	0.117
MS15c49b	5866	0.4527	9.332	3.189	1.884	1.049	0.1573	0.3911	1.591	2.148	4.222	0.118
MS24c99b	29701	0.2481	2.532	2.611	1.220	0.8587	0.2061	0.5834	-	1.840	3.605	0.139
MS34c49b	29156	0.1427	2.941	2.171	1.282	0.7138	0.2427	0.7475	-	1.539	3.048	0.164

### 9.2. Scale Transition Algorithm

Based on the dimensionless parameters summarized in **Table 3**, we calculate the dimensional parameters of five models of globular star clusters. We set the peripheral-body mass to half the mass of the Sun:  $m_{1,m} = 0.5 m_\odot$ . In the center of globular constellations, the density of stars can reach 100 to 1000 stars per cubic parsec [7]. With this in mind, for all models in dimensional form, we set the semi-axis of the orbit of first-layer bodies to  $a_{1,m} = 0.2$  pc, where one parsec (pc) is  $3.0856776 \times 10^{16}$  m.

Taking into account the values of the dimensionless masses in **Table 3**, the dimensional central-body mass will be

$$m_{0,m} = m_{1,m} \cdot m_0 / m_1, \tag{45}$$

and the dimensional mass of the entire structure,

$$m_{ss,m} = m_{0,m} + (N - 1) \cdot m_{1,m}. \tag{46}$$

Given the semi-axis of the orbit of first-layer bodies  $a_{1,m}$ , the geometric scale is

$$A_{m,m} = a_{1,m} / a_1 . \tag{47}$$

With the help of this scale, we find the semi-axis of the orbit of last-layer bodies  $a_{N2,m} = A_{m,m} \cdot a_{N2}$ . Given the values of  $A_{m,m}$  and  $m_{ss,m}$ , formula (27) can be used to determine the time factor:

$$k_{t,m} = \sqrt{G \cdot m_{ss,m} / A_{m,m}^3} . \tag{48}$$

The velocity coefficient  $k_{v,m}$  is calculated by formula (42). Using these coefficients, converting the angular momentum and energy to dimensionless form, we obtain expressions for their scale factors:

$$k_M = \frac{k_{v,m}}{A_{m,m} m_{ss,m}} ; k_E = \frac{(k_{v,m})^2}{m_{ss,m}} . \tag{49}$$

With the help of scale factors, the transition from dimensionless quantities to dimensional ones is carried out. For example, the dimensional period of revolution of outer-layer bodies is calculated as follows:  $P_{N2,m} = P_{N2} / k_{t,m}$

### 9.3. Dimensional Parameters of Simulated Globular Clusters

**Table 4** indicates the scale factors and dimensional values of globular clusters modeled with five multilayer structures. The body masses are given in solar masses; the semi-axes, in parsecs; and periods are in years. The last column gives the number of stars in a cubic parsec at the initial time. This value is defined as follows:

$$n_{pk} = \frac{3N}{4\pi (a_{N2,m})^3} . \tag{50}$$

The density of stars  $n_{pk}$  in **Table 4** changes from 355 for the 5-layer structure to 22 for the 34-layer structure. Since these are average densities, these values correspond to the observed densities of stars in the center of globular star clusters.

The revolution periods of stars in the first layer  $P_{1,m}$  vary from 120 to 170 thousand years (**Table 4**), and the revolution periods of stars in the last layer  $P_{N2,m}$ , from 1.2 to 12.7 million years. The periods of revolution of stars in constellations are much shorter than in the outer layer. For instance, in the ten-layer structure the period of revolution of body 4781 relative to body 4785 is 388 thousand years (**Figure 19(c)**), and that of body 4776 about body 4788 is 37.6 thousand years.

Taking into account the average value of  $r_{95rN2m}$  the diameter of these globular star clusters  $D_g = 2 \times 1.622 \times r_{95rN2m}$  varies from 3.2 pc for the 5-layer structure to 22 pc for the 34-layer structure. The diameter of observed globular star clusters varies from 20 to 100 pc, and the number of stars in them, from  $10^4$  to  $10^5$  [7]. Evidently, the globular cluster models based on the 24- and 34-layer structures satisfy these parameters.

The shape of the observed globular star clusters may differ from spherical, so such clusters are characterized by ellipticity [2]. Ellipticity is defined as the difference between the largest and smallest diameters, divided by the largest di-

ameter. In our Galaxy, the clusters NGC 7492, NGC 6144 and NGC 6273 have ellipticity of 0.24, 0.25 and 0.27, respectively [2]. The highest ellipticity of the simulated clusters, equal to 0.6, was exhibited by the 5-layer cluster. For other models, with an increase in the number of layers, the ellipticity approaches zero.

**Table 4.** Dimensional parameters of globular star clusters modeled with multilayer structures with the semi-axis of first-layer bodies  $a_{1,m} = 0.2$  pc and star mass  $m_{1,m} = 0.5 m_s$ , where 1 parsec (pc) =  $3.0856776 \times 10^{16}$  m. The solar mass is  $m_s = 1.989118 \times 10^{30}$  kg.

Structures	$m_{0,m^p}$ $m_s$	$m_{ss,m^p}$ $m_s$ $\times 10^3$	$A_{m,m^p}$ m, $\times 10^{17}$	$k_{t,m^p}$ 1/s, $\times 10^{-15}$	$k_{v,m^p}$ s/m, $\times 10^{-3}$	$a_{N2,m^p}$ pc	$P_{1,m^p}$ years, $\times 10^5$	$P_{N2,m^p}$ years, $\times 10^6$	$n_{pk}$ 1/pc <sup>3</sup>
MS05c99e	4901	5.644	4.733	2.658	0.7948	1	1.192	1.247	355
MS10c99b	4900	7.625	5.234	2.656	0.7192	2	1.193	3.024	163
MS15c49b	2426	5.358	5.883	1.869	0.9095	3	1.696	6.631	52
MS24c99b	4899	19.75	7.187	2.657	0.5236	4.8	1.192	6.957	64
MS34c49b	2426	17.00	8.646	1.869	0.6189	6.8	1.696	12.68	22

It is also noted [7] that deformation tails were found in the shape of all globular clusters for which high-quality optical images were obtained; in other words, there are deviations from spherical symmetry. Therefore, we may assume that the asymmetry of the 10-layer and 15-layer models of globular clusters in **Figure 7(b)** and **Figure 12(b)** is their quite acceptable shape.

In order to verify the results of the scale transition, the period of revolution of first-layer bodies was calculated from the dimensional parameters according to formula (8). In formula (8) for a circular orbit we have  $\alpha_1 = -1$ , the pericenter radius is  $R_p = a_1$ , the pericenter velocity  $v_p$  can be calculated by formula (9), and the interaction parameter  $\mu_1$ , by formula (6). Thus, the periods of revolution calculated up to the units of the fourth decimal place proved to be coincident with the periods calculated using the scaling approach.

The presented parameters of globular cluster models are of interest to scientists who develop cluster models based on an analysis of their brightness. These models are based on the Virial Theorem  $-U/T_{kin} = 2$ , where  $U$  is the potential energy of the cluster and  $T_{kin}$  is its kinetic energy. They are defined in a known manner; see for example equation (1.2) in [13]. Dimensionless values of  $T_{kin}$  and  $-U$  are given in **Table 3**, from which it follows that the ratio  $-U/T_{kin}$  varies from 1.960 to 1.986, *i.e.* is close to 2.

The total mechanical energy  $E = T_{kin} + U$  in the process of evolution of the presented models towards the end slightly decreases in absolute value in the 5-layer structure by 0.02%, in the 10-layer structure by 1.2%, and in the 15-layer structure by 0.87%. In statistical modeling of clusters, one important scale is the virial radius  $R_v = G \cdot m_{ss}^2 / (2|U|)$  [5]. As can be seen from **Table 3**, the value of  $R_v$  almost completely coincides with the outer radius  $a_{N2}$  for a 10-layer structure; in other cases,  $R_v$  is greater or less than  $a_{N2}$ .

### 9.4. The Rotation Periods of Stars and Their Temperatures

When considering the approaches and collisions of bodies in the three studied structures, the maximum spins and thermal energies were reported. In addition, the maximum values of velocities  $v_{mx}$  were indicated. With the help of scale factors, we find the dimensional values of the velocities, the periods of rotation of merged bodies  $P_{rp}$  and the increase in their temperature  $\Delta t$ . For determining the radii of stars in globular star clusters, we specify their average density  $\rho_{gk} = \rho_s = 1.406 \times 10^3 \text{ kg/m}^3$ , where  $\rho_s$  is the average density of the Sun. Then, the dimensional radii of the bodies can be determined from their dimensional masses  $m_m$ :

$$Ra_m = \left( \frac{3m_m}{4\pi\rho_{gk}} \right)^{1/3}. \quad (51)$$

The moments of inertia of bodies are defined as for a homogeneous globe:

$$J_m = 0.4m_m \cdot Ra_m^2. \quad (52)$$

The dimensional spins and thermal energies are calculated using the scale factors

$$S_{p,m} = S_p/k_M; \quad E_{t,m} = E_t/k_E. \quad (53)$$

Then, the dimensional periods of rotation of stars are defined as follows:

$$P_{rt,m} = 2\pi J_m / S_{p,m}. \quad (54)$$

For calculating the heating temperature  $\Delta t$  of merged stars, we specify their specific heat equal to the specific heat of water  $C_t = 1.183 \times 10^3 \text{ J/(kg-deg)}$ . Then, the increase in the temperature of merged bodies will be:

$$\Delta t = E_{t,m} / (m_m \cdot C_t). \quad (55)$$

The results of calculations performed according to these formulas are summarized in **Table 5**. The first five columns indicate the dimensionless spins, the thermal energies, and the maximum velocities. The values with subscript "0" refer to the central body, and those with subscript "1", to peripheral bodies. For a peripheral body, the maximum values of spins and thermal energies are given. These bodies with the maximum parameters in the 5- and 15-layer structures have doubled masses, and in the 10-layer structure, the body mass is  $5m_1$ . As already noted, bodies located near the center of structures have a maximum dimensionless velocity  $v_{mx}$ .

In the last five columns of **Table 5**, the dimensional values are given. The periods of rotation of the central body  $P_{r0,m}$  vary from 2 to 17 days, while the period of rotation of the peripheral body ( $P_{r1,m}$ ) reach thousandths of a day, which is equivalent to several minutes. The heating temperature of the central body  $\Delta t_0$  varies from several hundred to two thousand degrees, while that of the peripheral body ( $\Delta t_1$ ) reaches several tens of thousands of degrees. In the central region of the clusters, the highest velocity of star motion is equal to two tens of kilometers per second.

With the masses of bodies used in the models of globular star clusters, their

relative radii do not coincide with the relative radii at which the problem of interaction of bodies (28) was solved. Their rotation periods and temperatures  $\Delta t$  depend on the body radii. To make sure that the values in **Table 5** are reliable, the periods of rotation and temperatures were calculated for the initial dimensional radii of the bodies.

**Table 5.** Star rotation periods  $P_{rt}$  in days, the collision-induced heating temperatures  $\Delta t$  of stars in Kelvins, and the maximum velocities  $v_{mx}$  in km/s of stars in globular star clusters modeled with multilayered structures (in km/s).

Structures	Dimensionless quantities					Dimensional quantities				
	$S_{p0},$ $\times 10^{-7}$	$S_{p1},$ $\times 10^{-9}$	$E_{t0}$	$E_{t1},$ $\times 10^{-3}$	$v_{mx}$	$P_{rt0,mp}$ days	$P_{rt1,mp}$ days, $\times 10^{-3}$	$\Delta t_0,$ K	$\Delta t_1,$ K, $\times 10^{+4}$	$v_{mx,m}$ km/s
MS05c99e	-	2.71	-	3.24	14.3	-	1.549	-	2.447	17.99
MS10c99b	2.13	6.39	0.762	6.45	17.7	16.87	1.832	1938	3.215	24.61
MS15c49b	8.99	3.75	0.149	6.46	16.9	1.982	1.085	336.3	3.537	18.58

On average, the temperatures proved to be ten times higher. The temperatures are proportional to the squares of body velocities. At the initial parameters, the velocities are three times higher, which fact explains one order of magnitude higher temperatures.

At the initial parameters, the rotation periods were 60 times longer. The periods of rotation are inversely proportional to body velocities, and they vary in proportion to the squares of body radii. The radii of the bodies with the initial parameters are 15 times smaller. This explains the 60-fold increase in periods.

Thus, in order of magnitude, the increase in the temperature of stars and their periods of rotation in the models of globular star clusters presented in **Table 5** adequately reflect these properties of stars.

The processes of merging of bodies depend on their radii. The connection of radii with body masses differs from the connection of distances with masses in the interaction Equation (28). That is why for more accurate modeling of body parameters during the merging of bodies, it is necessary to specify the radii of bodies corresponding to the simulated star system.

The rotation periods and temperatures of peripheral bodies presented in **Table 5** are extreme. As it was shown in Section 8.3, the minimum values of spins and thermal energies are one or two orders of magnitude smaller. Therefore, on average, the temperatures  $\Delta t_1$  for peripheral bodies can be expected to have several times lower, and the rotation periods  $P_{rt1,mp}$  several times larger values.

### 9.5. Central-Body Models

One of the main problems concerning such stellar associations as globular star clusters and galaxies is the central-body mass: how big should it be? For the problem of interaction of bodies of a plane axisymmetric structure [18] [33],



there is an exact solution in the absence of a central body, that is, for  $m_0 = 0$ . However, such a structure is unstable. As a result of numerical experiments with a single-layer spherical structure [20] [21], it was found that such structures can be created with a relative central-body mass  $p_{m_0} < 0.95$ . Therefore, multilayer structures were created with certain margins at  $p_{m_0} = 0.99$ .

In a multilayer structure, the central-body mass, related to the mass of the entire structure, decreases with an increase in the number of layers from  $m_0 = 0.87$  for the five-layer structure to  $m_0 = 0.14$  for the 34-layer structure (Table 3). However, the dimensional central-body mass  $m_{0,m}$  remains equal to thousands of solar masses (Table 4). When modeling globular clusters, other researchers also obtain such masses of the central bodies [9]. However, in order to reduce the central-body mass, we will replace it with a model in the form of a multilayer structure similar to the above-considered structures. Let the mass of such a structure be equal to the central-body mass

$$m_{ss3,m} = m_{0,m} \tag{56}$$

and the outer semi-axis of the orbit is the fraction, equal to  $k_{a1}$ , of the semi-axis of the inner layer of the globular cluster:

$$a_{N23,m} = k_{a1} \cdot a_{1,m} \tag{57}$$

Here, the subscript “3” denotes the parameters of the model of the first central body. Subsequently, there will be more models of other central bodies. Two conditions (56)-(57) uniquely determine the parameters of this model.

**Table 6.** Models of central bodies in the form of multilayer structures under conditions (56)-(57) with  $k_{a1} = 0.5$ .

Structures	Models of the 1 <sup>st</sup> central body				Models of the 2 <sup>nd</sup> central body			
	$m_{03,m}$ $m_s$	$m_{13,m}$ $m_s$	$P_{13,m}$ years,	$P_{N23,m}$ years, *10 <sup>4</sup>	$m_{04,m}$ $m_s$	$m_{14,m}$ $m_s$	$P_{14,m}$ years,	$P_{N24,m}$ years
MS05c99e	4255	0.4341	4045	4.231	3695	0.3770	137.3	1436
MS10c99b	3149	0.3213	1664	4.217	2024	0.2065	23.20	588.2
MS15c49b	1073	0.2306	1534	5.998	474.7	0.1020	14.03	548.8
MS24c99b	1216	0.1240	719.9	4.200	301.6	0.0308	4.346	253.6
MS34c49b	346.1	0.0713	800.6	5.984	49.37	0.0102	3.780	282.6

Based on the parameters of the multilayer structures considered, central-body models were calculated. For a globular cluster model with  $N_2$  layers, a central-body model with the same number of layers was created. Table 6 summarizes the parameters of the models of the 1st central body with  $k_{a1} = 0.5$ , i.e. the outer size of the central-body model is equal to half the inner size of the multilayer structure. Given in Table 6 are the central-body mass  $m_{03,m}$  and the peripheral-body mass  $m_{13,m}$  (in solar masses), and the period of revolution of inner-layer bodies  $P_{13,m}$  and the period of revolution of outer-layer bodies  $P_{N23,m}$  (in

sidereal years). For the five-layer model, the central-body mass  $m_{0,m}$  has decreased from 4901 (Table 4) down to 4255 solar masses (Table 6), *i.e.*, this is an insignificant decrease. For the 34-layer structure, the central-body mass has decreased from 2426 to 346.1 solar masses, that is, by a factor of 7. In this structure, the peripheral bodies have a mass of  $m_{1,m} = 0.5$  solar masses, and in the central-body model, the peripheral-body mass is  $m_{13,m} = 0.0713$  solar masses. That is, also 7 times less. The period of revolution of bodies on the inner layer is  $P_{13,m} = 800.6$  years, and on the outer layer,  $P_{N23,m} = 59,840$  years. These periods are 212 times shorter than the corresponding periods in the globular cluster model (Table 4).

This central-body model models the central body of a multilayer structure, *i.e.* this is the model of the first central body. The central-body model also has a central body, *i.e.* this is a second central body. This body can also be substituted with a multilayer model according to conditions similar to (56)-(57). Table 6 summarizes the parameters of the model of the 2<sup>nd</sup> central body; those parameters are marked with the subscript "4". The mass of the 2<sup>nd</sup> central body  $m_{04,m}$  for its 34-layer model has decreased most significantly, namely, also by 7 times with respect to  $m_{03,m}$ . The peripheral-body mass  $m_{14,m}$  has decreased by the same factor. The periods of revolution  $P_{14,m}$  and  $P_{N24,m}$  have also decreased by 212 times compared to the corresponding periods of the model of the first central body.

In these central-body models with two 34-layer structures, the central-body mass is 49.37 solar masses. If we additionally use the model of a 3rd central body, then the central-body mass will be further decreased to seven solar masses. In this case, the central body will be surrounded by 34 layers of revolving bodies with a mass equal to one and a half Jupiter masses. On the inner layer, the period of revolution of bodies will be 6.5 days, and on the 34<sup>th</sup> layer, 1.3 years. There will be 29,155 peripheral bodies in total. Then, the same number of bodies with a mass equal to 0.0102 solar mass will be located in 34 layers with periods of revolution of 3.78 years in the 35<sup>th</sup> layer and 282.6 years in the 68<sup>th</sup> layer. The next 29,155 bodies with a mass of 0.0713 solar mass are located in 34 layers with periods of revolution of 800.6 years in the 69<sup>th</sup> layer and 59.84 thousand years in the 102nd layer. The 34 outer layers of this globular cluster contain 29,155 stars with a mass of 0.5 solar mass and periods of revolution of 169.6 thousand years in layer 103 and 12.68 million years in layer 136. All in all, this cluster contains 116,620 peripheral bodies revolving around the central body with a mass equal to 7 solar masses. The radius of the first layer is 0.13 AU, and that of the 136<sup>th</sup> layer, 6.8 pc, or  $2.06 \times 10^5$  AU. As it was already noted, the period of revolution of first-layer bodies here is 6.5 days, and that of bodies in the last layer, 12.68 million years.

Bodies in the inner layer with a mass equal to 1.5 Jupiter masses are not the sources of radiation, so they will shield the central body from light. In layers, starting from the 35<sup>th</sup> layer, the mass of bodies will increase, and their luminosity will appear first in the infrared range, then in the red, and then in other spectral ranges.

The scaling of the results of the performed studies makes it possible to foresee such a hierarchically folded multilayer structure of a globular star cluster with a moderate central-body mass. The high velocities of bodies and their close arrangement on the inner layers can contribute to their more frequent collisions than in the structures considered; this circumstance can facilitate the destruction of such structures. Therefore, in order to make sure that such star clusters are possible, it is necessary to create their models and study their evolution. Such models can be created based on the multilayer structures whose evolution from the initially organized state to the steady state has already taken place, for example, based on the 15-layer MS15c49b.dat structure at the time  $T = 0.779$ . Then, the study of the evolution of such globular clusters will take much less time.

Unlike in the 34-layer structure, for the 15-layer structure it will be necessary to create not three but several more central-body models. For example, with seven such models, the peripheral-body mass on the inner layer will be equal to 2.2 Jupiter masses. In this case, the period of revolution of such a body will be eight orders of magnitude shorter, which raises doubts about the stability of such a structure.

With three central-body models, the peripheral-body mass in the inner layer will be 51.4 Jupiter masses, its semi-axis will be  $1.96 \times 10^{-2}$  pc, or 4047 AU, and the period will be  $9.13 \times 10^{-2}$  years, or 33.4 days. In this case, the central-body mass will be equal to 238 solar masses, *i.e.* a value ten times less than without the central-body model (Table 4). The globular cluster will contain 23,465 bodies, and the parameters of its 15 outer layers will be such as indicated in Table 4 for the 15-layer structure. Seemingly, such a hierarchical model of a globular cluster will be stable.

## 10. Discussion

Usually, at modeling of globular star clusters, for example using the NBODY 6 program, the evolution of the shape of the globular cluster is investigated and the change of its statistical characteristics are studied, for example, changes in the distribution of mass along the radius of the cluster. In this case, the internal dynamics of the globular cluster are not considered, the trajectories of the stars are not studied, the processes during their collision are not investigated, for example, the appearance of rotational motion of the stars and their thermal energy, etc.

In the present study, the N-body problem (28) was solved in dimensionless form. Therefore, its results can be applied to stellar associations of different scales, such as planetary systems, globular clusters and galaxies. However, the relative sizes of the bodies in these associations are different. Therefore, the characteristics of processes when bodies collide will be different. In further studies these circumstances will be taken into account.

## 11. Conclusions

A method has been developed for constructing models of globular star clusters in the form of multilayer spherical structures. In this case, the central body of the

structure and the layer surrounding it are adopted as a new central body, around which the next layer is located.

As a result of the interaction of stars, they collide and merge together, and some stars get ejected from the structure. At the first stage, the rate of collisions is kept at a certain level, then it decreases by several times or, sometimes, by several tens of times, and the stage of steady cluster dynamics begins. The stars move in quasi-elliptical orbits around the center of mass of the cluster. The periods of revolution of stars in orbits increase with the increase in orbit sizes. With close passages of stars, the orbits change and their position in space also changes. Sometimes stars collide with each other or with the central body. Individual stars, when passing very close to other stars, can acquire a high velocity and leave the cluster.

Some of the stars moving around the center of mass of the cluster can unite forming constellations. In a constellation, there is a relative motion of stars around its center of mass.

The orbits of stars are located in different planes. Their orbital angular momentum changes due to the interaction, but the angular momentum of the entire cluster remains unchanged. In magnitude, it can reach half the sum of the modules of the orbital momenta of all stars.

When stars merge together, they acquire additional rotation and temperature. The axes of revolution of stars have different directions. The total angular momentum of the rotational motion does not coincide in direction with the total orbital momentum, and in magnitude it is hundreds of thousands times smaller.

The existence of a globular cluster is due to the attraction of bodies to the central body and due to the mutual attraction of stars to each other. With an increase in the number of layers, the relative central-body mass decreases from 0.87 in clusters with five layers to 0.14 in clusters with 34 layers. However, in absolute terms this mass remains at the level of several thousand solar masses. The developed central-body models in the form of multilayer structures show that the central-body mass can be reduced by one or two orders of magnitude. However, the speed of movement of stars on the inner layers becomes large, and this can lead to the destruction of the whole cluster. Apparently, there must be a minimum mass of the central body below which a globular cluster can no longer exist.

## Acknowledgements

The evolution of multilayer structures was studied on supercomputers of the Central Shared-Use Center of the Siberian Supercomputer Center, ICM&MG SB RAS, Novosibirsk, Russia.

This research project was carried out under Contract Agreement No. FWRZ-2021-0007 with RAS.

## Data Availability

The Galactica system for solving the  $N$ -body problem and studying its results is

available at <http://wgalactica.ru/smull1/smulski/GalactcW/>. The program for creating multilayer structures and the structure files mentioned in this paper are available at <http://wgalactica.ru/smull1/smulski/Data/MLSpStr/>.

## Conflicts of Interest

The author declares no conflicts of interest regarding the publication of this paper.

## References

- [1] King, I.R., Hedemann, E.J., Hodge, S.M. and White, R.E. (1968) The Structure of Star Clusters. V. Star Counts in 54 Globular Clusters. *The Astronomical Journal*, **73**, 456-491. <https://doi.org/10.1086/110648>
- [2] Harris, W.E. (1996) A Catalog of Parameters for Globular Clusters in the Milky Way. *The Astronomical Journal*, **112**, 1487-1488. <https://doi.org/10.1086/118116>
- [3] Heggie, D. and Hut, P. (2003). The Gravitational Million-Body Problem. Cambridge University Press. <https://doi.org/10.1017/cbo9781139164535>
- [4] Orlov, V.V., Rubinov, A.V. (2008) N-Body Problem in Stellar Dynamics: Textbook. St. Petersburg State University.
- [5] Portegies Zwart, S.F., McMillan, S.L.W. and Gieles, M. (2010) Young Massive Star Clusters. *Annual Review of Astronomy and Astrophysics*, **48**, 431-493. <https://doi.org/10.1146/annurev-astro-081309-130834>
- [6] Heggie, D.C. (2014) Modelling and Understanding Globular Clusters. ISIMA.
- [7] Loktin, A.V. and Marsakov, V.A. (2009) Lectures on Stellar Astronomy. Educational and Scientific Monograph. Southern Federal University. (In Russian)
- [8] Llorente de Andrés, F. (2024) Some Old Globular Clusters (and Stars) Inferring That the Universe Is Older than Commonly Accepted. *American Journal of Astronomy and Astrophysics*, **11**, 1-13. <https://doi.org/10.11648/j.ajaa.20241101.11>
- [9] Baumgardt, H., Makino, J. and Hut, P. (2005) Which Globular Clusters Contain Intermediate-Mass Black Holes? *The Astrophysical Journal*, **620**, 238-243. <https://doi.org/10.1086/426893>
- [10] Mackey, A.D., Wilkinson, M.I., Davies, M.B. and Gilmore, G.F. (2008) Black Holes and Core Expansion in Massive Star Clusters. *Monthly Notices of the Royal Astronomical Society*, **386**, 65-95. <https://doi.org/10.1111/j.1365-2966.2008.13052.x>
- [11] Cuevas-Otahola, B., Mayya, Y.D., Puerari, I. and Rosa-González, D. (2020) Mass-Radius Relation of Intermediate-Age Disc Super Star Clusters of M82. *Monthly Notices of the Royal Astronomical Society*, **500**, 4422-4438. <https://doi.org/10.1093/mnras/staa3513>
- [12] Tully, R.B., Rizzi, L., Dolphin, A.E., Karachentsev, I.D., Karachentseva, V.E., Makarov, D.I., *et al.* (2006) Associations of Dwarf Galaxies. *The Astronomical Journal*, **132**, 729-748. <https://doi.org/10.1086/505466>
- [13] Aarseth, S.J. (2003). Gravitational N-Body Simulations. Cambridge University Press. <https://doi.org/10.1017/cbo9780511535246>
- [14] Baumgardt, H. (2016) *n*-Body Modelling of Globular Clusters: Masses, Mass-to-Light Ratios and Intermediate-Mass Black Holes. *Monthly Notices of the Royal Astronomical Society*, **464**, 2174-2202. <https://doi.org/10.1093/mnras/stw2488>
- [15] King, I.R. (1966) The Structure of Star Clusters. III. Some Simple Dynamical Mod-

- els. *The Astronomical Journal*, **71**, 64-75. <https://doi.org/10.1086/109857>
- [16] McLaughlin, D.E. (2000) Binding Energy and the Fundamental Plane of Globular Clusters. *The Astrophysical Journal*, **539**, 618-640. <https://doi.org/10.1086/309247>
- [17] Smulsky, J.J. (2019) The Upcoming Tasks of Fundamental Science. Sputnik+ Publishing House. (In Russian) <http://www.ikz.ru/~smulski/Papers/InfPrZaFN.pdf>
- [18] Smulsky, J.J. (2003) The Axisymmetric Problem of Gravitational Interaction of N-Bodies. *Math Modeling*, **15**, 27-36. (In Russian) <http://www.ikz.ru/~smulski/sm11/Russian1/IntSunSyst/Osvnb4.doc>
- [19] Smulsky, J.J. (2015) Exact Solution to the Problem of N Bodies Forming a Multi-Layer Rotating Structure. *SpringerPlus*, **4**, Article No. 361. <https://doi.org/10.1186/s40064-015-1141-1>
- [20] Smulsky, J.J. (2016) Distributed Structures on the Sphere. Deposited in VINITI 22.08.2016, No. 112-V2016. (In Russian) <http://www.ikz.ru/~smulski/Papers/SphDsSt2.pdf>
- [21] Smulsky, J.J. (2019) Periodic Orbits of N Bodies on a Sphere. *Cosmic Research*, **57**, 459-470. <https://doi.org/10.1134/s001095251906008x>
- [22] Smulsky, J.J. (2015) Multilayer Coulomb Structures: Mathematical Principia of Microcosm Mechanics. *Open Access Library Journal*, **2**, 1-47. <https://doi.org/10.4236/oalib.1101661>
- [23] Smulsky, J.J. (2012) Galactica Software for Solving Gravitational Interaction Problems. *Applied Physics Research*, **4**, 110-123. <https://doi.org/10.5539/apr.v4n2p110>
- [24] Smulsky, J.J. (2018) Future Space Problems and Their Solutions. Nova Science Publishers. <http://www.ikz.ru/~smulski/Papers/InfFSPS.pdf>
- [25] Smulsky, J.J. (2012) The System of Free Access Galactica to Compute Interactions of N-Bodies. *International Journal of Modern Education and Computer Science*, **4**, 1-20. <https://doi.org/10.5815/ijmecs.2012.11.01>
- [26] Smulsky, J. (2014) Module of System Galactica with Coulomb's Interaction. *International Journal of Modern Education and Computer Science*, **6**, 1-13. <https://doi.org/10.5815/ijmecs.2014.12.01>
- [27] Smul'skii, I.I. and Krotov, O.I. (2015) Change of Angular Momentum in the Dynamics of the Solar System. *Cosmic Research*, **53**, 237-245. <https://doi.org/10.1134/s0010952515020094>
- [28] Smulsky, J.J. (2019) Angular Momentum Due to Solar System Interactions. In: Gordon, O., Ed., *A Comprehensive Guide to Angular Momentum*, Nova Science Publishers, 1-40. [http://www.ikz.ru/~smulski/Papers/CGAngMom1\\_2Cv.pdf](http://www.ikz.ru/~smulski/Papers/CGAngMom1_2Cv.pdf)
- [29] Laskar, J. (1996) Marginal Stability and Chaos in the Solar System. *Symposium—International Astronomical Union*, **172**, 75-88. <https://doi.org/10.1017/s0074180900127160>
- [30] Laskar, J., Correia, A.C.M., Gastineau, M., Joutel, F., Levrard, B. and Robutel, P. (2004) Long Term Evolution and Chaotic Diffusion of the Insolation Quantities of Mars. *Icarus*, **170**, 343-364. <https://doi.org/10.1016/j.icarus.2004.04.005>
- [31] Melnikov, V.P. and Smulsky, J.J. (2009) Astronomical Theory of Ice Ages: New Approximations. Solutions and Challenges. Academic Publishing House "Geo". <http://www.ikz.ru/~smulski/Papers/AsThAnE.pdf>
- [32] Smulsky, J.J. and Smulsky, Y.J. (2012) Dynamic Problems of the Planets and Asteroids, and Their Discussion. *International Journal of Astronomy and Astrophysics*, **2**, 129-155. <https://doi.org/10.4236/ijaa.2012.23018>

- [33] Smulsky, J.J. (1999) The Theory of Interaction. Publishing House of Novosibirsk University. (In Russian) [http://www.ikz.ru/~smulski/TVfulA5\\_2.pdf](http://www.ikz.ru/~smulski/TVfulA5_2.pdf)
- [34] Smulsky, J.J. (2004) The Theory of Interaction. Cultural Information Bank. [http://www.ikz.ru/~smulski/TVEnA5\\_2.pdf](http://www.ikz.ru/~smulski/TVEnA5_2.pdf)

## Discussion

### I. Celestial Mechanics and Dynamical Astronomy

August 30th 2023, I uploaded my paper “Development of multilayer models of globular star clusters and study of their evolution” to Submission system (SNAPP) of the journal “Celestial Mechanics and Dynamical Astronomy” in Collection “Gravitational Stellar and Galactic Dynamics”. I am attaching the text of the cover letter below.

#### *Cover Letter 1*

The paper considers models of globular star clusters. Algorithms and programs have been developed that make it possible to create a globular star cluster that does not break down during their further gravitational interaction. The evolution of several models is considered by numerical solution of the N-body problem. We studied the dynamics of stars and their trajectories in various cases of interactions.

When stars collide, they merge and acquire angular momentum and thermal energy. These characteristics are used to determine the rotation periods and temperatures of the stars. In the process of interaction, several stars are combined into constellations. Their quantitative compositions, the trajectories of motion of stars in them have been studied, and their number in the models of globular clusters has been determined.

The models of the central body in the form of a set of bodies are considered. They make it possible to reduce the mass of the central body by 2–3 orders of magnitude.

Spherical dwarf galaxies, galactic nuclei and their surrounding halos also have a spherical shape. Since the studies were carried out both in dimensional and dimensionless form, many of the results obtained are also applicable to these objects.

The present work considers problems that belong to the field “Collection: Gravitational Stellar and Galactic Dynamics”, in particular to the following problems: Binary stellar dynamics, Engulfments and explosions in stellar systems, Stellar collisions, Galactic dynamics, Galaxy formation, Disk, bulge and halo dynamics.

-----  
On November 10, 2023, my paper was rejected in the following decision by the Journal.

**From:** Gravitational Stellar and Galactic Dynamics

**Sent:** Friday, November 10, 2023, 19:36 +05:00

**Subject:** Decision on your submission to Celestial Mechanics and Dynamical Astronomy

Ref: Submission ID 781af574-1e6b-4007-ab85-6ee479e3dcf2

Dear Dr. Smulsky,

Your manuscript entitled "Development of multilayer models of globular star clusters and study of their evolution" has now been assessed. If there are any reviewer comments on your manuscript, please find them below.

Regrettably, the above submission has been rejected for publication in Celestial Mechanics and Dynamical Astronomy.

Thank you for the opportunity to consider your work. I am sorry that we cannot be more positive on this occasion and hope you will not be deterred from submitting future work to Celestial Mechanics and Dynamical Astronomy.

Kind regards, Alessandra Celletti, Editor, Celestial Mechanics and Dynamical Astronomy

#### **COMMENTS FROM THE ASSOCIATE EDITOR:**

I'm afraid that the two expert reviewers have raised serious enough concerns about your manuscript such that it is not suitable for publication in Celestial Mechanics and Dynamical Astronomy. However, the detailed comments by each of the reviewers are useful and will hopefully be helpful for your future work.



*My comment:* Please note that some places in my published article have been changed. These changes will be noted in my responses to the reviewers.

### **Reviewer Comments:**

#### **Reviewer 1**

This work presents a model to evolve star clusters. The work is hefty in terms of number of pages, but it lacks rigour to make this a publishable paper. A new method to solve collisional dynamics needs to demonstrate a few basic tests:

1. For equal-mass systems, the core collapses after approximately 15 initial half-mass relaxation times (Cohn 1980). This contraction of the core is the result of energy exchange in interactions trying to establish isothermal conditions and the negative heat capacity of self-gravitating systems (Lynden-Bell & Eggleton 1980). No mention of core collapse is made, in fact, "collisions" are only mentioned in the context of physical collisions.
2. Mass segregation: when bodies have different masses, the more massive objects should migrate to the centre as the result of dynamical friction. No mention of the evolution of bodies with different masses is made.
3. A demonstration that energy is conserved and a comparisons to other (more time consuming) methods. I have also checked the paper by the author from 2012 in which the Galactica method is presented, and no such tests are presented there either.

Apart from these major concerns, some other concerning claims were made, such as globular cluster ages older than the age of the Universe.

#### **Reviewer 2**

##### ***General comment***

The manuscript presents an interesting method to model the initial conditions of a system of bodies that could be used to reproduce after dynamical evolution using Galactica the observed and expected features of stellar systems such as Globular Clusters and Galaxies. However, several major concerns should be addressed by the author in order to reconsider this article for its publication:

Some introductory sections lack classical references to classical works and more up-to-date ones (King, Baumgardt, and Heggie's works are necessary, however, other sources are missing that need to be included):

1. The extensive and useful review by Zwart et al. 2018, discussing some properties of Star Clusters in general, emphasizing its connection with younger clusters  
<https://arxiv.org/pdf/1002.1961.pdf>
2. The classical catalogue of Globular Cluster by Harris: Harris WE. 1996. AJ 112:1487
3. The work by Mackey et al. 2008 on the core expansion of clusters that describes how clusters could reach a Globular Cluster phase: <https://doi.org/10.1111/j.1365-2966.2008.13052.x>
4. The work by Cuevas-Otahola et al. 2021 describing how the relation between mass and radius from the initial phases of clusters may lead or not to a Globular Cluster configuration:  
<https://doi.org/10.1093/mnras/staa3513>
5. The work by Mc Laughlin et al. 2000 describing important properties of Globular Clusters and very relevant scaling relations: <https://iopscience.iop.org/article/10.1086/309247/fulltext/40856.text.html>

Following the previous point, the work requires more background regarding the clusters' evolution until they reach the Globular Cluster configuration, for which the previous works may settle the basis to include such a background.

The use of Wikipedia is completely discouraged since it is not peer-reviewed. The author should remove the reference named Globular 2023 and include the previous references instead along with a brief background on the globular clusters' evolution and properties.

The work discusses very relevant points on the evolution of a system of bodies considering collisions, escapes, and mergers among other effects. However, as I will mention in the following sections of this review, several parts of the manuscript. For instance, in the first sections, it seems that colliding particles are not taken into for the computations but later in the following sections a detailed description

of mergers and collisions is included. Hence, the paper should be deeply reorganized to avoid those contradictions.

Also, regarding the initial conditions, they seem very idealized conditions, as I will describe later.

The manuscript should be proofread and a language and grammar revision performed, using either proofreading services or the help of a native-speaking colleague.

***The following general comments are minor:***

The sign “÷” is confusing, I strongly suggest replacing it with “-“ throughout the manuscript.

The reference to distances should be consistent throughout the manuscript since some distance variables were named using ‘r’ and in other sections using ‘d’. Those details should be carefully reviewed by the author.

Figure axes format is not suitable for easy reading. The author needs to make axes and labels bigger and if possible increase the images' resolution.

In addition, the following particular comments should also be addressed:

***Abstract***

The abstract is quite technical and requires some additional background highlighting the relevance of the type of algorithm introduced by the author (in addition to that mentioned at the end of the abstract). The details of the layers may be summarized since they are fully described in the algorithms. Re-writing the abstract and moving the focus to the relevance rather than fine details would increase the impact of the work significantly and would help other readers from different areas to benefit from reading this manuscript. For example, the author could include a phrase explicitly stating more differences between the presented proposal and deterministic models, and some further applications, indicating the differences in execution times.

***Introduction***

The use of Wikipedia is discouraged due to the lack of a reliable peer-review process for those content. Hence, a list of peer-reviewed sources with provided structural parameters needs to be included (the suggested list is in the general comment). Right after, the density quantity  $100 \div 1000$  seems odd. The author should check that and include a new reference or refer to a previously cited one. The diameters mentioned by the author are quite big, since observationally, globular clusters have diameters predominantly shorter than 40 pc, for instance in the globular clusters catalog by Harris. These values should be taken with caution since establishing the absolute boundaries of clusters is a challenging task, for this reason, the used parameters to parameterize clusters' sizes are half-mass radius.

In the Milky Way, the total number of GCs is challenging to be estimated. However, rough estimates have been done. I suggest citing some works supporting such a number, for example, the following one [https://www.aanda.org/articles/aa/full\\_html/2019/10/aa36135-19/aa36135-19.html](https://www.aanda.org/articles/aa/full_html/2019/10/aa36135-19/aa36135-19.html).

Caution should be taken with the estimated ages of clusters larger than the estimated age of the universe. A brief sentence should be included to explain those large ages above 13.7 Gyr, for example, if they are computed from old-ages isochrones fitting.

The last sentence in the second paragraph states a risky assumption that is not correctly supported. Indeed there are a lot of spherical objects in the universe but it is not quite common, it is common among old objects, since in young stellar associations, the most observed shape is not spheric. For example young stellar associations such as open clusters like Hyades, among others. I suggest re-writing this paragraph emphasizing that the spherical shape is common among old clusters such as GCs, which is a consequence of virialization.

In the fifth paragraph, in the sentence “With the help of IMG” a “the” is missing right before IMF”.

In the introduction and throughout 5e manuscript I suggest replacing “So,..” with “Hence, ..” or “Thus,..” for the sake of formality.

In paragraph eleven it would be better to write: “For solving the N-body problem, we have developed a system called Galactica”. The URL should be moved to a footnote. The author should

include a brief description of the micro-word term and its relevance to the manuscript, or remove the comment.

In paragraph thirteen the author should elaborate on why the Galactica system avoids the instability reached by other authors in the literature. Such difference should be clearly stated since it gives more reliability to the use of Galactica rather than other traditional approaches in stellar dynamics. If the difference is due to the lack of regularization it should be stressed here rather than in upcoming paragraphs.. It is crucial since regularization has been a traditional ingredient in typical Nbody prescriptions such as in the Nbody codes family, and it would increase the impact of the new proposal introduced by the author.

### ***Section 2***

In the second paragraph thru authors should briefly explain the implications of considering circular orbits only.

The construction of the evenly spaced bodies in the rings seems an odd idealization since due to the discrete nature of the layers, there might be bodies with initial positions not covered by any layer. For this reason, the author should stress the reasons for this choice, since a higher space coverage of the initial conditions seems to require more computational resources than those used by the traditional Nbody codes. Figure 2 seems a good representation however more details should be included in the manuscript since it seems that many computations are required to generate points with no equal distances such as body 99th and body 1. The author should give more details on the computation of the accuracy term EPS.

With the proposed prescriptions how does the author avoid having two changes from rotated layers lying in the same position?

### ***Section 3***

The author claims “After the interaction for some time, the bodies will become evenly distributed over space”. Such a statement seems to be a consequence of the simplified assumed initial conditions, since in the majority of cases we notice that clusters tend to show some increase in entropy. Virialization of the cluster is expected indeed, but several processes need to take place (for example core collapse). The author should include some details on this subject since the statement is very relevant.

In equation 26, in the time factor, the author should explain what the 100 stands for.

After equation 28, describe  $r_{jk}$  (distances but in previous reference to distances the letter d was used instead by the author”). The notation should be consistent throughout the manuscript.

In general, this section is very informative, however, it should be summarized, and the details on the files' names and the resulting outputs should be moved to the appendix, leaving here only the summary of the algorithm's purpose and its relevance regarding the cluster dynamics (virialization, orbits, etc). The technical coding details should not be in the body of the manuscript. A useful resource for highlighting the relevance and strength of the code is a flowchart, which could show this section a glance at the algorithm operation to the readers.

### ***Section 4***

There is a typo in the first paragraph “perimeters” should be “parameters”

The names of the files in the figure and across the section should be moved to a footnote.

Is the author using any correction to account for the effect of the excluded collisions in the simulation or is the author estimating to any extent the possible change in the outcome when excluding the collisions?

Why does the author suggest Adding new bodies to the layers manually in the file fn3fvinp.dat. That could change the initial conditions dramatically.

Is there any special treatment in the algorithm for effects such as two-body relaxation, and the formation of hard and soft binaries?

### ***Section 5***

A summary of the treatment of bodies' motions and interactions performed by Galactica should be included and compared to that in other tools such as the Nbody codes family by Aarseth

Section 5.2 is well written and the operation of Galactica for interactions and trajectories seems accurate, however, my main concern is the initial conditions set described in previous sections.

### ***Section 5.3***

In this section, distances are referred to as  $R$ , whereas in the previous one  $r$ , and at the beginning of the manuscript  $d$ .  $R$  is more often used to refer to radii and  $D$  for diameters or distances. I recommend using the same notation throughout the manuscript.

### ***Section 5.4***

If the author uses  $d$  for distances in previous sections,  $R_p$  will be a good notation for the pericenter.

### ***Section 5.5***

After equation 33 the word “eliminating” is not accurate. I suggest writing something like: “equating expressions 33 and 32 yields”

After equation 34 the word “excluding” is not accurate. I suggest writing something like: “equating expressions 33 and 34 it follows”

### ***Section 6.2***

Right after Fig 8, the distance is referred to using  $r$ . The author should check the notation following the comments in the previous sections.

In the paragraph starting: “As already noted, the distances...”, a period is missing before “For some of these bodies...”.

### ***Section 6.3***

In previous sections, the author refers to the removal of bodies and avoiding collisions. However, in this section, there is a thorough treatment of bodies’ merging and dynamics. It is not clear which part of the algorithm performs these interesting calculations and the previous sections are confusing regarding this point. Please state clearly the details behind these calculations. Does Galactica handle them? If so, please give a brief explanation or if it is not the case, give a detailed explanation.

### ***Section 6.4***

This section gives hints on the collision treatment. For this reason, a reference to this section should be made to clarify that collisions are indeed considered, rather than the confusing statement in previous sections.

### ***Section 8.1***

Right after Figure 17, the term  $In_x$  is not previously described. It should be explicitly stated the meaning of such a term that is related to the number of layers. At the end of that paragraph, the last sentence has a grammatical error it should be: “the last structure (Fig. 16d) shows almost no differences from a sphere”.

Regarding the discussion of Fig. 17, the authors recall the relation between velocity and radius which scales or velocity inversely proportional to the square root of the radius. However, there is an increase at larger radii, which is described following a “non-linear” relation. I have several concerns here: in the first place, Eq. 41 is indeed linear (with a small slope), since the equation shown is of the form  $v_l = b + a \cdot r_l$ . On the other hand, the physical reason behind that increase in velocity (beyond the multiplication by the velocity coefficient  $k_v$ ) should be clearly stated.

### ***Section 8.2***

In the first paragraph, the author refers to “kinematic momentum” whereas in the paragraph before Table 2 the author refers to kinetic. The vocabulary needs to be unified to avoid confusion.

In the paragraph right after the tables, the sentence “In each layer, the orbits of the bodies are rotated according to one and the same algorithm” is not clear. What does the author mean by “to one and the same algorithm”? The sentence should be rephrased to clarify the point.

### ***Section 8.3***

In the first paragraph starting with “The spin of the central body is...” the sentence “In this case, if one look”, is wordy. Please rephrase it to improve the readability.

### ***Section 8.4***

Following the comments in the previous sections, caution should be taken with the notation throughout the manuscript, keeping either  $d$  or  $r$  for distances in a consistent way.

### **Section 9.3**

The assumptions regarding the initial conditions used for the simulations are accurate for Globular Clusters, however, the mentioned observational values are not accurate, since GCs do not have large radii as reported in several catalogs such as the GCs catalog by Harris. I recommend as in the introduction correcting the radii as masses observed quantities and include some classical references as suggested in the comment in the introduction.

I strongly discourage the use of Wikipedia as a reference source since it is not peer-reviewed by experts. The author should remove the reference to Wikipedia and include classical and verified literature sources regarding the observational structural values of GCs. A suggested list of verified references is included in the comments regarding the introduction and should be included.

### **Section 9.4**

There is a typo after equation 54, in “theirspecific” a blank space is missing.

### **Section 9.5**

As a closing point to this section, a comparison with Nbody codes such as those developed by Aarseth is necessary. Also a comparison of the execution times as mentioned in previous comments. The latter is to increase the impact of the manuscript, rather than just focusing the closing comment of this section on the specific simulation details alone.

On February 6, 2024, I sent the Editor of the Journal a response to her decision of November 10, 2023.

Dear Dr. Alessandra Celletti,

I have revised my paper "Development of multilayer models of globular star clusters and study of their evolution" in accordance with the reviewers' comments and attach it in the file DMMGSCE2\_1.doc.

I have also attached my response to the reviewers in the file ReplayRefSm.doc, as well as the reviewers' comments in the file CelMecDecision.doc.

Sincerely yours

Prof. Joseph J. Smulsky

A chief scientist of the Institute of Earth's Cryosphere,  
doctor of physical-mathematical sciences,  
professor of theoretical and applied mechanics,  
Institute of Earth's Cryosphere, Tyum. SC of SB RAS, Federal Research Center  
Malygina Str. 86,  
625026, Tyumen, Russia.  
Tel. +7-3452-68-87-14; E-mail: [jsmulsky@mail.ru](mailto:jsmulsky@mail.ru);  
<https://www.ikz.ru/~smulski/smul1/>.

### **Response to the first Reviewer's comments**

Reviewer 1, made several general comments on the article, based on the results of approximate analytical estimates of the N-body problem. It must be borne in mind that these estimates introduce a number of assumptions and simplifications, which often lead to conclusions that are not related to the actual interactions of bodies.

1. In point 1, the reviewer states that the core collapses for a system of equal mass. This statement is incorrect, since the concentration of bodies towards the center or their expansion is determined by their velocities: at low velocities the bodies will tend to the center and at large velocities they will tend to infinity.

2. Mass segregation of bodies of different masses is not relevant to my work, since it considers the interaction in a system with a central body and peripheral bodies of the equal mass.

3. The reviewer notices that the article lacks a demonstration that energy is conserved. I additionally provided kinetic and potential energies in Table. 3, and before paragraph 9.4 I give their explanation. These results show that the total mechanical energy is conserved.

The accuracy of integration of the N-body problem in the Galactica program is controlled by changes in momentum and angular momentum. Mechanical energy, as the sum of kinetic and potential energies, is not suitable for monitoring the accuracy of solving the N-body problem. An interacting N-body system is a changing system. For such a mechanical system, the work of forces depends on the path; work along a closed path is not zero, so the forces are not potential. In this case, the mechanical energy does not remain constant during the solution of the differential equation of motion. With strong changes in the system, mechanical energy can change by 50% or more, and then when the system returns to its previous state, the total energy also returns to its original value.

In addition, when bodies collide, mechanical energy is spent on their rotation and heating. When bodies collide, the angular momentum is spent only on the rotation of the bodies. And this part can be taken into account. Therefore, the change in angular momentum is the most reliable indicator of the accuracy of solving the N-body problem.

Let me give you an example. For a 15-layer structure, the relative change in angular momentum at the beginning of integration is  $2 \cdot 10^{-16}$ , and at the end there is  $5.8 \cdot 10^{-5}$ . Such control of precision is not possible using mechanical energy.

4. The article does not state that the age of globular clusters is greater than the age of the Universe. The article presents the results of determining the age of globular clusters by astronomers at 19.2 billion years, and the age of the Universe is not mentioned in the article. The value of 19.2 billion years is greater than the age of 13.7 billion years, which is assigned to the Universe according to the Big Bang hypothesis. But this hypothesis contradicts all the provisions of theoretical and celestial mechanics, as well as contradicts observation, and therefore is erroneous [1].

However, since the estimate of the age of astronomical objects is quite arbitrary, in the article I changed the words “19.2 billion years” to “more than 10 billion years”.

1. Smulsky, J.J. (2021). Dark Matter and Gravitational Waves. *Natural Science*, 13, 76-87. doi:10.4236/ns.2021.133007. <https://www.scirp.org/journal/paperinformation.aspx?paperid=107880>.

### **Response to the second Reviewer's comments**

Reviewer 2's comments contain the following parts: General Note, Abstract, Introduction. The following are comments by section: Section 2, Section 3, and so on. In accordance with these parts, what follows is my response to Reviewer 2's comments.

#### ***General comment***

In the first sentence, the reviewer formulates the essence of the work and gives it an assessment: “The manuscript presents an interesting method to model the initial conditions of a system of bodies that could be used to reproduce after dynamical evolution using Galactica the observed and expected features of stellar systems such as Globular Clusters and Galaxies.” I agree with this reviewer's opinion.

Further, the reviewer suggests taking into account a number of classic works and not using a source such as Wikipedia. I fully took into account these reviewer's suggestions in the revised text of the article.

There are also a few stylistic notes here that I took into account as well.

Regarding the note about the axes in the figures. I looked at all the drawings. Small inscriptions on the axes are available on some of the graphs in Fig. 5, 8 and 13, and refer to three-dimensional images. These images, along with the axes, were made in MathCad and are provided for illustration purposes. All the necessary dimensions of the trajectories are available on the two-dimensional graphs.

#### ***Abstract***

I changed the beginning of the Abstract to explain the relevance of the article.

#### ***Introduction***

I took into account all the reviewer's comments and suggestions.

#### ***Section 2***

The article has been added an explanation about circular orbits and EPS accuracy.

**Explanation 1** about the discrete nature of the layers. When creating a structure, bodies are in layers. Some time after the bodies interact, they will be between the layers.

**Explanation 2** to the reviewer's question. To avoid various negative results, the algorithms for all rotations are carefully developed and then tested on various examples.

### **Section 3**

**Explanation 3** to the question of uniform distribution. In order for an interacting system of bodies not to have a tendency to collapse or to continuously expand, two conditions are necessary: 1) the initial conditions are correctly specified; 2) high accuracy of problem solving.

These two conditions are met in this work.

**Explanation 4** for the number "100". This number is explained above by formula (26): "Time  $T$  is expressed in hundreds of periods of revolution  $P_1$ ".

**Explanation 5** about the designation of distances. I replaced the designation  $R_{ik}$  with  $r_{ik}$ . In other cases, the designation "r" from the word "radius" is not suitable for the length  $l$  of the line on which the bodies are located and the distance  $d$  between the bodies in equations (17) – (21).

**Explanation 6** about the MLSpStr2 program. I agree with the reviewer that this section is very informative. This is due to the fact that I briefly describe the program for creating models of globular clusters. Without this writing, the reader will not understand how such a model is created. The flowchart in this case will be less clear and will require more description. And in the Appendix it would be possible to place the MLSpStr2 program.

I believe that the MLSpStr2 program for constructing a cluster will help researchers study processes in various star systems in more depth. Therefore, I made it freely available and provide a link to it.

### **Section 4**

The error has been corrected.

**Explanation 7** about file names. File names are also names of structures, so they must be given in the text.

**Explanation 8** about collisions. During the interaction of bodies, collisions are not excluded. At the stage of creating the structure, close positions of bodies at the points of self-intersection of the line of their location are eliminated by correcting the number of bodies  $N_3$  in the layer. When the positions of the bodies in all layers are determined, then their velocities are calculated. Therefore, a stable structure with a new number of bodies is created.

**Explanation 9** about binaries stars. In the Galactica program, when bodies approach each other, the step is automatically reduced so that the accuracy of the problem does not decrease. Therefore, no other algorithms are required for binaries stars.

### **Section 5**

**Explanation 10** about NBODY programs. A comparison of the Galactica program with other programs is given in the Introduction. There are hundreds of programs to solve the N-body problem. The Introduction presents of the comparison of the Galactica program results with three programs: NBODY 6, the French school of celestial mechanics (Laskar et al.) and NASA. For example, NBODY 6 uses three derivatives, and the Galactica program uses 6. According to our research, each derivative reduces the error in angular momentum by three orders of magnitude, that is, 6 derivatives reduce the error by  $6 \cdot 3 = 18$  orders of magnitude [2] - [3]. In NBODY 6, according to the Hermite method, derivatives are calculated at the beginning and end of the step, which reduces the error by two orders of magnitude. Therefore, in general, in NBODY 6 the error in angular momentum will decrease by  $3 \cdot 3 + 2 = 11$  orders of magnitude. Therefore, its accuracy is 7 orders of magnitude worse than the Galactica program.

2. Smulsky J.J. (2012). The System of Free Access Galactica to Compute Interactions of N-Bodies. I. J. Modern Education and Computer Science, 11, 1-20. DOI: 10.5815/ijmeecs.2012.11.01. <http://www.ikz.ru/~smulski/Papers/Galct14E2J.pdf>.

3. Smulsky, J.J. (2018) Future Space Problems and Their Solutions. Nova Science Publishers, New York, 269 p. ISBN: 978-1-53613-739-2. <http://www.ikz.ru/~smulski/Papers/InfFSPS.pdf>.

**Explanation 11.** I am pleased with the words of the reviewer: “Section 5.2 is well written and the operation of Galactica for interactions and trajectories seems accurate...”. Namely, the results of the Galactica program indicate the accuracy of its work. This is especially visible in Fig. 10, which shows trajectories during collisions and mergers of bodies. I am sure that none of the existing programs for solving N-body problems can give such results. And these results provide a lot of new knowledge about processes in stellar systems.

About the reviewer's concerns about the initial conditions. At the beginning of the interaction of bodies, the structure of the system does not change for a time equal to several periods of revolution of the bodies of the first layer. Does not change if the initial conditions are set correctly! If there is the slightest mistake in them, the structure immediately begins to change and may even collapse. Therefore, inaccuracies in the initial conditions are immediately visible.

**Section 5.3**

I talked about the designation “ $r$ ” in Explanation 5.

**Section 5.4**

I'm glad the reviewer approved of “ $R_p$ .”

**Section 5.5**

Comments are taken into account.

**Section 6.2**

The comment has been taken into account.

**Section 6.3 and Section 6.4**

**Explanation 12.** As I already wrote in Explanation 7, the positions of the bodies are adjusted when the structure is created by the MLSpStr2 program. The interactions of the bodies are calculated by the Galactica program, and if the bodies collide, they merge into one body.

**Section 8.1**

**Explanation 13.** The parameter  $Inx$  is explained in section 3, before formula (24).

The error has been corrected.

**Explanation 14** about increasing velocity. An explanation of the increase in velocity is given in the second paragraph before formula (41): “... the velocity decreases unless the mass of the bodies increases so much that its influence becomes predominant” i.e. the increase in velocity at radius  $r$  is due to the increase of the mass of bodies contained inside a sphere of radius  $r$ .

**Section 9.3 and Section 9.4**

The comments were taken into account.

**Section 9.5**

I mentioned the comparison of the NBODY 6 and Galactica programs in terms of theoretical accuracy values in Explanation 10. For a more detailed comparison, it is necessary to solve the same problem with these programs. This is a lot of work, and also meaningless.

As I already noted, there are hundreds of programs to solve N-body problems. Their creators are highly qualified specialists. One of them is Dr. Sverre Aarseth, who dedicated his entire life to creating the NBODY series of programs. However, all these programs work well on the class of tasks for which they were created. If the task belongs to a different class, then these programs may not work well.

Based on the functions that are available in the NBODY 6 program, I see that the results obtained using Galactica cannot be obtained using NBODY 6. On the other hand, the Galactica program is not suitable for solving traditional problems based on IMF with additional algorithms for binary stars, tidal forces, operations with receding bodies, etc. With these additions, Galactica will lose its accuracy and benefits.

If the reviewer is interested, then I can prepare initial conditions for a globular cluster with a large number of bodies. This problem can be solved using NBODY 6. The reviewer now has an understanding of what kind of globular cluster structure can be created. Therefore, he can formulate requirements that it reflect to the greatest extent the problems that exist with globular clusters. In accordance with these requirements, I will create such a model of a globular cluster and send the file with it to the reviewer.



In conclusion of my response to the reviewers, I would like to express my gratitude to them for their comments and suggestions.

I especially want to note the great and high-quality work of the second reviewer. Thanks to this work, I delved deeper into the problem of globular clusters and saw new prospects for further research.

-----  
**My comment:** On the same day, February 6, 2024, I received the following message from the editor-in-chief of the Journal.

**From:** Prof. Alessandra Celletti

**Sent:** Tuesday, February 6, 2024, 20:47 +05:00

**Subject:** Re: Decision on your submission to Celestial Mechanics and Dynamical Astronomy

Dear Dr. Smulsky,

unfortunately your paper has been rejected on 10 November 2023.

Of course you are free to submit a new paper through SNAPP (and not directly to me), but it should not include a reply to the reviewers, since it will be treated as a new submission.

Best regards, Alessandra Celletti.

\*\*\*\*\*

Prof. Alessandra Celletti

Department of Mathematics

University of Rome Tor Vergata

<http://www.mat.uniroma2.it/~celletti>

Governing Board member and Vice-President of ANVUR

"Italian National Agency for the evaluation

of Universities and Research Institutes"

<https://www.anvur.it/en/personae/alessandra-celletti-2/>

February 7 2024, I uploaded my paper to Submission system (SNAPP) of the journal in Collection "Innovative computational methods in Dynamical Astronomy". I am attaching the text of the cover letter below.

#### *Cover Letter 2*

The paper considers models of globular star clusters. Algorithms and programs have been developed that make it possible to create a globular star cluster that does not break down during their further gravitational interaction. The paper describes a program MLSpStr2 for creating stable globular star clusters. To solve the N-body problem, the Galactica program, also created by the author, is used to study the evolution of the clusters. Compared to similar programs, it has increased accuracy. The evolution of several models is considered by numerical solution of the N-body problem. We studied the dynamics of stars, their trajectories in various cases of interactions.

*The two, three and four paragraphs are the same as in Cover Letter 1.*

The present work considers problems that belong to the field "Innovative computational methods in Dynamical Astronomy".

-----  
On February 11, 2024, my paper was rejected in the following decision by the Journal.

**From:** "Innovative computational methods in Dynamical Astronomy

**Sent:** Tuesday, February 11, 2024, 17:58

**Subject:** Re: Decision on your submission to Celestial Mechanics and Dynamical Astronomy

Ref: Submission ID 9c4b6950-b32e-4586-8c0c-efc7aafe060b

Dear Dr Smulsky,

Your manuscript entitled "Development of multilayer models of globular star clusters and study of their evolution" has now been assessed. If there are any reviewer comments on your manuscript, please find them below.

Regrettably, the above submission has been rejected for publication in *Celestial Mechanics and Dynamical Astronomy*.

Thank you for the opportunity to consider your work. I am sorry that we cannot be more positive on this occasion and hope you will not be deterred from submitting future work to *Celestial Mechanics and Dynamical Astronomy*.

Kind regards,

Alessandra Celletti, Editor, *Celestial Mechanics and Dynamical Astronomy*

On February 12, 2024, I sent the Editor of the Journal such letter.

**From:** [Joseph J. Smulsky](#)

**Sent:** Monday, February 12, 2024 12:32 PM

**To:** [Innovative computational methods in Dynamical Astronomy](#)

**Cc:** Dr. Alessandra Celletti

**Subject:** Re: Decision on your submission to *Celestial Mechanics and Dynamical Astronomy*

Dear Dr. Alessandra Celletti,

I have resubmitted my paper "Development of multilayer models of globular star clusters and study of their evolution" as you recommended doing in your letter dated February 6, 2024: "Of course you are free to submit a new paper through SNAPP (and not directly to me), but it should not include a reply to the reviewers, since it will be treated as a new submission".

Why is my paper being rejected now?

Sincerely yours

Prof. Joseph J. Smulsky

On February 19, 2024, I received such letter of the Editor of the Journal.

**From:** Prof. Alessandra Celletti

**Sent:** Monday, February 19, 2024, 21:36 +05:00

**Subject:** Re: Decision on your submission to *Celestial Mechanics and Dynamical Astronomy*

Dear Dr. Smulsky,

as I said in my previous message, we could not treat your paper as a revision, but rather as a new submission.

You submitted your new paper, but the opinion of the associate editor was that it could not be "considered a new manuscript because it is not substantially and sufficiently different from the previously rejected manuscript".

I hope this clarifies.

Best regards, Alessandra Celletti.

On February 21, 2024, I sent the Editor of the Journal such letter.

**From:** [Joseph J. Smulsky](#)

**Sent:** Wednesday, February 21, 2024 5:27 PM

**To:** [Prof. Alessandra Celletti](#)

**Subject:** Re: Decision on your submission to *Celestial Mechanics and Dynamical Astronomy*

Dear Dr. Alessandra Celletti,

The associate editor's decision is incorrect. My paper has been revised in accordance with the reviewers' comments. A list of all the reviewers' comments, their detailed analysis, and a list of all changes in the paper are given in my reply to the reviewers in the file *ReplayRefSm.doc*.

However, you insisted that I am submitting a new paper through SNAPP and not upload this reply: "but it should not include a reply to the reviewers, since it will be treated as a new submission." Since the further passage of the paper depended on the associate editor, then you should have familiarized him with my answer. Therefore, the rejection of my paper was entirely your fault.

As for the associate editor, then his activities do not correspond to the interests of the scientific journal, if by these interests we mean the spread of truth and not the spread of misconceptions and lies.

The previous decision of the associate editor on my paper also testifies to this. From the review of the first reviewer, the superficial nature of the review is visible to the naked eye. The reviewer only read the Introduction to the paper, and of the four his comments, two are not relevant to the paper, one indicates the reviewer's superficial understanding of the basics of mechanics, and the fourth comment about the age of the Universe is false.

The second reviewer worked deeply on my paper and offered a number of useful tips that I took into account. He also asked many questions, and he did not understand a number of places. This is not surprising, since the paper is large, it contains 60 pages. And to understand everything in it you need to read it two or three times.

In my answer to these questions and to the passages that the reviewer did not understand, I gave 14 explanations. In a number of places, the second reviewer admires the results I obtained in the paper. Therefore, his review is not negative, but positive. This is an ordinary review by a research scientist of material previously unknown to him, which implies further dialogue between the author and the reviewer.

However, the associate editor rated these reviews as negative and misled you, so you rejected this paper.

Modern fundamental science is in a deep crisis: it propagates misconceptions and impedes the spread of truth [1]. Almost all of its constructions are based on hypotheses. This is the first cause. The second cause is the assessment of scientific activity: it is assessed not by the content of scientific results, but by their place of publication.

In modern physics and astrophysics, an imaginary macro-world has been created with big explosions, black holes, dark matter, dark energy and other equally ridiculous fantasies. All of them contradict the basics of mechanics. Therefore, it seemed that Celestial mechanics, continuing the traditions of Galileo, Newton, Laplace, Euler and many others, was supposed to set a barrier to these fantasies. However, your journal is not such a barrier, but, on the contrary, is a disseminator of all these misconceptions of Mainstream science.

My paper presents a new way of non-hypothetical knowledge of the world around us. It examines the question of what, in accordance with the laws of mechanics, a globular cluster of stars should be so that it can exist for a long time. The properties of a globular cluster obtained in this way provide answers to many questions that could not previously be obtained in the way in which such associations as globular clusters and galaxies are currently studied.

In conclusion, in the file IntScTrib4\_4J.pdf I attach my paper [1], which should be read by everyone who strives to understand the real world.

1. Smulsky J.J. International Scientific Tribunal. *Ann Rev Resear.* 2023; 10(3): 555786. DOI: 10.19080/ARR.2023.10.555786. <https://juniperpublishers.com/arr/pdf/ARR.MS.ID.555786.pdf>.

Sincerely yours

Prof. Joseph J. Smulsky

On February 24, 2024, I received such letter of the Editor of the Journal.

**From:** Prof. Alessandra Celletti

**Sent:** Monday, February 24, 2024, 23:49 +05:00

**Subject:** Re: Decision on your submission to Celestial Mechanics and Dynamical Astronomy

Dear Prof. Smulsky,

the associate editor analyzed the paper as well as your reply letter in an attempt to make a fair assessment of the submission. Unfortunately, the associate editor concluded that there are no substantial elements of novelty in the new manuscript; the only changes are minor.

I put in copy Dr. Frank Schulz, Springer editor.

Best regards, Alessandra Celletti.

On February 26, 2024, I sent the Editor of the Journal such letter.

**From:** [Joseph J. Smulsky](#)

**Sent:** Monday, February 26, 2024 6:53 PM

**To:** [Prof. Alessandra Celletti](#)

**Subject:** Re: Decision on your submission to Celestial Mechanics and Dynamical Astronomy

Dear Prof. Alessandra Celletti,

You write that the associate editor decided to reject my paper taking into account the corrected paper and my Reply to the reviewers.

Based on these same materials, you decided to continue reviewing the paper. That is, the associate editor also rejected your decision.

I presented this paper as part of the “**Collection:** Gravitational Stellar and Galactic Dynamics” headed by Dr. Daniel Pfenniger, Dr. Dimitri Veras and Dr. Alessandra Celletti. That is, you are not only the editor-in-chief, but also a well-known specialist in the field to which my paper relates. Therefore, your associate editor here also showed his unsuitability to be an associate editor of a scientific journal.

I think that you did the right thing by sending a copy of your letter to your superior manager Dr. Frank Schulz, Springer editor. Apparently, he will make the right decision and fire the associate editor, or both of you.

So, my paper was reviewed, in my answer I explained the parts that the reviewers did not understand, and I made the additions they recommended to the paper. The paper needs to be published. Its publication will have a beneficial effect on the development of celestial mechanics!

Sincerely yours

Prof. Joseph J. Smulsky

**My comment:** Since 2010, I have submitted five papers to the journal Celestial Mechanics and Dynamical Astronomy.

1. "Theory of the Earth's rotation for numerical integration", January 2010, published as “The Influence of the Planets, Sun and Moon on the Evolution of the Earth’s Axis”.
2. "Asteroids Apophis and 1950 DA: 1000 years orbit evolution and possible use" by Smulsky J.J. and Smulsky Ya.J., December 2010.
3. “Exact solution to the problem of N bodies forming a multi-layer rotating structure”, 2015.
4. “Advances in mechanics and outlook for future mankind progress”, 2016.
5. “Development of multilayer models of globular star clusters and study of their evolution”, 2023.

And all of them were rejected by the Journal editors. Now these papers are published. Readers are given the opportunity to compare and evaluate the contribution to the treasury of knowledge about the world that these papers and all the papers published in Celestial Mechanics and Dynamical Astronomy have made.

## **II. An International Journal of Astronomy, Astrophysics and Space Science (Astrophysics and Space Science).**

On February 16, the paper was submitted to the journal via the Submission System with the following cover letter.

### ***Cover Letter 3***

*The first four paragraphs are the same as in Cover Letter 1.*

The present work considers problems that belong to the field of the Astrophysics and Space Science.

On April 17, 2024, my paper was rejected in the following decision by the Journal.

**Subject:** Decision on your submission to Astrophysics and Space Science

**Date:** April 17 2024. 2:33

**Ref:** Submission ID 69e72b34-b5c6-4c0f-86d2-61853c9b70e5

Dear Dr Smulsky,

Despite trying very hard and inviting over a dozen potential reviewers, I haven't been able to find one willing to take on the review of your manuscript "Development of multilayer models of globular star clusters and study of their evolution".

As it would be unfair to further delay your paper, I consider it the better option to return the manuscript, with my apologies that despite my best efforts I haven't been able to secure a report on it.

Thank you for the opportunity to review your work. I hope you will not be deterred from submitting future work to Astrophysics and Space Science.

Kind regards,

Elias Brinks, Editor in Chief, Astrophysics and Space Science.

**My comment:** Over the course of two months, the editor invited more than 10 potential reviewers, and no one expressed a desire to review the paper. I think that this is evidence of a crisis in contemporary fundamental science: it has plunged into an imaginary world, so its representatives are not able to review a paper that reveals the mechanisms of the functioning of the real world. Now the paper is published, and the reader can agree with me, or, on the contrary, justify the refusal of 10 potential reviewers to review the paper.

### III. Journal of Astrophysics and Astronomy

On April 22, the paper was submitted to the journal via the Submission System with the following cover letter.

#### *Cover Letter 4*

*The first four paragraphs are the same as in Cover Letter 1.*

The present work considers problems that belong to the field of the Journal of Astrophysics and Astronomy.

On May 1, 2024, my paper was rejected by the Journal in the following decision.

**From:** Annapurni Subramaniam

**Subject:** Decision JOAA: Your manuscript entitled Development of multilayer models of globular star clusters and study of their evolution - [EMID:f65abaa71ca648b3]

**Date:** Wednesday May 1, 2024. 15:21 +05:00

Ref.: Ms. No. JOAA-D-24-00067

Development of multilayer models of globular star clusters and study of their evolution  
Journal of Astrophysics and Astronomy

Dear Prof. Smulsky,

I regret to inform you that I am unable to accept the paper mentioned above for publication in Journal of Astrophysics and Astronomy. Please find enclosed the referee's comments which could be of some use to you.

In consultation with the Editorial Board members, I regret to inform you that your paper does not warrant publication in the Journal of Astrophysics and Astronomy.

Thank you for submitting your paper to this Journal.

Dear Author,

We find that your article has 28% similar text with text in an already published material by you. This is a large fraction of similar text and the manuscript cannot be considered as original. We cannot process this manuscript any further. You may revise and resubmit it as a fresh manuscript.

Best regards,

Chief Editor, JoAA Journal, Editorial Office, Journal of Astrophysics and Astronomy.

On May 2, 2024, I sent the Editor of the Journal such letter.

**From:** [Joseph J. Smulsky](#)

**Sent:** Thursday, May 2, 2024 3:37 PM

**To:** [Annapurni Subramaniam](#)

**Subject:** Re: JOAA: Your manuscript entitled Development of multilayer models of globular star clusters and study of their evolution - [EMID:f65abaa71ca648b3]

Dear Dr. Annapurni Subramaniam,

Chief Editor  
JoAA Journal,

My paper “Development of multilayer models of globular star clusters and study of their evolution” (Ref.: Ms. No. JOAA-D-24-00067) was rejected according to the following statement: “We find that your article has 28% similar text with text in an already published material by you”.

This statement is incorrect, since the materials of the paper in English were not published.

Sincerely yours

Prof. Joseph J. Smulsky

**My comment:** I have not received a response to my letter.

When a paper is analyzed by programs such as Antiplagiat or CrossCheck, the journal sends the author a report from this program. In this case, I was not sent such a report. The Antiplagiat program report, previously provided by another journal, gave the paper's originality as 89.92%. Therefore, the 72% originality reported by the JoAA Journal editor was clearly incorrect.

Now the paper has been published, and the reader can draw his own conclusion about its originality.

The work of the Antiplagiat program is the work of artificial intelligence. About 5 years ago, the report of this program was accompanied by a Warning that its results cannot serve as the basis for a final decision. The editor makes the decision based on the author's response. Now the final decision is made by Artificial Intelligence. Everyone should understand what awaits us if we are managed with the help of Artificial Intelligence.

This is, firstly. And secondly, such Artificial Intelligence is a very convenient tool for realizing one's interests, i.e. for corruption. Apparently, this option is used in this case.

I would like to note for your information that there are now services that offer to rework a published paper so that Antiplagiat will consider it original, and it can be republished, apparently even changing the authors. This operation is also carried out with the help of artificial intelligence!

#### IV. Journal of Modern Physics

**From:** [Joseph J. Smulsky](#)

**Sent:** Monday, May 6, 2024 11:15 AM

**To:** [Sarry Sun](#)

**Subject:** Re: Issue plans: Journal of Modern Physics (JMP) Invites Exceptional Authors to Submit Papers

Dear Ms. Sarry Sun,

Editor of the Journal of Modern Physics,

In the file DMMGSCE2\_4.doc I send you my paper “Development of multilayer models of globular star clusters and study of their evolution” for publishing in Journal of Modern Physics, Vol. 11, No. 8, July 2024, \*Special Issues\*, -Gravitation, Astrophysics and Cosmology.

Sincerely yours

Prof. Joseph J. Smulsky

On May 14, 2024, I have received Acceptance Letter from the Journal.

**From:** [jmp@scirp.org](mailto:jmp@scirp.org)

**Sent:** Monday, May 14, 2024 06:01 +05:00

**Subject:** JMP: Acceptance Letter for Paper ID: 7505310

Dear Dr. Joseph Smulsky,

Warm greetings from the Journal of Modern Physics (JMP).

We are pleased to inform you that your paper entitled "Development of multilayer models of globular star clusters and study of their evolution" has been accepted for publication.

To proceed with the publication process, kindly complete the following three procedures within a week:

Step 1: Submit the Article Processing Charge payment of \$1199 by clicking the payment link [click here](#)

Step 2: Complete the Copyright Transfer process.

Step 3: Revise your paper according to the comments on the system, format it using our template, and upload the revised version in Word or Latex (with its PDF version) using the system. Please highlight the revisions in red color and send us a response letter on the comments if available. The template and review comments are available in the system. If the size of the reformatted file exceeds 4MB, kindly send it via email.

Please feel free to contact us if you have any questions.

Best regards, Jane Gao, JMP Editorial Office.

### **Reviewer 1**

Journal of Modern Physics (JMP)

Development of multilayer models of globular star clusters and study of their evolution (7505310)  
The initial models of globular clusters are very important in N-body simulations. However, it is not easy to get stable models. This manuscript presents a method for constructing models of globular star clusters in the form of multilayer spherical structures. Models with 5, 10 and 15 layers are tested, and their evolution has been studied in detail. The dynamical processes of globular clusters and the change of some properties such as positions, velocities, merge, rotation and temperature are discussed.

#### ***1. General comments***

This manuscript studies the creation of stable globular cluster models, which can be used for N-body simulations of such clusters. The feature of the new method of this paper is that it constructs models of globular star clusters in the form of multilayer spherical structures. This method is thought to be more accurate than some other method, e.g., that used by NBODY 6. This is interesting and helpful for N-body studies of globular clusters. The process of how to build such globular cluster models and the evolution of some examples of such models have been investigated.

#### ***2. Improvements that you could suggest on the paper***

Although this manuscript has been prepared carefully, in particular, it shows many detailed formulae and figures, I have some suggestions to improve this paper.

- 1) In the abstract, it is better to give some suggestions about how to build accurate and stable cluster models.
- 2) At the end of section 1, I suggest to give a short introduction about the structure of paper.
- 3) In section 3, it is better to give some description about the relation of different layers when building multilayer structures.
- 4) About the models with 5, 10 and 15 layers, I hope to have a clear comparison of them. This may help the readers to see the difference and then choose appropriate number of layers to build their models.
- 5) After the conclusion, I suggest to add a discussion section, to give some comparison with other methods such as that used by N-body 6, and compare to the observation of at least one or two typical globular clusters. It is also better to clarify the shortcomings of the new method used by this paper.
- 6) In addition, the paper seems somewhat long. A shorter one may be welcome. Besides, according to the policy of the journal, research manuscripts typically range from 10 to 30 pages in length. Please try to shorten it to approximately 50 pages.

#### ***Notes on format:***

1. To facilitate the typesetting process, we kindly ask you to provide us with the **Word version** of your paper. If your paper contains many equations or symbols, please also include the PDF file to avoid any potential text corruption in the Word version. If you don't have the Word version, you can submit **the LaTeX file along with its PDF format**, which is also acceptable.

#### ***PS: For equations,***

1) Except for constants like  $e$ ,  $\pi$ ,  $i$ , functions such as  $\sin$ ,  $\exp$ ,  $\ln$ ,  $\Gamma$ , and some special symbols like  $\Delta$ ,  $\Sigma$ , all other equations will be presented in italic form. 2) Matrices and vectors should be presented in bold and italic form.

If you have any specific requirements for equations, please inform us in advance.

2. The references are not cited correctly in the paper. Here are the rules:
  - 1) References at the end of the paper should be numbered in order like 1, 2, 3 and so on.
  - 2) All the references should be quoted in the main body.
  - 3) The references mentioned in the main body should be written like [1], [2], [3] and so on.
  - 4) The order of references mentioned in the paper should be shown from small to large, which means reference [1] should be shown before references [2] (for the first time they are quoted).
3. Ensure that all figures and tables (if any) are in the correct order and are referenced in the text.
4. High-resolution figures should be submitted for clarity.
5. **All equations should be editable and created using equation editor.**
6. Figures and tables will be positioned either at the top or bottom of the page according to typesetting rules. If you have any special layout requirements, please let us know when submitting the revised version.
7. Avoid including excessive references in the abstract. If needed, limit the number of references to three.
8. It is essential to carefully review your paper before submitting the final version, as major revisions will not be permitted once the revised edition has been received.

### ***1. Summary***

This is an interesting study on numerical analysis of an N-body problem. Especially the use of the software is impressive.

### ***2. General comments***

This manuscript is also interesting for high-school students, because the software is applied to the well-known Coulomb force.

### **Reviewer 2**

ID: 7505310

Title: Development of multilayer models of globular star clusters and study of their evolution

In the manuscript, the author examines models of globular star clusters by analyzing their luminosity and other observational parameters. The objective of this work is to develop stable models of globular clusters based on the principles of mechanics. By employing an exact solution for the axisymmetric gravitational interaction of N-bodies, single-layer spherical structures were created and subsequently combined into multilayer models of globular clusters. The manuscript describes the algorithm and program used for this creation process. Through solving the problem of gravitational interaction of N-bodies, the evolution of 5-, 10-, and 15-layer structures was studied. During inter-body interactions, the initial specially organized structure transitions to one where bodies are uniformly distributed in space. This results in a decrease in the number of inter-body collisions, leading the globular cluster model to achieve a stable form. The manuscript also considers the collisions of bodies and the acquisition of rotational motion and thermal energy by them. By scaling the dimensions, the results were recalculated to match the conditions of globular star clusters.

### ***1. General comments***

Broadly speaking, I think the work is well referenced and of interest to the astrophysics and respective gravity community. There is, however, lack of stronger motivation for some of the assumptions used in the analyses. For example:

### ***2. Improvements that you could suggest on the paper***

- 1) First of all, the introduction and motivation must be improved and it is not aimed to general reader.
- 2) The specific shape chosen in this work should be further motivated. What are the advantages or the justification of this paper choice against any other?
- 3) Current version motivation does not explain why the authors need to study the multilayer models of global star clusters.
- 4) In equation (24), author mention that AUV but not mentioned about Asm. There should be more detail about Asm.



- 5) Write down complete detail For Equation (27), how you are getting these expressions.
- 6) The author should spend some words about Equation 50.
- 7) There are several typographical (grammar, punctuation etc) errors that need to be fixed after careful rounds of reading.
- 8) Provide more detail in the conclusion section for better understanding.
- 9) The author speaks of "determinism" of the classical, Newtonian, N-body problem. I do not understand what he means by "determinism" in this case, because it is known that since the pioneering studies of the 3-body problem by Poincare, the N-body problem is prototype of an ergodic system.

On May 27, 2024, I sent the JMP Editorial Office such letter.

**From:** [Joseph J. Smulsky](#)

**Sent:** May 27, 2024 12:49

**To:** Jane Gao

**Subject:** Re: JMP: Acceptance Letter for Paper ID: 7505310

Dear Jane Gao,  
JMP Editorial Office,

Today I uploaded Copyright Form and my paper "Development of multilayer models of globular star clusters and study of their evolution", corrected according to the reviewer's suggestions, into the Paper Submissions system.

I am attaching the paper in the files DMMGSCE2\_6.doc and DMMGSCE2\_6.pdf.

I took into account all the reviewers' suggestions, their list, and my answers to them are attached in the Author'sResponses.doc file.

Sincerely yours

Prof. Joseph J. Smulsky

#### **Author's response to Reviewer 1's comments**

The author's response is highlighted in blue.

1. In the abstract, it is better to give some suggestions about how to build accurate and stable cluster models.

The following text has been added to the Abstract.

It is necessary to set the coordinates, velocities and masses of the stars so that as a result of their gravitational interaction the globular cluster is not destroyed. This is not an easy task, and it has been solved in this paper.

2. At the end of section 1, I suggest to give a short introduction about the structure of paper.

The following text has been added at the end of section 1.

The structure of the paper is as follows. The method for constructing globular clusters is described at the beginning. The evolution of 5, 10, and 15-layer globular cluster models is then considered. Then their general properties are described. These studies were carried out in dimensionless form. Further, the results obtained are presented in dimensional form in the scale of a globular cluster. At the end of the paper, models of the central body are studied, which make it possible to reduce its mass by tens of times.

3. In section 3, it is better to give some description about the relation of different layers when building multilayer structures.

The relation of different layers is represented by formula (16). The relation is expressed in the fact that the mass of the inner layer is added to the mass of the central body. The text before formula (16) explains this.

4. About the models with 5, 10 and 15 layers, I hope to have a clear comparison of them. This may help the readers to see the difference and then choose appropriate number of layers to build their models.

The following text has been added at the end of section 7.

In the considered 5, 10, and 15-layer models of globular clusters, the arrangement of the layers relative to each other, the number of bodies in the first layer, and the number of layers changed. All of

them are stable and do not destroy. Therefore, with the variations considered, it is possible to create models of globular clusters with any number of layers in them.

5. After the conclusion, I suggest to add a discussion section, to give some comparison with other methods such as that used by N-body 6, and compare to the observation of at least one or two typical globular clusters. It is also better to clarify the shortcomings of the new method used by this paper.

Before the Conclusions, I added the following section 10.

### 10. Discussion

Usually, at modeling of globular star clusters, for example using the NBODY 6 program, the evolution of the shape of the globular cluster is investigated and the change of its statistical characteristics are studied, for example, changes in the distribution of mass along the radius of the cluster. In this case, the internal dynamics of the globular cluster are not considered, the trajectories of the stars are not studied, the processes during their collision are not investigated, for example, the appearance of rotational motion of the stars and their thermal energy, etc.

In the present study, the N-body problem (28) was solved in dimensionless form. Therefore, its results can be applied to stellar associations of different scales, such as planetary systems, globular clusters and galaxies. However, the relative sizes of the bodies in these associations are different. Therefore, the characteristics of processes when bodies collide will be different. In further studies these circumstances will be taken into account.

### Author's response on Referee 2's comments

The author's response is highlighted in blue.

1. First of all, the introduction and motivation must be improved and it is not aimed to general reader.

In the Introduction, I tried to describe the problem so that it would be understandable to a wide range of readers. The paper discusses many different problems, so some readers may be unfamiliar with some problems. However, using the references provided in the paper, such a reader will be able to get acquainted with them.

2. The specific shape chosen in this work should be further motivated. What are the advantages or the justification of this paper choice against any other?

3. Current version motivation does not explain why the authors need to study the multilayer models of global star clusters.

The answer to p. 2 and p. 3. The motivation is in the Abstract and Introduction. Every new reader has their own special interests that they would like answered. If the reviewer had specified his interest, I could then provide that specific motivation in my response. There is a lot of material in the paper, and I have no doubt that any interested reader will find answers to his interests in it.

As stated in the Abstract: "The goal of this work is to create stable models of globular clusters based on the laws of mechanics." Typically, models of globular clusters are considered as "black boxes". After reading my paper, the reader will see how bodies "live" in such a "black box". Therefore, many questions about the existence of globular clusters will become clear, and there will be no need to put forward hypotheses about the supposed structure of globular clusters. This is my motivation.

4. In equation (24), author mention that  $AU$  but not mentioned about  $A_{sm}$ . There should be more detail about  $A_{sm}$ .

$A_{sm}$  – mentioned in the third paragraph of section 3: " $A_{sm}$  is the semi-axis of the orbits of first-layer peripheral bodies in astronomical units (AU)."

5. Write down complete detail For Equation (27), how you are getting these expressions.

Equation (27) was obtained by transforming the dimensional differential equation of motion into the dimensionless one (28). This is shown in my work [25], the reference to which is given at the beginning of the paragraph before formula (26): "A file of initial conditions such as MS15c49b.dat uses dimensionless values [25]."

6. The author should spend some words about Equation (50).

Equation (50) is the ratio of the number of stars in a globular cluster to its volume in cubic parsecs. This is stated before formula (50): “The last column gives the number of stars in a cubic parsec at the initial time.”

7. There are several typographical (grammar, punctuation etc) errors that need to be fixed after careful rounds of reading.

I read the paper again and corrected the typographical errors I noticed.

8. Provide more detail in the conclusion section for better understanding.

At the suggestion of the first reviewer, I added a Conclusion paragraph, which stated what the reviewer suggested.

There is a lot of new material in the paper, so there may be many points to conclude. If the second reviewer had a specific suggestion, I would have taken it into account in this Conclusion.

9. The author speaks of "determinism" of the classical, Newtonian, N-body problem. I do not understand what he means by "determinism" in this case, because it is known that since the pioneering studies of the 3-body problem by Poincare, the N-body problem is prototype of an ergodic system.

How “determinism” is understood in the paper is stated in the fourth paragraph of the Introduction: “In deterministic models, each body has its own size, mass, coordinates, and velocity. The gravitational interaction of each such body with any other body is investigation. Therefore, the position and velocity of any body are known at any time.”

10. I express my gratitude to the reviewer for his interest in my paper and his comments. I find them quite useful.

On July 29, 2024, I have received such letter from the Journal.

**From:** jmp@scirp.org

**Sent:** July 29, 2024, 12:05 +05:00

**Subject** paper is published on JMP: Vol.15 No.8 2024! [ID: 7505310]

Dear Dr. Joseph Smulsky,

I hope this email finds you well. I am excited to inform you that your manuscript has been published in the latest issue (Vol.15 No.8 2024) of Journal of Modern Physics (JMP). You can access it at <https://www.scirp.org/journal/JMP/>.

We wish you further progress in your research field and hope to hear more news from you soon. Please do not hesitate to contact us if you have any questions.

Best regards, Cindy Zhang, JMP Editorial Office, Scientific Research Publishing.